Universidade Estadual de Londrina

GUILHERME DELFINO SILVA

EFFECTIVE FIELD THEORIES FOR QUANTUM SPIN LIQUIDS AND FRACTONIC SYSTEMS

Londrina
2021

GUILHERME DELFINO SILVA

EFFECTIVE FIELD THEORIES FOR QUANTUM SPIN LIQUIDS AND FRACTONIC SYSTEMS

Dissertação de mestrado apresentada ao Departamento de Física da Universidade Estadual de Londrina, como requisito parcial à obtenção do título de Mestre.

Orientador: Prof. Dr. Pedro Rogério Sérgi Gomes

Londrina
2021

Ficha de identificação da obra elaborada pelo autor, através do Programa de Geração Automática do Sistema de Bibliotecas da UEL

Silva, Guilherme Delfino.
Effective Field Theories for Quantum Spin Liquids and Fractonic Systems / Guilherme Delfino Silva. - Londrina, 2021.
95 f. : il.

Orientador: Pedro Rogério Sérgi Gomes.
Dissertação (Mestrado em Física) - Universidade Estadual de Londrina, Centro de Ciências Exatas, Programa de Pós-Graduação em Física, 2021.
Inclui bibliografia.

1. Teorias Efetivas - Tese. 2. Líquidos Quânticos de Spin - Tese. 3. Sistemas Fractônicos - Tese. 4. Modelos Exatamente Solúveis - Tese. I. Sérgi Gomes, Pedro Rogério. II. Universidade Estadual de Londrina. Centro de Ciências Exatas. Programa de Pós-Graduação em Física. III. Título.

CDU 53

GUILHERME DELFINO SILVA

EFFECTIVE FIELD THEORIES FOR QUANTUM SPIN LIQUIDS AND FRACTONIC SYSTEMS

Dissertação de mestrado apresentada ao Departamento de Física da Universidade Estadual de Londrina, como requisito parcial à obtenção do título de Mestre.

BANCA EXAMINADORA

_____

Orientador: Prof. Dr. Pedro Rogério Sérgi Gomes
Universidade Estadual de Londrina - UEL

_____

Prof. Dr. Rodrigo Gonçalves Pereira
Universidade Federal do Rio Grande do Norte - UFRN

_____

Prof. Dr. Carlos André Hernaski
Universidade Tecnológica Federal do Paraná - UTFPR

Londrina, 15 de fevereiro de 2021.

Agradecimentos

Quero agradecer imensamente ao meu orientador Pedro Gomes que guiou meus passos para me que me tornasse um pesquisador em Física Teórica. Ele me proporcionou experiências inestimáveis como contatos com outros pesquisadores e novas colaborações, vários conselhos pessoais e me cedeu muito de seu tempo, que contribuíram enormemente para minha formação como físico e como ser humano. Fico feliz em dizer que ele se tornou um amigo.

Agradeço aos meus pais Elizabete e Joaquim, à minha namorada Geovana Maria, e a toda a minha família que me apoiaram ao longo de todo este percurso. Em especial, quero agradecer à minha prima Amabile Mariano, às minhas tias Roselei Delfino e Elizete Delfino e à minha avó Jacira Lopes que me proporcionaram casa, comida, companhia, amor e carinho enquanto me dedicava ao aprendizado da Física. Sem eles, eu nunca seria capaz de chegar aqui.

Agradeço aos inúmeros amigos que fiz em minha jornada na Física, que espero levar comigo para o resto da minha vida. Não me atrevo a cita-los pois sei que me esqueceria de alguém e isso não seria justo. Em especial, agradeço aos meus amigos Julio Toledo e Samuel Gomes que tive o prazer de compartilhar a maior parte dos meus dias em Londrina, estudando, discutindo, me divertindo e até mesmo procrastinando. Sem eles, a jornada até aqui seria muito mais dura e difícil.

Quero agradecer a todos os professores que tive durante minha formação educacional. Em especial, agradeço a Maria de Lourdes Anjos, minha professora do Ensino Médio, por todo o apoio e material didático que me proporcionou quando ingressei no curso de Física e a Paula Bienzobaz que, além de uma grande professora, tem se mostrado uma amiga valiosa. Ela me incentivou fortemente a seguir o que eu realmente queria na minha carreira acadêmica e é, de alguma forma, a responsável por esse trabalho.

Agradeço também aos membros da banca, os professores Rodrigo Gonçalves Pereira e Carlos André Hernaski que aceitaram avaliar este trabalho. Agradeço também aos professores suplentes Paula Fernanda Bienzobas e Renann Lipinski Jusinskas.

Por fim, gostaria de agradecer ao CNPq pelo apoio financeiro e ao Departamento de Física da UEL pelo apoio estrutural.

DELFINO, Guilherme. **Teorias Efetivas para Líquidos Quânticos de Spin e Sistemas Fractônicos**. 2021. Dissertação de mestrado (Mestrado em Física) – Universidade Estadual de Londrina, Londrina, 2021.

Resumo

Em uma classe especial de fases da matéria, o emaranhamento quântico desempenha um papel importante nas propriedades de baixas energias do sistema. Ele pode atuar como um mecanismo que leva à quase-partículas não locais e a uma degenerescência robusta do estado fundamental. Dois exemplos de tais fases, que são objetos deste trabalho, são os Líquidos Quânticos de Spin gappeados e os sistemas Fractônicos. Nosso objetivo é investigar descrições efetivas, em termso de teorias de campos, para vários modelos exatamente solúveis de líquidos de spin bidimensionais e sistemas fractônicos em $3D$. Fazemos isso tomando o limite do contínuo da teoria depois de usar um mapa explícito entre os graus de liberdade micro e macroscópicos. Além do estudo de modelos de rede bem conhecidos, também propomos um modelo de rede de fractonico do Tipo-I em $2D$, que é exatamente solúvel e ordernado topologicamente. Além disso, este trabalho revisa alguns mecanismos para fractons, como modelos exatamente solúveis, construções de camadas acopladas e abordagens *bottom-up* para descrições efetivas.

Palavras-chave: Teorias Efetivas. Líquidos Quânticos de Spin. Sistemas Fractônicos. Modelos Exatamente Solúveis.

DELFINO, Guilherme. **Effective Field Theories for Quantum Spin Liquids and Fractonic Systems** . 2021. Master Thesis (Masters of Science in Physics)– Universidade Estadual de Londrina, Londrina, 2021.

Abstract

In a special class of phases of matter, the quantum entanglement plays a major role in the low-energy properties of the system and may act as a mechanism for robust non-local quasi-particles and ground state degeneracy. Two examples of such phases, which are the subject of this work, are gapped Quantum Spin Liquids and Fractonic systems. Our purpose is to investigate topological-like effective field theories descriptions for several exactly solvable models of $2D$ quantum spin liquids and $3D$ fractonic systems. We do that by taking the continuum limit of the theory after using an explicit map between the micro and macroscopic degrees of freedom. Moreover, besides the study of well known lattice models, we also propose a $2D$ Type-I lattice fracton model, which is exactly solvable and is topologically ordered. In addition to those, this work reviews a few fracton mechanisms, such as exactly solvable models, coupled-layer constructions, and bottom-up approaches to effective descriptions.

Keywords: Effective Field Theories. Quantum Spin Liquids. Fracton Systems. Exactly Solvable Models.

Lista de ilustrações

Sumário

Introduction

In our physical understanding so far, nature behaves differently in distinct energy scales, which are in general decoupled from each other [1]. These simple features are the keystones in order to isolate a given phenomenon and study it. In addition, physical systems also present distinct qualitative properties as the number of constituents N is increased. Indeed, as we increase N new phenomena are able to emerge and the description of the system may eventually become quite complicated [2]. Depending on how large N is, new approaches and theories are needed in order to describe the physics of such systems. Roughly,

$$\begin{aligned} N &\sim 1 \quad \text{Quantum mechanics} \\ N &\sim 10-100 \quad \text{Atomic Physics} \\ N &\sim 100-10^5 \quad \text{Chemistry} \\ N &\gtrsim 10^5 \quad \text{Condensed matter physics.} \end{aligned}$$

In the last few decades, condensed matter physics has been an effervescent research area with interdisciplinary interests, ranging from pure theoretical descriptions to quantum computing technology. In this way, it provides a rich laboratory to develop and test theoretical ideas describing interesting phenomena. With the proper technology, materials can be submitted to extreme conditions of temperature and external fields, so that quantum effects are macroscopically visible. Such systems are denoted as quantum matter, where impressive phenomena may emerge due to high-entanglement and strong interactions among the constituents [3].

Quasi-particle excitations with exotic properties are a signature of a strong coupled physical system. Within the context of quantum matter, quasi-particles usually emerge in topologically ordered systems [4, 5]. The most prominent example is the Quantum Hall system [6]. Such excitations are called *anyons* and possess intriguing properties like fractional charge and statistics [7]. In the last decades, new kinds of topologically ordered systems were discovered, as the Quantum Spin Liquids (QSL) and, more recently, the so-called fractonic phases.

Quantum Spin Liquids are quantum phases of matter whose topological ordering properties emerge from spin fluctuations [8]. This is in contrast with the Quantum Hall fluids, where the topological nature follows from correlations between charged degrees of freedom. In QSL, the quantum states present a high degree of entanglement between all spins of the system. It means that one cannot perform a local measurement in the system without affecting all other spins. The severe entanglement of the quantum states is the essential ingredient for the emergence of exotic properties, as non-local quasi-particles and

robust gapped states [4]. Although they may be very complicated systems, they provide beautiful theoretical descriptions along with deep physical insights.

Fractons were firstly realized in certain $3D$ lattice models involving only local interactions between spin degrees of freedom [9, 10, 11]. In addition to certain topological aspects, they exhibit even more exotic properties, such as restricted mobility: they typically move in planes, lines or are completely immobile [12, 13]. Furthermore, certain low-energy properties carry ultraviolet information (UV/IR mixing), in contradiction to the usual property of decoupling of scales [14]. These unusual characteristics make the problem of finding low-energy descriptions very challenging. Nevertheless, several approaches for fractonic systems have been proposed, as gapless higher-rank gauge theories [15], topological-like gapped field theories [16, 17, 18], stacks of coupled layers [19], and parton constructions [20].

The theoretical description of the above systems can be done in principle from two perspectives. One can start from a microscopic description, with an underlying lattice structure, or one can start directly from the macroscopic point of view, in terms of low-energy descriptions. The central purpose of this work is to investigate the interplay between these two approaches in the context of QSL and fractonic systems. We consider several exactly solvable lattice models and discuss how to find the corresponding effective field theories. The main original results contained in this work are:

i) Derivation of the low-energy effective field theory for the $\mathbb{Z}_N$ Toric code;

ii) Derivation of an effective description for the Wen plaquette model;

iii) Construction of a two-dimensional Type-I fracton model;

iv) Derivation of an effective field theory for the above fracton model;

v) Study of general properties of $2D$ Chern-Simons-like fractonic theories.

This work is organized as follows. In Chapter 1, we review general properties of topological field theories, which are useful throughout the work. In addition, we briefly review QSL and fracton phenomenology. In order to acquire some intuition about lattice models and their effective field theories, in Chapter 2, we study $2D$ topologically ordered systems, such as the $\mathbb{Z}_2$ lattice gauge model and exactly solvable QSL models (Toric Code and Wen Plaquette model). In Chapter 3, we study three $3D$ exactly solvable lattice fracton models: the X-Cube, Chamon, and Haah codes. In Chapter 4, we discuss the coupled layers construction, which is able to perturbatively recover the X-cube model from coupled stacks of $2D$ Toric codes. In Chapter 5, we investigate bottom-up approaches for continuum effective field theories for fractonic systems. Finally, in Chapter 6, we explicitly derive the effective field theory in a top-down approach for the X-Cube model, the Chamon code, and also for a $2D$ Type-I fracton system.

1 Topological Phases of Matter

In this chapter we review some properties of topological quantum field theories, as the emergence of anyons and the ground state degeneracy. In addition, we review some properties of quantum spin liquids and we briefly summarize the main characteristics of fractonic phases of matter.

1.1 Topological Quantum Field Theory

Topological Quantum Field Theories (TQFT) are a class of quantum field theories which are an indispensable keystone in modern theoretical physics. TQFT emerge naturally in the low-energy limit of effective theories for topological phases of matter as, for example, the Quantum Hall Effect. For the purposes of this work, we discuss two types of topological quantum field theories, namely, Abelian Chern-Simons and BF theories.

Chern-Simons theories are expressed as local terms in the Lagrangian for gauge fields. They can be seen as "kinetic terms" for gauge fields which are able to capture topological aspects of the underlying manifold and gauge group. Let us consider the Abelian Chern-Simons action defined over three dimensional manifold $\mathcal{M}$

$$S_{CS} = \frac{k}{4\pi}\int_{\mathcal{M}} d^3x \epsilon^{\mu\nu\rho} a_\mu \partial_\nu a_\rho, \tag{1.1}$$

with a_μ an $U(1)$ gauge field and k a dimensionless parameter, called the Chern-Simons level. For the case in which the underlying gauge group is non-Abelian, cubic terms $\sim a_\mu a_\nu a_\rho$ also contribute for the CS action. Although the CS theory can only be defined on $2+1$ dimensions, in section 5.2 we will see a generalization of it in order to describe $3+1$ dimensional systems.

Up to boundary terms, the Chern-Simons theory is invariant under gauge transformations $a_\mu \to a_\mu + \partial_\mu \alpha$. It is also invariant under the Poincare group. We can see the topological character of the Chern-Simons term by noting that it does not depend on the metric of the manifold $\mathcal{M}$. It is also commonly written as

$$S_{CS} = \frac{k}{4\pi}\int_{\mathcal{M}} a \wedge da \tag{1.2}$$

with a a one-form, d the exterior derivative and $\wedge$ the wedge product between them. The Chern-Simons theory does not require a metric space, that is, the notion of distances and angles are not important for its physics. The theory is invariant under manifolds continuous deformations. In mathematics, we call such transformations homeomorphisms and that is the reason we call such field theory topological. As we will see in the following and through examples in Section 2, the topological aspect of such theories plays a major role in the robustness of the low-energy properties of topological phases of matter.

Let us now analyze the physics contained in the Chern-Simons theory. Let $f_{\mu\nu} = \partial_\mu a_\nu - \partial_\nu a_\mu$ ne the $U(1)$ gauge invariant field strength associated to the a_μ fields. The classical theory has the equations of motion

$$f_{\mu\nu} = 0 \quad \Leftrightarrow \quad da = 0, \tag{1.3}$$

which tell us the local physics it contains is trivial: There are no gauge invariant propagating degrees of freedom. Let j a one-form subjected to the conservation law $d \star j = 0$. The coupling to matter fields can be performed by the current term $\mathcal{L}_{CS} - a \wedge \star j$, which leads to classical equations of motion

$$f_{\mu\nu} = \frac{2\pi}{k} \epsilon_{\mu\nu\rho} j^\rho, \quad j^\mu = (\rho, j^1, j^2). \tag{1.4}$$

It attaches magnetic flux to the matter density $2\pi\rho = kB$. This is, together with its topological aspect, the most striking feature of Chern-Simons theories. The role of the CS theory is to attach magnetic flux to the excitations, which transmutes their statistics. In the process to exchange two identical particles, they feel an Aharonov-Bhom effect due to their attached magnetic field, which contributes to the statistical phase [21]

$$\nu = \frac{1}{2k}. \tag{1.5}$$

For $\nu = 0$ and $\nu = 1$ we have bosons and fermions, respectively. For arbitrary ν, we have *anyons*.

Even in the presence of matter, the CS theory has no propagating degrees of freedom. Upon quantization, it will give us a fully gapped theory. Albeit it has a gapped spectrum, it may gives us interesting physics. If the underlying manifold $\mathcal{M}$ has nontrivial topology, nontrivial physics may emerge. In this case, another class of gauge invariant objects are present in the theory: Wilson loops. Wilson loops are holonomies around non-contractible closed loops γ on the manifold

$$W(\gamma) = \exp\left(i \oint_\gamma a \right). \tag{1.6}$$

For simplicity, let us consider the case in which the manifold is homeomorphic to a $T^2 \times \mathbb{R} =_{homeo} \mathcal{M}$, with T^2 a genus 1 torus. In coordinates, it means the opposite edges in both directions x and y of a plane are identified, as in Figure 1. For such case, where the manifold topology is nontrivial, large gauge transformations α are allowed. Such transformations receive this name because they have a global aspect and cannot be continuously deformed into the identity $\alpha = 0$. Namely

$$\alpha(x, y) = \frac{2\pi n_1 x_1}{L_1} + \frac{2\pi n_2 x_2}{L_2}, \quad n_1, n_2 \in \mathbb{Z}. \tag{1.7}$$

They wind around the two spatial directions of the $L_1 \times L_2$ torus n_1 times around a given direction and n_2 around the other. This class of gauge transformations leave the Wilson

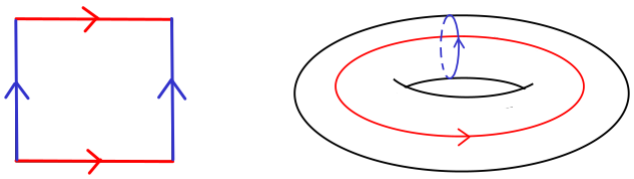

Figura 1 – Torus as a plane with identified edges. In such topological space there are two non-contractible loops.

loops invariant

$$a_i \to a_i + \frac{2\pi n_i}{L_i}, \quad W(\gamma_i) \to \exp\left(i \oint_{\gamma_i} a_i dx^i + 2\pi n_i\right) \tag{1.8}$$

with γ_i being a closed curve around the i-th direction of the torus.

Under canonical quantization, a non-vanishing commutator is induced between the conjugated fields a_1 and a_2

$$[a_1(\vec{x},t), a_2(\vec{y},t)] \equiv -\frac{2\pi i}{k}\delta^{(2)}(\vec{x}-\vec{y}) \tag{1.9}$$

and consequently

$$W(\gamma_1)W(\gamma_2) = e^{\frac{2\pi i}{k}} W(\gamma_2)W(\gamma_1). \tag{1.10}$$

The above expression tell us that the ground state is $k-$fold degenerated. In fact, for a genus g manifold, the ground state is k^g-fold degenerate [6], indicating the CS sensitivity to the manifold topology. The global aspect of such operators indicate us how robust is the ground state degeneracy. Any local operator to be added in the Lagrangian does not split the degeneracy, in contrast to usual quantum theories.

Other class of TQFT frequently used in this work is the BF theory. BF-theories can be thought as generalizations of Chern-Simons theories for arbitrary spacetime dimensions D. In general, they involve topological interaction terms $A \wedge \mathrm{d}B$, with a a one-form and c a $(D-2)-$form fields

$$S_{BF} = \frac{k}{2\pi}\int_{\mathcal{M}} a \wedge dc. \tag{1.11}$$

As the CS theory, the above action contains no local gauge invariant degrees of freedom. Instead, the relevant degrees of freedom are the Wilson lines and their "dual", t'Hooft operators

$$W(\gamma) = \exp\left(i \oint_{\gamma} a\right) \quad \text{and} \quad V(\Sigma) = \exp\left(i \oint_{\Sigma} c\right), \tag{1.12}$$

for a closed curve γ and a closed $(D-2)$-surface. From now, we are mainly interested in the case $D = 2+1$ dimensions. In this case, both the Wilson and t'Hooft operators are

string-like, c is the topological conserved current, and the BF term corresponds to the coupling of the current with a vector field a.

The physics contained in the BF theory is very similar to Chern-Simons in the sense that it is sensitive to the topology of the underlying manifold $\mathcal{M}$ and it attaches magnetic flux to matter in the presence of external currents. The main difference is that, when put on a nontrivial manifold, large-gauge transformations leave both operators (1.12) invariant. In the case that $\mathcal{M} =_{homeo} T^2 \times \mathbb{Z}$, for any closed loops which transverse the system in the 1 and 2 directions, the operators obey

$$W(\gamma_2)V(\gamma_1) = e^{\frac{2\pi i}{k}} V(\gamma_1)W(\gamma_2) \quad \text{and} \quad V(\gamma_2)W(\gamma_1) = e^{\frac{2\pi i}{k}} W(\gamma_1)V(\gamma_2). \tag{1.13}$$

Each one of the algebras (1.13) have a k-dimensional representation, leading to a k^2-fold ground state degeneracy. It can be seen by considering the set $\{|n_x, n_y\rangle\}$ of $\mathcal{A}_x$ and $\mathcal{A}_y$ eigenstates with eigenvalues $\mathcal{A}_i |n_x\rangle = e^{2\pi i n_i/k} |n_x\rangle$. From the algebras in (1.13) we see that

$$V(\gamma_1) \left(W(\gamma_2) |n_x, n_y\rangle\right) = e^{\frac{2\pi i(n_x-1)}{k}} \left(W(\gamma_2) |n_x, n_y\rangle\right) \tag{1.14}$$

$$V(\gamma_2) \left(W(\gamma_1) |n_x, n_y\rangle\right) = e^{\frac{2\pi i(n_y+1)}{k}} \left(W(\gamma_1) |n_x, n_y\rangle\right), \tag{1.15}$$

with $n_i = 0, \ldots, k-1$ for $i = 1$ and 2. The role of the $V(\gamma_i)$ operator is either to measure the c flux through the i direction or to insert a flux through the $i_\perp$ direction. The same is valid for the $W(\gamma)$ operators. In general, for a manifold $\mathcal{M}$ with genus g the ground state degeneracy is k^{2g} [6].

In summary, TQFT are very useful to describe topological phases of matter and are able to account for the ground state degeneracy, the fully gapped spectrum, the phase robust character and the emergence of quasi-particles.

1.2 Quantum Spin Liquids

Quantum spin liquids (QSL) are insulating phases of spin-materials that do not present spontaneous magnetization, even at very low temperatures ($T \sim 0$). Such phases usually present interesting features, as the presence of excitations with fractional statistics and the emergence of gauge fields. The high entangled nature of these phases provides their nontrivial properties, which make them of great interest in physics, and also make them challenging.

There are many spin liquid phases which behave differently, amid a bunch of these present the same geometrical symmetries. Thereby, dealing with order transitions between such phases, Landau theory of phase transitions is not applicable: a topological phase transition theory is required. It is important to say that not all spin liquids present topological ordering, as gapless QSL for example [4]. Also worth of mention, is that QSL may exist in both $2+1$ and $3+1$ dimensions [22].

Unfortunately, so far QSL were not experimentally observed, and their study hides some giant difficulties. The high degree of interaction needed among the constituents of the system and the difficulty to deal with decoherence in ordinary materials are the main difficulties in experimental QSL research.

In the theoretical context, the strongly interacting character of QSL usually makes them non-perturbative systems. In this fashion, even the theoretical description of QSL is not an easy task. There are several approaches which have been used to study and explore QSL physics, as slave-particles decomposition and mean-field theory. We will explore exactly solvable gapped quantum spin liquids, as the two-dimensional lattice models Toric Code and Wen Plaquette model (See Chapter 2).

Let H_{QSL} be a quantum lattice Hamiltonian describing a gapped quantum spin liquid. Its ground state usually presents a certain kind of entangled ordering, which is not magnetic since

$$\langle 0|\, \vec{S}_i \,|0\rangle = 0, \tag{1.16}$$

where i represents the lattice site.

Such property plays an important role in QSL. If we allow perturbations in the original Hamiltonian

$$H = H_{QSL} - \sum_i \vec{h} \cdot \vec{S}_i, \tag{1.17}$$

we see that they have no crucial role in lifting the ground state degeneracy. This is a consequence of the robust topological character of the ground state degeneracy.

The high degree of entanglement may allow non-local excitations, that is, excitations that can only be created by non-local operators. Although the system may be constituted of only bosonic spin degrees of freedom, excitations with fractional quantum numbers may emerge as a result of the underlying entanglement.

The work in Ref. [8] provides an extensive review on the topic, regarding theoretical advances and potential experimental platforms of QSL.

1.3 Fractons

A general feature of topological phases of matter is the emergence of quasi-particles with exotic properties, such as fractional statistics and fractional charge. In fractonic topological phases of matter, quasi-particles with "fractional mobility" appear. Such particles are called fractons and have their mobility restricted to sub-manifolds. They are called sub-dimensional particles and, for three dimensional systems, are usually classified as:

- Fractons - Excitations whose mobility is completely restricted, they cannot move at all as individual excitations;

- Lineons - Particles which can move only along lines;
- Planons - Particles which can move only along two dimensional manifolds, usually planes.

We refer as fractonic phases of matter physical systems whose excitations are fractons. Such phases are topologically ordered in the sense that they present topological properties, as ground state topology dependence, robust phenomenology against perturbations and emergent quasi-particles. Although there are several works in three-dimensional gapped fracton systems, it is believed that they do not exist in $2+1$ dimensions. We propose an example of such system, both in the lattice and in continuum, in Section 6.1.

Even though fracton phases are topologically ordered, they are not truly topological. General properties of such systems are UV/IR mixing and that the ground state degeneracy depends on the size of the system. In contrast to truly topological systems (See Section 1.1), the fractonic ones are not invariant under continuous deformations. Within the context of fractonic systems, they are usually classified in two groups:

- Type I - Fractons per se are immobile particles. However, they are able to move along the system as part of bound states with other fractons;
- Type II - Fractons do not move at all.

The dependence of ground state degeneracy (GSD) on the system size places a big challenge in finding continuous field descriptions of such systems. One of the main principles of effective field descriptions is the decoupling of the physics in distinct scales. The fact that the long wavelength physics must take into account what happens on short lengths goes against the renormalization group philosophy and signals an IR/UV scales mixing in the underlying field theory [14]. In this sense, effective field theories for fractons cannot be TQFT's, but must be, somehow, similar to them.

2 Two-dimensional Quantum Spin Liquids Lattice Models and Effective Field Theories

In this chapter we will study the properties of two-dimensional lattice models as well as their Effective Field Theories (EFT). First, we will study, in some details, the properties of the $\mathbb{Z}_2$ lattice gauge theory and its corresponding EFT. Then, we will study other two $2D$ lattice models, the Toric Code and Wen Plaquette model, which are both exactly solvable models and correspond to gapped quantum spin liquids.

2.1 $\mathbb{Z}_2$ Lattice Gauge Theory

The $\mathbb{Z}_2$ lattice gauge theory is the simplest gauge theory that presents nontrivial topological order: defined on a torus, its ground state has a four-fold topological degeneracy. Due to its simplicity, in this section we study this system in a very detailed way. We mainly follow the references [4] and [23].

Let Λ be a $L \times L$ square lattice, constituted by N sites (vertices of the lattice), with periodic boundary conditions in both directions, forming a torus. We define a qubit degree of freedom on every link ℓ of the lattice. It is useful to denote the link $\ell = (ij)$ in terms of the sites i and j that it connects to.

The Hilbert space per link $\mathcal{H}_\ell$ is two-dimensional and the total Hilbert space is given by the product of them $\mathcal{H} = \prod_\ell \otimes \mathcal{H}_\ell$. Albeit $\dim(\mathcal{H}) = \prod_\ell \dim(\mathcal{H}_\ell) = 2^{2N}$, we do not observe this amount of physical states. The role of the $\mathbb{Z}_2$ gauge structure is to identify different qubit configurations as the same physical state. In order to fully characterize the physical properties of this system, we will define a subspace $\mathcal{H}_{phys}$ composed of all the physical states.

In order to define the quantum Hamiltonian of this system, we write the local operators which act on the qubits in terms of the Pauli operators Z_ℓ and X_ℓ. The Hamiltonian is defined as

$$\mathcal{H}_{\mathbb{Z}_2} = -g \sum_p \prod_{\ell \in \partial p} Z_\ell - t \sum_\ell X_\ell, \tag{2.1}$$

where g and t are coupling constants, p is a square plaquette and ∂p is its boundary. Let us denote the set of four links ℓ connected to the lattice site i as the star set s_i and consider the local operator

$$G_i = \prod_{\ell \in s_i} X_\ell, \tag{2.2}$$

which obeys $G_i^2 = 1$. This operator anti-commutes with the Z_ℓ Pauli operator if $\ell \in s_i$ and trivially commutes with it otherwise. In another words it "flips" the z-component spin of the four qubits lying in the star s_i

$$G_i Z_\ell G_i = -Z_\ell, \quad \ell \in s_i. \tag{2.3}$$

These operators generate the $\mathbb{Z}_2$ gauge structure for the model, locally acting on the sites. The identity element of this group is the non-action of G_i in any site, that is, the identity operator $\mathbb{I} = \prod \otimes \mathbb{I}_\ell$. As mentioned before, the gauge structure identifies different qubit configurations as the same physical state. We say that two qubit configurations $|\psi_1\rangle, |\psi_2\rangle \in \mathcal{H}$ are gauge equivalent if $|\psi_2\rangle = G|\psi_1\rangle$ for some element G of the $\mathbb{Z}_2$ gauge group . This relation define an equivalence relation which enable us to define a physical Hilbert space $\mathcal{H}_{phys} \cong \mathcal{H}/\sim$ identifying all the equivalent spin configurations with an unique physical state.

The Hamiltonian $\mathcal{H}_{\mathbb{Z}_2}$ is invariant under gauge transformations

$$[G_i, \mathcal{H}_{\mathbb{Z}_2}] = 0 \quad \forall i \in \Lambda, \tag{2.4}$$

which follows from the fact that there is always an even number of Z_ℓ operators emanating from each site i.

The dimension of the physical Hilbert space is $\dim(\mathcal{H})$ divided by the number of independent gauge transformations. Naively, since there are N lattice sites, one can think that there are 2^N independent gauge transformations. However, to correctly count $\dim(\mathcal{H}_{phys})$ it is useful to introduce the Invariant Gauge Group (IGG). The IGG is a subgroup of $\mathbb{Z}_2$ gauge group, composed by all the elements that leave all qubit configurations invariant. For this model, the IGG contains only two elements: the G_i action in every lattice site and the identity element:

$$IGG = \{\prod_{\forall i \in \Gamma} G_i, \mathbb{I}\}. \tag{2.5}$$

The existence of a nontrivial Invariant Gauge Group causes a reduction of the number of independent gauge transformations. To see this, let us consider two spin configuration $|\psi_1\rangle, |\psi_2\rangle \in \mathcal{H}$ and keep in mind that, by definition, $\tilde{G}|\psi\rangle = |\psi\rangle$ for any $|\psi\rangle \in \mathcal{H}$ and $\tilde{G} \in IGG$. Then, if these two spin configurations are gauge equivalent $|\psi_2\rangle = G|\psi_1\rangle$ for some element G of the $\mathbb{Z}_2$ gauge group, it is also gauge equivalent for an element $G\tilde{G}$, since $|\psi_2\rangle = G(\tilde{G}|\psi_1\rangle) = G\tilde{G}|\psi_1\rangle$. The two distinct group elements G and $G\tilde{G}$ actually perform the same gauge transformation, as ilustred in Figure 2. In general, for a finite gauge group $\mathcal{G}$, the number of independent gauge transformation is given by the coset $\mathcal{G}/IGG$. In our case there are $2^N/2$ independent gauge transformations and then $2^{2N}/\left(2^N/2\right) = 2^{N+1}$ distinct physical states, gauge inequivalent to each other.

The g and t parameters of the Hamiltonian set two energy scales. In the following, we analyze how the system behaves in extreme limits of such parameters. What we see

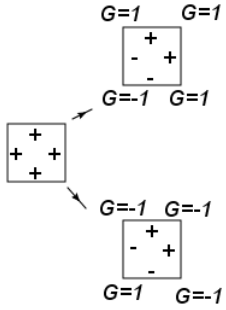

Figura 2 – Two distinct gauge group elements lead to the same qubit configuration. Both elements are identified in the coset $\mathcal{G}/IGG$.

is that this system present different behaviors depending on the relation between those parameters. In one regime we have a topological deconfined phase and in the other we have a non-topological confined phase:

- $g \gg t$: For $t \to 0$, the ground state minimizes the plaquette terms B_p with eigenvalues $+1$ for every p. We can explicitly find the system ground state introducing the product state $|\Uparrow\rangle = \prod_\ell \otimes |\uparrow_\ell\rangle$, with $|\uparrow_\ell\rangle \in \mathcal{H}_\ell$. Although this state minimizes the system energy, it is not invariant under gauge transformations. One can construct a gauge invariant ground state performing the gauge transformation

$$|0\rangle = \prod_{i\in\Lambda} (1 + G_i) \, |\Uparrow\rangle \, . \tag{2.6}$$

  The energy of such states is

$$E_0 = -gN, \tag{2.7}$$

  and the low-energy excitations, siting in the plaquette p, correspond to negative eigenvalue states of the plaquette operator B_p. We call such excitations *visions* and they correspond to a nontrivial $\mathbb{Z}_2$ flux through a plaquette. They can be created by applying the X_ℓ Pauli operator on some link ℓ. The fact that every link is shared by two plaquettes forces these excitations to be created in pairs. The local action of the Pauli operator on a link creates two excitations. In order to have a locally isolated excitation, one must apply a X_ℓ operators along a string. Explicitly, let γ^* be a string defined in the dual lattice with endpoints in the plaquettes a and b, then

$$B_p \left(\prod_{\ell\in\gamma^*} X_\ell \, |0\rangle \right) = f_p \left(\prod_{\ell\in\gamma^*} X_\ell \, |0\rangle \right), \quad \text{with} \quad f_p = \begin{cases} -1, \ p = a \text{ or } b, \\ +1, \ \text{otherwise}, \end{cases} \tag{2.8}$$

  which tell us this state has one excitation in each endpoint of γ^*, as indicated in the Figure 3.

  There are no local operators which creates a single $\mathbb{Z}_2$ excitation - this characteristic is topological in the sense that it survives to perturbations and to the introduction

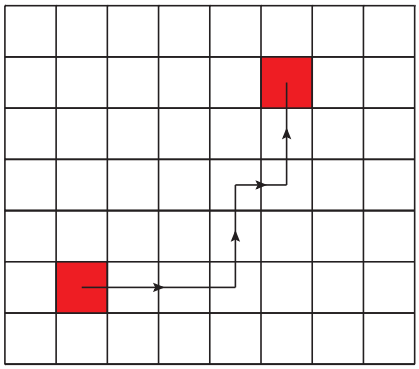

Figura 3 – Visions (red plaquettes), created in the endpoints of the string γ^* in the dual lattice. The notation $\ell \in \gamma^*$ means that the link ℓ crosses γ^*.

of new degrees of freedom. This phase is gapped: the energetic cost to create a pair of excitations is very large $\Delta E \sim 4g$. The gapped character of topological phases makes them very robust against perturbations.

The topological character of this phase becomes clear once we realize that the ground state is not unique. Actually, defined on a torus, the ground state has a four-fold degeneracy. Indeed, we have a hint of such degeneracy if we try to label our physical states through the gauge invariant $\mathbb{Z}_2$-flux through a plaquette p. Since there are N plaquettes with eigenvalues $B_p = \pm 1$ under the constraint

$$\prod_p B_p = 1, \tag{2.9}$$

we have only $2^N/2$ gauge invariant labels, which cannot label all the 2^{N+1} physical states.

Let us show explicitly the degeneracy, by showing at first that the gauge group operators G_i do not exhaust the set of commuting operators with the Hamiltonian. Define the non-local operators

$$V_1 = \prod_{\ell \in \gamma_1^*} X_\ell \quad , \quad V_2 = \prod_{\ell \in \gamma_2^*} X_\ell \tag{2.10}$$

$$W_1 = \prod_{\ell \in \gamma_1} Z_\ell \quad , \quad W_2 = \prod_{\ell \in \gamma_2} Z_\ell \tag{2.11}$$

with γ_a and γ_a^*, for $a = 1, 2$, closed paths along the i-axis of the torus defined on the lattice and the dual lattice, respectively (Figure 4). From their definition, follows from the Pauli operators algebra that

$$V_1 W_2 = -W_2 V_1, \quad V_2 W_1 = -W_1 V_2, \tag{2.12}$$

with all other commutators vanishing. The W_a operators are called Wegner-Wilson loop operators and they play an important role in our analysis because they are gauge invariant objects $[W_a, G_i] = 0$.

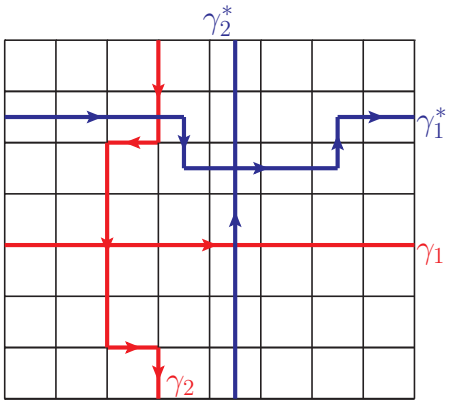

Figura 4 – Closed strings in the direct and dual lattice along both x_1 and x_2 directions.

When V_1 or V_2 act on the ground state $|0\rangle$, they flip every spin located at the links which cross these x_1 or x_2 lines. Since $[V_1, H] = [V_2, H] = 0$ the states

$$V_1 |0\rangle , \quad V_2 |0\rangle , \quad \text{and} \quad V_1 V_2 |0\rangle \tag{2.13}$$

are also eigenstates of $\mathcal{H}_{\mathbb{Z}_2}$ with energy E_0. One could ask if these three states are not simply gauge equivalent configurations to $|0\rangle$. They are not. Note that the ground state $|0\rangle$ obeys

$$W_1 |0\rangle = |0\rangle \quad \text{and} \quad W_2 |0\rangle = |0\rangle . \tag{2.14}$$

The eigenvalue of the W_a operators is a gauge invariant quantity, that is, there is no way to change it through gauge transformations. From the anti-commutation relation (2.12) follows that all other states in (2.13) have different gauge invariant eigenvalues. As an example:

$$W_2 V_1 |0\rangle = -V_1 W_2 |0\rangle = -V_1 |0\rangle \quad \text{and} \quad W_1 V_1 |0\rangle = V_1 W_1 |0\rangle = V_1 |0\rangle . \tag{2.15}$$

Similar analysis follows for the other two states. Thus, these are indeed four physical degenerate states. Now, the $2^N/2$ gauge invariant B_p and the four fold degeneracy are enough to characterize every$2^N/2 \times 4 = 2^{N+1}$ states.

At non-zero t, we can consider it as a perturbation. Albeit this term may break symmetries, it is not able to break the ground state degeneracy until the L-th order in perturbation theory. The perturbation term $\sim -tX_\ell$ acts on the link ℓ and flips its spin. In order to the perturbation lead a ground state (2.13) into another it must be able to invert a whole line of spins. If the linear size of the system is L, then it only happens at L-th order. In the thermodynamic limit $L \to \infty$ the energy splitting between the states (2.13) $\Delta E \sim g\,(t/g)^L$ vanishes. Actually, the four-fold degeneracy is robust against any local perturbation and is the most important feature of the $\mathbb{Z}_2$ gauge theory.

- $g \ll t$: This phase consists of a non-aligned phase. The eigenstates of the X_ℓ operator with positive eigenvalue is $|\Rightarrow_\ell\rangle$ and, for $g = 0$, the ground state of the system is simply $\prod_\ell \otimes |\Rightarrow_\ell\rangle$. It is not hard to see that the gauge structure is now trivial: every gauge transformation (2.2) maps any state in $\mathcal{H}$ into itself (modulo a global phase). Thus, trivially $\mathcal{H}_{phys} \cong \mathcal{H}$ and $\dim \mathcal{H}_{phys} = 2^{2N}$. We can successfully use the 2^{2N} eigenvalues of the operators X_ℓ to completely label the physical states.

  The energy of the ground state is $E_0 = -2Nt$ and the gap to the first excited state is $\Delta E \sim 2t$, which does not go to zero, for large t, even in the thermodynamic limit. In contrast to the topological phase, in this phase, the excitations can be individually created by a local application of the Z_ℓ operator and the ground state is no longer degenerate. We call this phase the trivial phase.

Thus, to summarize, in the $g \gg t$ phase, the ground state is degenerated and has $\mathbb{Z}_2$ visions as low-energy excitations. We call this phase the $\mathbb{Z}_2$ deconfined phase. In the $g \ll t$, the ground state is non-degenerated and the low-energy excitations are just qubits oriented against the field t. We call this phase the $\mathbb{Z}_2$ confined phase by the simply fact that the visions do not appear in the spectrum.

Effective Field Theory

Based on the work in Ref. [23] we are able to find an effective field theory which captures the phenomenology present in the $\mathbb{Z}_2$ lattice gauge model (2.1). In order to get a continuum theory, we embed the discrete $\mathbb{Z}_2$ gauge structure into a continuous $U(1)$ group. Let us introduce $U(1)$-compact gauge fields $A_{i,\alpha}$ situated at the link $\ell = (i, i + \hat{e}_\alpha)$ between the sites i and $i + \hat{e}_\alpha$ with $\alpha = 1, 2$. The discrete and continuum degrees of freedom are related by [23]

$$Z_{ix} \to \exp\left(i\eta_i A_{ix}\right) \quad \text{and} \quad Z_{iy} \to \exp\left(-i\eta_i A_{iy}\right), \quad \text{with} \quad \eta_i = (-1)^{i_x + i_y}. \tag{2.16}$$

In general, the effective $U(1)$ gauge theory presents distinct UV physical properties than the original $\mathbb{Z}_2$ model. We expect, however, that both theories describe the same physics not in all energy scales but only in the infrared limit. Based on this argument, a potential term $\sim -L\cos(2A_{i\alpha})$ is added in the Hamiltonian in an *ad hoc* way so that the configurations $A_{i\alpha} = 0, \pi$ are favored in the large L limit.

In order to replicate the Pauli operators anti-commutation algebra, we introduce conjugated "electric fields" $E_{i\alpha}$

$$[A_{i\alpha}, E_{j\beta}] = i\delta_{ij}\delta_{\alpha\beta}, \tag{2.17}$$

with the identification

$$X_{i\alpha} \to \exp\left(\pi i \eta_i E_{i\alpha}\right). \tag{2.18}$$

Since $A_{i\alpha}$ is a periodic variable, $E_{i\alpha}$ has integer eigenvalues.

The Hamiltonian, in terms of the $U(1)$ field is

$$\mathcal{H}_{U(1)} = -K\sum_{\square}\cos\left(\epsilon_{\alpha\beta}\Delta_\alpha A_{i\beta}\right) + h\sum_{i,\alpha}E_{i\alpha}^2 - L\sum_{i\alpha}\cos\left(2A_{i\alpha}\right), \tag{2.19}$$

where $\Delta_\alpha f_i \equiv f_{i+\hat{e}_\alpha} - f_i$. The first term in (2.19) follows from the plaquette terms and the second one were added to provide dynamics to the fields. It is worth to mention that the Gauss law is $\Delta_\alpha E_{i\alpha} = 0$ is compatible with our matter-free theory $G_i = +1$.

Although we have been referring to A as an $U(1)$ gauge field, the third term in (2.19) is not invariant under gauge transformations $A_{i,\alpha} \to A_{i,\alpha} + \Delta_\alpha f_i$. In order to ensure gauge invariance, we use the *Stueckelberg* trick, i.e., we promote the gauge parameter to a dynamical field which transforms appropriately under local transformations. It corresponds to introduce a matter field Θ_i, with the corresponding conjugated momenta $\hat{N}_i$, and to couple it to the gauge field

$$\begin{aligned}\mathcal{H}_{U(1)} &= -K\sum_{\square}\cos\left(\epsilon_{\alpha\beta}\Delta_\alpha A_{i\beta}\right) + h\sum_{i,\alpha}E_{i\alpha}^2 \\ &- L\sum_{i\alpha}\cos\left(\Delta_\alpha\Theta_i - 2A_{i\alpha}\right) + \widetilde{h}\sum_i \hat{N}_i^2,\end{aligned} \tag{2.20}$$

with $[\Theta_i, \hat{N}_j] = i\delta_{ij}$. In this fashion $\mathcal{H}_{U(1)}$ is invariant under gauge transformations $A_{i\alpha} \to A_{i\alpha} + \Delta_\alpha f_i, \Theta_i \to \Theta_i + 2f_i$. We see that The field $H_i \equiv \exp(i\Theta_i)$ possesses charge 2 under the gauge group $U(1)$.

We now take the continuum limit of the Hamiltonian (2.20), which describes gapped matter coupled to an $U(1)$ compact gauge field. The $U(1)$ group topology causes the proliferation of monopole instanton solutions throughout the system, making even the symmetric phase completely gapped [24]. In the continuum limit of (2.20), the monopoles degrees of freedom Φ are taken into account by an external Lagrangian $\mathcal{L}_{mon}(\Phi)$ so that the continuum Lagrangian is given by

$$\begin{aligned}&\mathcal{L}_{U(1)} = \mathcal{L}_H + \mathcal{L}_{\text{mon}}\,, \quad \text{with} \\ &\mathcal{L}_H = \left|\left(\partial_\mu - 2iA_\mu\right)H\right|^2 + g|H|^2 + u|H|^4 + K\left(\epsilon_{\mu\nu\lambda}\partial_\nu A_\lambda\right)^2,\end{aligned} \tag{2.21}$$

where the new parameters are functions of the old ones. The continuum gauge transformation of the fields, by its turn, reads $A_\mu \to A_\mu + \partial_\mu f$ and $H \to He^{i2f}$.

The two phases of (2.21) correspond to the two phases of (2.1), which can be accessed by tuning the g parameter below or above the critical value g_c. For $g > g_c$, in which $\langle H\rangle = 0$, the matter field H decouples and the monopoles proliferate $\langle\Phi\rangle \neq 0$, giving rise to a confining gapped phase. There is no topological order and it corresponds to the confining phase of (2.1).

For $g < g_c$, $\langle H\rangle \equiv H_0 \neq 0$ is responsible for the Higgs mechanism which gives the $U(1)$ gauge fields a mass. This is a deconfined phase, where the monopoles are not condensed $\langle\Phi\rangle = 0$. Although the amplitude degree of freedom H_0 is frozen, there are

nontrivial topological excitations associated with Higgs field phase. As H goes q times around a vortex it gains a phase of $2\pi q$ at the time that a gauge flux of

$$\int d^2x \ (\partial_1 A_2 - \partial_2 A_1) = \pi q \tag{2.22}$$

is trapped in the vortex core [25]. Such point-like defects have finite energy and correspond to the $\mathbb{Z}_2$ visions in the lattice model. Because of the presence of the monopoles source term the trapped flux is only defined modulo 2π implying that q is only defined *mod* 2, precisely as $\mathbb{Z}_2$ visions require.

Finally, we can argue that in the Higgs phase, the EFT for the $\mathbb{Z}_2$ lattice model is a BF theory. We note that the Higgs phase of (2.21) can be dualized to a topological theory. To see it, let us consider a Higgs field with charge p under the $U(1)$ gauge field a

$$D\tilde{\phi} = (\partial - ipa)\tilde{\phi}. \tag{2.23}$$

In the Higgs phase the radial mode of the field is frozen and we focus on the dynamics of the phase degree of freedom $\tilde{\phi} = me^{i\phi}$, dictated by

$$m^2(\partial_\mu \phi - pa_\mu)(\partial_\mu \phi - pa_\mu) + \frac{1}{4e^2} f_a^2. \tag{2.24}$$

In the strict low-energy limit $m \to \infty$ all local degrees of freedom are swept away since the a_μ field becomes pure gauge $a_\mu = \frac{1}{p}\partial_\mu \phi$. In fact, the low-energy physics is determined by global degrees of freedom which depends on the underlying manifold topology. In order to understand this point, we shall manipulate the Lagrangian to make it explicit. First, we dualize the scalar field ϕ to a new gauge field b

$$\partial_\mu \phi \equiv b_\mu. \tag{2.25}$$

The scalar-gauge duality is accompanied by the pure gauge constraint

$$\epsilon_{\mu\nu\rho}\partial_\nu b_\rho = 0, \tag{2.26}$$

which can be enforced through Lagrange multipliers c_μ. In this fashion, the Lagrangian (2.24) is equivalently written as

$$m^2(b_\mu - pa_\mu)(b_\mu - pa_\mu) + \frac{1}{2\pi}\epsilon_{\mu\nu\rho}c_\mu \partial_\nu b_\rho + \frac{1}{4e^2} f_a^2. \tag{2.27}$$

Now we shift the field $b_\mu \to b_\mu + pa_\mu$

$$m^2 b^2 + \frac{1}{2\pi}\epsilon_{\mu\nu\rho}c_\mu \partial_\nu b_\rho + \frac{p}{2\pi}\epsilon_{\mu\nu\rho}c_\mu \partial_\nu a_\rho + \frac{1}{4e^2} f_a^2, \tag{2.28}$$

and integrate it out

$$\frac{1}{2(4\pi)^2 m^2} f_c^2 + \frac{p}{2\pi}\epsilon_{\mu\nu\rho}c_\mu \partial_\nu a_\rho + \frac{1}{4e^2} f_a^2. \tag{2.29}$$

It is now explicit that, in the deep infrared $m, e^2 \to \infty$, the long-distance physics is dominated by BF topological field theory

$$\frac{p}{2\pi}\epsilon_{\mu\nu\rho}c_\mu\partial_\nu a_\rho. \tag{2.30}$$

Thus, we see that the EFT for the Higgs phase of the $\mathbb{Z}_2$ gauge lattice model corresponds to the BF theory with quantized level $p = 2$. For a generalized $\mathbb{Z}_N$ gauge lattice model, it would correspond to $p = N$. By the analysis in Section 1.1 we see that it correctly captures the N^2 ground state degeneracy of a generalized $\mathbb{Z}_N$ lattice gauge theory.

The usage of *ad hoc* arguments and the dual photon duality obscures the precise relation between the lattice and the BF continuum degrees of freedom. As an alternative, in the next section we propose to use a map, as in Ref. [18], to explicitly find the BF theory from the lattice in a more direct way.

2.2 Toric Code

In contrast to the $\mathbb{Z}_2$ gauge lattice model, which we could only solve for some regime in the space of parameters, the toric code is an exactly solvable model. Indeed, the toric code can be thought as the topological phase of the $\mathbb{Z}_2$ gauge model, with the addition of star interacting terms. As we will investigate, there are two kinds of excitations in this model, which carry nontrivial mutual statistics. Here we follow the discussion in [26] and [8].

The Toric Code is a two-dimensional model proposed by Kitaev [26], with a two-dimensional Hilbert space in each link of a square lattice given by the following Hamiltonian

$$H_{TC} = -J_e\sum_i A_i - J_m\sum_p B_p, \quad J_e, J_m > 0, \tag{2.31}$$

with the sum over plaquettes p and lattice vertices i. In the above expression, the star operator

$$A_i = \prod_{\ell\ltimes i} X_\ell, \tag{2.32}$$

is the product of the X Pauli operators on the four links ℓ connected to the site i. The plaquette operator

$$B_p = \prod_{\ell\in\partial p} Z_\ell, \tag{2.33}$$

is a product of the Z Pauli operator on the boundary ∂p of a plaquette p.

All the operators A_s and B_p commutes among themselves for every sites and plaquettes

$$[A_i, A_j] = [B_p, B_{p'}] = [A_i, B_p] = 0. \tag{2.34}$$

The two first commutators vanish since they involve only one "flavor" of Pauli operators (X for the star and Z for the plaquette operators) and they trivially commute among themselves. The last commutator vanishes trivially for the cases in which A_i and B_p do not share any link. For the case in which the site i relies on a corner of the plaquette p, they share two links and their commutation follows from the algebra:

$$\begin{aligned}
[A_i, B_p] &= X_1X_2Z_5Z_6[X_3X_4, Z_3Z_4] && (2.35)\\
&= X_1X_2Z_5Z_6\left(X_3Z_3\underbrace{\{X_4, Z_4\}}_{0} - \underbrace{\{X_3, Z_3\}}_{0}Z_4X_4\right) && (2.36)\\
&= 0, && (2.37)
\end{aligned}$$

with the links 3 and 4 being the two common shared links.

Since all the operators are compatible we can find the ground state exactly. The ground state is characterized by positive eigenvalues of A_i and B_p for every site and plaquette of the lattice. Let $\{s_\ell\}$ be the set of eigenvalues at the links ℓ in a given spin configuration and $B_p(s) = \prod_{\ell\in\partial p} s_\ell$ a measure of the plaquettes eigenvalues. If $B_p(s) = -1$, we say there is a vortex on the plaquette p in the spin configuration $\{s_\ell\}$.

Let $|\uparrow\uparrow\ldots\rangle = \prod_\ell \otimes |\uparrow\rangle_\ell$, with $Z_\ell |\uparrow\rangle_\ell = +1 |\uparrow\rangle_\ell$ and let

$$P_i \equiv \frac{(1 + A_i)}{2} \tag{2.38}$$

be the star projector in the lattice vertex i. Then, the ground state of this model is explicitly given by

$$|0\rangle = \prod_i P_i |\uparrow\uparrow\ldots\rangle . \tag{2.39}$$

This is, indeed, the ground state of the Hamiltonian since $A_i |0\rangle = |0\rangle$ and $B_p |0\rangle = |0\rangle$ for every vertex i and plaquette p, namely

$$\begin{aligned}
A_i |0\rangle = A_i \prod_j P_j |\uparrow\uparrow\ldots\rangle &= \underbrace{A_iP_i}_{P_i} \prod_{j\neq i} P_j |\uparrow\uparrow\ldots\rangle && (2.40)\\
&= \prod_j P_j |\uparrow\uparrow\ldots\rangle = |0\rangle \quad \forall i,
\end{aligned}$$

where we have used the fact that $A_iP_i = A_i (1 + A_i)/2 = (A_i + 1)/2 = P_i$. In addition,

$$\begin{aligned}
B_p |0\rangle &= B_p \prod_i P_i |\uparrow\uparrow\ldots\rangle\\
&= \prod_i P_i \underbrace{B_p |\uparrow\uparrow\ldots\rangle}_{+1|\uparrow\uparrow\ldots\rangle} = |0\rangle , \quad \forall p. && (2.41)
\end{aligned}$$

Since $X_\ell |\uparrow\rangle_\ell = |\downarrow\rangle_\ell$ and the star operator involves a product of X operators, the action of A_i on the product state $|\uparrow\uparrow\ldots\rangle$ is to flip the up spins of the four links connected

to the site i. The product of projector P_i on all the vertices i will flip spins in such way that (2.40) and (2.41) are satisfied. In order to have $B_p(s) = +1$ everywhere, there must be an even number of flipped spins connected to each lattice vertex i, which is geometrically achieved by flipped spins along closed loops. At the same time, in order to have $A_i(s) = +1$ everywhere, $|0\rangle$ must be a superposition of all such closed loop states. This is necessary since, at every measure of the star operator $A_i |0\rangle$, we flip all the spins connected to i (spins up goes to spins down and vice-versa) and because (2.40) we still need to recover the original state. This state is highly entangled and is an example of a string-net condensate [27].

In a loop configuration basis, we can write the ground state as a superposition of spin configurations $\{s\}$ such that it contains no vortices:

$$|0\rangle = \sum_{\{s:w_p(s)=1\forall\ p\}} c_s |s\rangle . \tag{2.42}$$

As previously argued, the application of the star operator A_i in this state maps a loop configuration $|s\rangle$ into another one, mapping the state $|0\rangle$ into itself, which tell us that all the c_s are of equal weight. If the lattice is defined in a plane, the previous discussions are enough to completely determine the ground state of the system. However, this does not hold if the system is defined in nontrivial topological spaces.

Let us impose periodic boundary conditions, or equivalently, define our lattice on a torus. There are more than one ground state. In fact, in a $g = 1$ genus topological space, the ground state is four-fold degenerate. We can vizualize this degeneracy through the introduction of the Wilson loop variables

$$w_\gamma(s) = \prod_{\ell\in\gamma} s_\ell, \quad \gamma = \gamma_1, \gamma_2, \tag{2.43}$$

with γ_1 and γ_2 two non-contractible loops wrapping the torus. As in the case of the $\mathbb{Z}_2$ gauge lattice model, the presence of these global excitations keep the energy of these states the same since they do not create local excitations $B_p = -1$ nor $A_s = -1$. In this way, we have four different ground states:

$$|0_{\omega_{\gamma_1}\omega_{\gamma_2}}\rangle = \sum_{\{s:B_p(s)=1\forall\ p\}} c_{\omega_{\gamma_1}\omega_{\gamma_2}} |s\rangle \tag{2.44}$$

Let us now study the excitations of this model. Excitations corresponding to the star operators that are characterized by $A_i(s) = -1$ in the vertex i and are pairwise created above the ground state at the endpoints i_1 and i_2 of the string operator

$$W_\gamma^{(e)} = \prod_{\ell\in\gamma} Z_\ell. \tag{2.45}$$

We call each $A_i(s) = -1$ excitation an "electric" particle e, which correspond to the state

$$|i_1, i_2\rangle = W_\gamma^{(e)} |0\rangle . \tag{2.46}$$

The energetic cost to create a single e particle is $2J_e$.

Analogously, we call the vortex excitations $B_p(s) = -1$ magnetic particles m. The energetic cost to create a single m particle above the ground state is $2J_m$ and they are created in the plaquette endpoints of the dual lattice string

$$W_{\gamma^*}^{(m)} = \prod_{\ell \in \gamma^*} X_\ell. \tag{2.47}$$

If the endpoints of γ^* are located at the plaquettes p_1 and p_2, the quantum state corresponding to the pair of m excitations created above the ground state is given by

$$|p_1, p_2\rangle = W_{\gamma^*}^{(m)} |0\rangle . \tag{2.48}$$

So far we know that the excitation spectrum corresponds to well localized excitations of the type e or m which carry $\mathbb{Z}_2$ charge. To fully characterize them, it is natural to ask about the particle statistics. Let us consider the braiding operator R_{ab} which exchanges the particles a and b. The Figures 5, 6, 7, 8 and 9 were borrowed from Ref. [28].

$R_{ab} =$ 

Figura 5 – The braiding operator.

$R_{ba} \cdot R_{ab} =$ 

Figura 6 – Two exchanges.

When the two particles are distinguishable, R_{ab} give us the sense of mutual statistics. Let us consider an initial state $|\psi_{init}\rangle$ which contains both an electric and a magnetic excitations. Let us move the e particle around the m particle around a closed loop $\mathcal{L}$

$$|\psi_{\text{fin}}\rangle = \prod_{\ell \in \mathcal{L}} Z_\ell \, |\psi_{\text{init}}\rangle . \tag{2.49}$$

Using the Stoke's theorem

$$\prod_{\ell \in \mathcal{L}} Z_\ell = \prod_{p \in \mathcal{A}} B_p, \tag{2.50}$$

with $\mathcal{A}$ being the area contained in $\mathcal{L} = \partial\mathcal{A}$. Then, since we have a m particle $B_p = -1$ inside $\mathcal{L}$

$$|\psi_{\text{fin}}\rangle = - \, |\psi_{\text{init}}\rangle , \tag{2.51}$$

which indicates us a nontrivial statistics. The process is graphically represented in Figure 7.

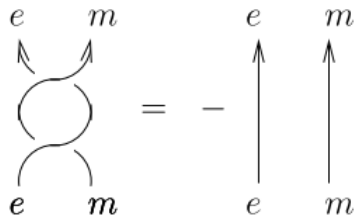

Figura 7 – Braiding of e and m particles.

Doing the same procedure, we find that the e and m particles are bosons (Figure 8).

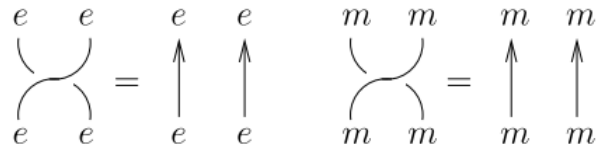

Figura 8 – The electric and magnetic excitations are bosons.

Not all the excitations in this model are bosons. The nontrivial mutual statistics allow us to construct, however, a composite particle which has nontrivial statistics. Consider the bound state $\epsilon = e \times m$. As it is graphically represented in Figure 9, the ϵ particle is a fermion.

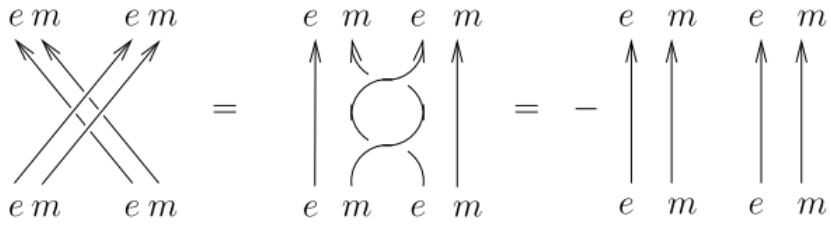

Figura 9 – The composite excitation ϵ is a fermion.

To summarize, the fusion rules of the toric code excitations are

$$e \times e = 1 \qquad e \times m = \epsilon \tag{2.52}$$

$$m \times m = 1 \qquad e \times \epsilon = m \tag{2.53}$$

$$\epsilon \times \epsilon = 1 \qquad m \times \epsilon = e. \tag{2.54}$$

The action of the Pauli operators on any one of the ground states is to create excited states, which are orthogonal to $|0\rangle$. In this fashion, we see that in fact the states

are not magnetically ordered

$$\langle 0|\, Z_\ell \,|0\rangle = 0 \quad \text{and} \quad \langle 0|\, X_\ell \,|0\rangle = 0. \tag{2.55}$$

Such property plays an important role in quantum spin liquids. If we allow perturbations on the original Hamiltonian (2.31)

$$H = H_{TC} - h_z \sum_\ell Z_\ell - h_x \sum_\ell X_\ell \tag{2.56}$$

we see that they have no crucial role in lifting the ground state degeneracy $\langle H\rangle = \langle H_{TC}\rangle - \langle h_z \sum_\ell Z_\ell + h_x \sum_\ell X_\ell\rangle = \langle H_{Tc}\rangle$. This is just a consequence of the robust topological character of the ground state degeneracy. In fact, for an $L \times L$ periodic square lattice, only perturbations in $L-$th order in h_z and h_x would be enough to connect two distinct ground states.

The ground state (2.42) is an example of a string-net condensate state. Such states with non-local excitations naturally leads to topological phases of matter [27]. In the section 4.1 we will see that the ground state of the X-Cube model, when constructed from two-dimensional Toric Code layers, corresponds to a condensate of strings. In such states, fermions and bosons may emerge in the system, associated to the endpoints of the strings. Wen proposed such mechanism as a way to unify bosons and fermions [4].

Generalization to the $\mathbb{Z}_N$ case

Generalization to the $\mathbb{Z}_N$ case is possible through the introduction of the $\mathbb{Z}_N$ Pauli operators (See Appendix A). As argued in [29], the $\mathbb{Z}_N$ Toric code can be thought as the $\mathbb{Z}_N$ lattice gauge model in the presence of charged matter. In this fashion, the Toric Code EFT is also given by a continuum BF topological theory. It is defined on a square lattice with the Hamiltonian given by

$$H_{TC} = -J_m \sum_p B_p - J_e \sum_i A_i + h.c., \quad J_e, J_m > 0 \tag{2.57}$$

with the sum on plaquettes p and lattice vertices i. In the above expression, the star and plaquette operators are written in terms of the $\mathbb{Z}_N$ Pauli operators

$$A_i = \prod_{\ell \ltimes i} X_\ell, \quad B_p = \prod_{\ell \in \partial p} Z_\ell. \tag{2.58}$$

The $\mathbb{Z}_N$ degrees of freedom located at the links have a sense of orientation, more specific, $X_{-\ell} = X_\ell^\dagger$ where $-\ell$ refers to the inverted orientation of the link ℓ. In 2.58 the star operators are defined so that all links point towards i and the plaquette operators are defined so that the links are oriented in the anti-clockwise orientation.

Analogously to the $N = 2$ case, in the $\mathbb{Z}_N$ Toric Code all operators commute so that the ground state for H_{TC} can be explicitly found. If the lattice is equipped with

periodic boundary conditions we find that the ground state is not unique, but is N^2-fold degenerated. It holds for any values of $J_e > 0$ and $J_m > 0$.

The system is completely gapped and excitations above the ground state are created at the endpoints of the open line operators

$$W(\gamma) = \prod_{\ell \in \gamma} Z_\ell \quad \text{and} \quad V(\gamma^*) = \prod_{\ell \cap \gamma^*} X_\ell, \tag{2.59}$$

where γ and γ^* are strings on the lattice dual lattice, respectively. The excitations created by $W(\gamma)$ are commonly called *electric* particles or charges (e particles) and the ones associated to $V(\gamma^*)$ are called *magnetic* particles or vortices (m-particles). Electric excitations are localized at site i and magnetic at plaquette p and correspond to eigenvalues of the operators $\tilde{A}_i \equiv A_i + A_i^\dagger$ and $\tilde{B}_p \equiv B_p + B_p^\dagger$,

$$\tilde{A}_i \left|\psi\right\rangle = 2\cos\left(2\pi/N\right)\left|\psi\right\rangle \quad \text{and} \quad \tilde{B}_p \left|\psi\right\rangle = 2\cos\left(2\pi/N\right)\left|\psi\right\rangle. \tag{2.60}$$

Such excitations have an energetic cost of $4J_{e/m}\cos\left(2\pi/N\right)$. Excitations with "charge" q and "vorticity" n, both quantities defined *mod* N, can be created at the endpoints of higher order string operators $W(\gamma)^q \left|0\right\rangle$ and $V(\gamma^*)^n \left|0\right\rangle$. In this fashion, $\tilde{A}_i \left|\psi\right\rangle = 2\cos(2\pi q/N)\left|\psi\right\rangle$ and $\tilde{B}_p \left|\psi\right\rangle = 2\cos(2\pi n/N)\left|\psi\right\rangle$. There are other operators that commute with the Hamiltonian and can be used to characterize excitations. In contrast to the operators $\tilde{A}_i$ and $\tilde{B}_p$, the Hermitian operators $\bar{A}_i = i\left(A_i - A_i^\dagger\right)$ and $\bar{B}_p$ (similarly defined) are able to distinct between excitations and anti-excitations. They obey

$$\bar{A}_i Z_\ell \left|0\right\rangle = a\ Z_\ell \left|0\right\rangle \quad \text{and} \quad \bar{A}_i Z_\ell^\dagger \left|0\right\rangle = -a\ Z_\ell^\dagger \left|0\right\rangle \tag{2.61}$$

with $a \equiv 2\sin\left(2\pi/N\right)$.

Although the elementary excitations e and m are bosons, they have nontrivial mutual statistics. When we move an electric excitation with charge q around a magnetic excitation with vorticity n, the wavefunction acquires a nontrivial phase

$$\left|\psi_f\right\rangle = \omega^{qn}\left|\psi_i\right\rangle. \tag{2.62}$$

For the case of the usual toric code model, $N = 2$, this gives $(-1)^{qn}$, showing that the composite excitation with $q = n = 1$ is a fermion.

The Toric code is invariant under both time-reversal $\mathcal{T}$ (see Appendix A)

$$\mathcal{T} : X \mapsto \omega^* X \quad \text{and} \quad \mathcal{T} : Z \mapsto \omega^* Z^\dagger \tag{2.63}$$

and charge conjugation

$$\mathcal{C} : X \mapsto X^\dagger \quad \text{and} \quad \mathcal{C} : Z \mapsto Z^\dagger. \tag{2.64}$$

The $\mathcal{C}$ transformation is a charge conjugation operation in the sense that it maps the $\mathbb{Z}_N$ Toric code e and m excitations into their $\mathbb{Z}_N$ antiparticles. The action $\mathcal{C} : W(\gamma) \mapsto W(\gamma)^\dagger = W(-\gamma)$ and $\mathcal{C} : V(\gamma^*) \mapsto V(\gamma^*)^\dagger = V(-\gamma^*)$ has precisely the effect of exchanging particles and anti-particles (and vortices and anti-vortices) $a \leftrightarrow -a$.

Effective Field Theory

Now we shall derive the low-energy effective field theory for the $\mathbb{Z}_N$ toric code model by following the method developed in [18]. The basic idea is to represent the spin operators in terms of fields that are well-defined in the continuum limit, namely,

$$X_\ell \equiv \exp\left(it^{(1)} K A\left(\ell\right)\right) \tag{2.65}$$

and

$$Z_\ell \equiv \exp\left(it^{(2)} K A\left(\ell\right)\right). \tag{2.66}$$

In this representation, K is a 2×2 anti-symmetric matrix

$$K = \begin{pmatrix} 0 & k \\ -k & 0 \end{pmatrix} \quad \text{and} \quad K^{-1} = \begin{pmatrix} 0 & -\frac{1}{k} \\ \frac{1}{k} & 0 \end{pmatrix}, \tag{2.67}$$

where the precise value of k will be fixed by demanding that these operators satisfies the $\mathbb{Z}_N$ algebra (A.1). The vectors t's are chosen as

$$t^{(1)} = (1,0) \quad \text{and} \quad t^{(2)} = (0,1) \tag{2.68}$$

and $A(\ell)$ corresponds to the column vector

$$A(\ell) = \begin{pmatrix} A_1(\ell) \\ A_2(\ell) \end{pmatrix}, \tag{2.69}$$

with the components satisfying the nontrivial commutation relation

$$[A_a(l), A_b(l')] \equiv -2\pi i (K^{-1})_{ab} \delta_{l,l'}. \tag{2.70}$$

By writing explicitly the operators (2.65) and (2.66),

$$X_\ell = \exp\left(ikA_2(\ell)\right) \quad \text{and} \quad Z_\ell = \exp\left(-ikA_1(\ell)\right), \tag{2.71}$$

we see that in order to reproduce the $\mathbb{Z}_N$ algebra (A.1), we set

$$k \equiv \frac{1}{N}. \tag{2.72}$$

Now we are ready to derive the low-energy effective field theory. Let us specify a link as $\ell \equiv (i, \alpha)$, i.e., with its origin at the site i and with α indicating the corresponding direction and orientation, $\alpha = \pm 1, \pm 2$. In this way, it is convenient to encode the information of different directions in terms of independent fields, namely,

$$\begin{aligned} A_1\left(i,1\right) \quad &\Leftrightarrow \quad b_1\left(i + \frac{\hat{e}_1}{2}\right), \\ A_1\left(i,2\right) \quad &\Leftrightarrow \quad b_2\left(i + \frac{\hat{e}_2}{2}\right), \\ A_2\left(i,1\right) \quad &\Leftrightarrow \quad a_2\left(i + \frac{\hat{e}_1}{2}\right), \\ A_2\left(i,2\right) \quad &\Leftrightarrow \quad -a_1\left(i + \frac{\hat{e}_2}{2}\right). \end{aligned} \tag{2.73}$$

The new fields a_i and b_i are located at the links. In terms of these fields, the commutation relation (2.70) splits in

$$\left[a_1(i+\frac{\hat{e}_2}{2}), b_2(j+\frac{\hat{e}_2}{2})\right] = 2\pi i N \delta_{ij} \tag{2.74}$$

and

$$\left[a_2(i+\frac{\hat{e}_1}{2}), b_1(j+\frac{\hat{e}_1}{2})\right] = -2\pi i N \delta_{ij}. \tag{2.75}$$

According to the identifications in (2.73), the star and plaquette operators read

$$A_i = \exp\left[i\frac{1}{N}\left(a_2(i+\frac{\hat{e}_1}{2}) - a_2(i-\frac{\hat{e}_1}{2}) - a_1(i+\frac{\hat{e}_2}{2}) + a_1(i-\frac{\hat{e}_2}{2})\right)\right] \tag{2.76}$$

and

$$B_p = \exp\left[-i\frac{1}{N}\left(b_1(i+\frac{\hat{e}_1}{2}) + b_2(i+\hat{e}_1+\frac{\hat{e}_2}{2}) - b_1(i+\frac{\hat{e}_1}{2}+\hat{e}_2) - b_2(i+\frac{\hat{e}_2}{2})\right)\right]. \tag{2.77}$$

In the continuum limit, they reduce to

$$A_i \sim \exp\left[i\frac{1}{N}\left(\partial_1 a_2 - \partial_2 a_1\right)\right] \tag{2.78}$$

and

$$B_p \sim \exp\left[-i\frac{1}{N}\left(\partial_1 b_2 - \partial_2 b_1\right)\right]. \tag{2.79}$$

Consequently, the continuum limit of the Hamiltonian (2.57) is

$$H \sim -J_e \int d^2x \cos\left[\frac{1}{N}\left(\partial_1 a_2 - \partial_2 a_1\right)\right] - J_m \int d^2x \cos\left[\frac{1}{N}\left(\partial_1 b_2 - \partial_2 b_1\right)\right]. \tag{2.80}$$

Now it is immediate to construct an effective action describing its low-energy properties. The ground state corresponds to the case where all the cosines are maximized. This can be implemented in the action through Lagrange multipliers. We can write the effective action describing the low-energy properties of the toric code as

$$S_{eff} = -\int dt d^2x \frac{1}{2\pi N}\left[b_1\partial_0 a_2 - b_2\partial_0 a_1 - b_0\left(\partial_1 a_2 - \partial_2 a_1\right) - a_0\left(\partial_1 b_2 - \partial_2 b_1\right)\right]. \tag{2.81}$$

The first two terms of this action imply the commutation relations (2.74) and (2.75), whereas the remaining ones correspond to the ground state constraints, implemented via the Lagrange multipliers a_0 and b_0. The theory (2.81) is nothing else but the BF action

$$S = \int_{T^2\times\mathbb{R}} d^3x \frac{1}{2\pi N}\epsilon^{\mu\nu\rho} a_\mu \partial_\nu b_\rho. \tag{2.82}$$

We can bring this to a more conventional normalization by rescaling the fields $a_\mu \to N a_\mu$ and $b_\mu \to N b_\mu$. With this, the action becomes

$$S = \int_{T^2\times\mathbb{R}} d^3x \frac{N}{2\pi}\epsilon^{\mu\nu\rho} a_\mu \partial_\nu b_\rho, \tag{2.83}$$

together with the commutation relations properly rescaled,

$$\Big[a_1(\vec{x}), b_2(\vec{x}')\Big] = \frac{2\pi i}{N}\delta(\vec{x}-\vec{x}') \tag{2.84}$$

and

$$\Big[a_2(\vec{x}), b_1(\vec{x}')\Big] = -\frac{2\pi i}{N}\delta(\vec{x}-\vec{x}'). \tag{2.85}$$

This leads correctly to a N^2-fold ground state degeneracy.

Let us examine how the discrete symmetries $\mathcal{T}$ and $\mathcal{C}$ act on the fields of the continuum theory. This can be extracted from the corresponding transformations of the spin operators, translating them to the fields according to (2.71). Under time-reversal $\mathcal{T}$, the fields transform as

$$\begin{aligned} a_0 \to a_0' &= -a_0 & b_0 \to b_0' &= b_0 \\ a_1 \to a_1' &= a_1 - \frac{2\pi}{l} & b_1 \to b_1' &= -b_1 + \frac{2\pi}{l} \\ a_2 \to a_2' &= a_2 - \frac{2\pi}{l} & b_2 \to b_2' &= -b_2 + \frac{2\pi}{l}, \end{aligned} \tag{2.86}$$

where l is the lattice spacing. Under charge conjugation $\mathcal{C}$, the fields transform as

$$\begin{aligned} a_0 &\to -a_0 & b_0 &\to -b_0 \\ a_i &\to -a_i & b_i &\to -b_i. \end{aligned} \tag{2.87}$$

It is immediate to check that these transformations leave the action (2.83) invariant. It is also interesting to consider the theory coupled with external currents. Coming from the lattice, there is a clear identification of particle and vortex currents. The fields a are associated with the star operator (2.78) and then can be coupled with a particle current j^a. On the other hand, the fields b are associated with the plaquette operator (2.79) and a can be coupled with a vortex current j^b. The gauge invariant coupling $\int a\cdot j^a + b\cdot j^b$ imply the following transformations of the currents

$$\mathcal{T}: \begin{cases} (j_0^a, j_i^a) \mapsto (-j_0^a, j_i^a), \\ (j_0^b, j_i^b) \mapsto (j_0^b, -j_i^b), \end{cases} \quad \text{and} \quad \mathcal{C}: \begin{cases} (j_0^a, j_i^a) \mapsto (-j_0^a, -j_i^a), \\ (j_0^b, j_i^b) \mapsto (-j_0^b, -j_i^b), \end{cases} \tag{2.88}$$

which are the expected transformations for particle and vortex currents [30].

We shall see now how the line operators of the continuum theory follow immediately from the map (2.71). Consider the closed Wilson lines of electric type

$$W(\gamma) \equiv \prod_{\ell\in\gamma} Z_\ell, \quad \gamma = \gamma_1, \gamma_2, \tag{2.89}$$

where γ_1 and γ_2 are lines that wrap around the torus in the directions x_1 and x_2. Mapping them into their continuum version we have that, in the x_1 direction

$$\begin{aligned} W(\gamma_1) &= \exp\left(-\sum_{i\in\gamma_1} iA_1(i+\frac{\hat{e}_1}{2})\right) = \exp\left(-i\sum_{\ell\in\gamma_1} b_1(\ell)\right) \\ &\sim \exp\left(-i\int_{\vec{x}}^{\vec{x}+N_1\hat{e}_1} dx_1 b_1(x)\right) = \exp\left(-i\oint_{\gamma_1} dx_1 b_1(x)\right), \end{aligned} \tag{2.90}$$

where we have used that there are N_1 sites in the x_1 direction and $\vec{x} \sim \vec{x} + N_1\hat{e}_1$ are the same geometrical point. In the same way, for the curve γ_2, we obtain

$$W(\gamma_2) = \exp\left(-i \oint_{\gamma_2} dx_2 b_2(x)\right). \tag{2.91}$$

Proceeding similarly for the magnetic operator, it follows that

$$V(\gamma^*) = \exp\left(-i \oint_{\gamma} dx_i a_i\right). \tag{2.92}$$

The algebra

$$V(\gamma_1^*)W(\gamma_2) = e^{\frac{2\pi i}{N}} W(\gamma_2)V(\gamma_1^*), \quad V(\gamma_2^*)W(\gamma_1) = e^{\frac{2\pi i}{N}} W(\gamma_1)V(\gamma_2^*), \tag{2.93}$$

following from (2.74) and (2.75) ensures the N^2-fold ground state degeneracy, as discussed in the Chapter 1.

One further check we can do in the EFT is to study the mutual statistics of excitations. In the presence of vortex with vorticity n located at $\vec{x}_0$, $j_0^b = n\delta^{(2)}(\vec{x} - \vec{x}_0)$, the flux constraint associated with b_0 is

$$\frac{N}{2\pi}\epsilon^{ij}\partial_i a_j = n\delta^{(2)}(\vec{x} - \vec{x}_0). \tag{2.94}$$

In this way, as we move a q-charged electric excitation around a closed path C that includes $\vec{x}_0$, the wavefunction acquires an Aharonov-Bhom phase

$$\exp\left\{iq \oint_{\partial R} a_i dx^i\right\} = \exp iq \int_R \epsilon^{ij}\partial_i a_j dx_1 dx_2 = \exp\left(\frac{2\pi i q n}{N}\right) = \omega^{qn}. \tag{2.95}$$

This result is precisely the mutual statistics we have found in (2.62).

2.3 Wen Plaquette Model

We study now the $\mathbb{Z}_N$ version of the Wen plaquette (WP) model [31]. It is defined on a two-dimensional periodic square lattice with $\mathbb{Z}_N$ degrees of freedom lying on the sites, with the Hamiltonian written in terms of commuting projectors. Hence, we can proceed similarly to the previous case in order to derive the low-energy effective theory. The Hamiltonian reads

$$H_{WP} = -\frac{1}{2}\sum_i g_i \left(\hat{F}_i + \hat{F}_i^\dagger\right), \tag{2.96}$$

where

$$\hat{F}_i \equiv X_i Z_{i+\hat{e}_1} X^\dagger_{i+\hat{e}_1+\hat{e}_2} Z^\dagger_{i+\hat{e}_2} \tag{2.97}$$

and all $g_i > 0$. This model is also exactly solvable due to the simultaneously commutation of all the plaquette operators (commuting projectors),

$$[\hat{F}_i, \hat{F}_j] = 0 \quad \text{and} \quad [\hat{F}_i, \hat{F}_j^\dagger] = 0, \tag{2.98}$$

which lead to a gapped topologically ordered system. As the low-energy physics depends whether the number of sites of the lattice along each direction is even or odd, we shall study the three cases separately.

2.3.1 Even × Even Lattice

Let us firstly consider an even by even lattice, where all the sites have a well defined parity. We divide the plaquette operators in the Hamiltonian in odd and even sites

$$H_{WP} = -\frac{1}{2}\left(g_1 \sum_{i\in\Lambda_{even}} \hat{F}_i + g_2 \sum_{i\in\Lambda_{odd}} \hat{F}_i\right) + h.\,c., \tag{2.99}$$

where i belongs to the even sub-lattice Λ_{even} if $i_x + i_y$ is even and to the odd sub-lattice Λ_{odd} if $i_x + i_y$ is odd. We also refer to the plaquette operators $\hat{F}_i$ themselves as even or odd according to the parity of the corresponding site i. Similarly, we call a given plaquette even (even) if its inferior leftmost site is even (odd), as shown in Figure 10.

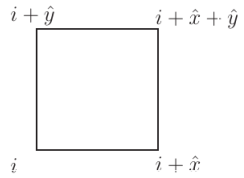

Figura 10 – We call a given plaquette even if $i \in \Lambda_{even}$ and odd if $i \in \Lambda_{odd}$.

For the $N \neq 2$ the Hamiltonians (2.96) and (2.99) are not invariant under time-reversal as defined in the Toric code model (2.63). The plaquette operators transform as $\mathcal{T} : \hat{F}_i \to \hat{F}'_i = X_i Z^\dagger_{i+e_1} X^\dagger_{i+e_1+e_2} Z_{i+e_2}$, and then cannot be mapped into $\hat{F}_i$ nor $\hat{F}^\dagger_i$. However, as discussed in [32], in the case of an even × even square lattice, the $\mathbb{Z}_N$ WP model is remarkably equivalent to the Toric code. This means that the time-reversal symmetry of the Toric code must corresponds to a different discrete symmetry in the WP model. Indeed, in addition to the charge conjugation defined in (2.64), the Hamiltonian (2.99) is also invariant under

$$\mathcal{T}' : \begin{cases} X \mapsto \omega^* X \ \text{ and } \ Z \mapsto \omega^* Z, & \text{for } X \text{ and } Z \text{ belonging to even plaquettes,} \\ X \mapsto \omega^* X^\dagger \ \text{ and } \ Z \mapsto \omega^* Z^\dagger, & \text{for } X \text{ and } Z \text{ belonging to odd plaquettes.} \end{cases} \tag{2.100}$$

The $\mathcal{T}'$ symmetry can be thought as a charge conjugation operation, but only for one type of excitations (the odd plaquettes). We will see that it is precisely the Toric code $\mathcal{T}$ symmetry analogue.

On an even × even lattice, the WP model contains two types of non-contractible string operators that play the same role as $W(\gamma)$ and $V(\gamma^*)$ in the Toric code. Let the

paths γ and γ^* lie on the even and odd plaquettes, respectively. We define the Wilson operators on even plaquettes (Figure 11)

$$W(\gamma) = \prod_{i\in\gamma} P_i, \quad \text{with} \quad P_i = \begin{cases} Z_i, \ i \in \Lambda_{even}, \\ X_i, \ i \in \Lambda_{odd}, \end{cases} \tag{2.101}$$

and, in a similar way, the 't Hooft loop operators on odd plaquettes (Figure 12)

$$V(\gamma^*) = \prod_{i\in\gamma^*} P_i, \quad \text{with} \quad P_i = \begin{cases} X_i, \ i \in \Lambda_{even}, \\ Z_i, \ i \in \Lambda_{odd}. \end{cases} \tag{2.102}$$

Let $\eta_i = i_x + i_y$ the parity of the site i in which the corresponding two line operators

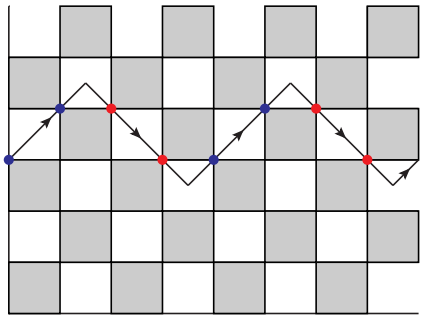

Figura 11 – Wilson line operators crossing the system in the horizontal direction on the even (white) plaquettes. It is an alternating product of Z (blue dots) or X (red dots) depending if the site is even or odd.

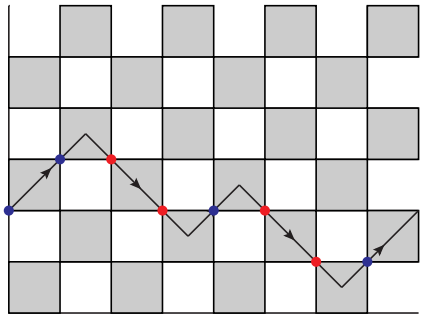

Figura 12 – t'Hooft line operators crossing the system in the horizontal direction on the odd (black) plaquettes. It is an alternating product of Z (blue dots) or X (red dots) depending if the site is odd or even.

intersect. They satisfy

$$W(\gamma_x)V(\gamma_y^*) = e^{\frac{2\pi i}{N}(-)^{\eta_i}} V(\gamma_y^*)W(\gamma_x) \quad \text{and} \quad W(\gamma_y)V(\gamma_x^*) = e^{\frac{2\pi i}{N}(-)^{\eta_i}} V(\gamma_x^*)W(\gamma_y), \tag{2.103}$$

which leads to a N^2-fold ground state degeneracy. Excitations created above the ground state are described by open line operators. The excitations, corresponding to even and odd plaquettes, are created at the endpoints of W and V strings and are analogous to the

electric and magnetic particles of the Toric code, respectively. In order to find the EFT for the even × even WP model, we map the even and odd degrees of freedom into fields A and B as

$$\begin{aligned} X = e^{iA_1} \quad &\text{and} \quad Z = e^{-iA_2} \quad \text{for even plaquettes,} \\ X = e^{iB_1} \quad &\text{and} \quad Z = e^{-iB_2} \quad \text{for odd plaquettes.} \end{aligned} \tag{2.104}$$

These are precisely the maps (2.71) up to a rescaling of the fields by a factor of N.

Nontrivial commutation rules occur only between even and odd plaquette operators. This is translated in nontrivial commutation relation between A and B fields

$$[A_a(\vec{x}), B_b(\vec{y})] = \epsilon_{ab}\frac{2i\pi}{N}\delta_{\vec{x},\vec{y}}. \tag{2.105}$$

In terms of the fields (2.104), the even plaquette operators are represented as

$$\hat{F}_{i\in\Lambda_{even}} = \exp i\left[A_2\left(i\right) - A_1\left(i+\hat{e}_1\right) - A_2\left(i+\hat{e}_1+\hat{e}_2\right) + A_1\left(i+\hat{e}_2\right)\right] \tag{2.106}$$

and the odd plaquette operators as

$$\hat{F}_{i\in\Lambda_{odd}} = \exp i\left[B_2\left(i\right) - B_1\left(i+\hat{e}_1\right) - B_2\left(i+\hat{e}_1+\hat{e}_2\right) + B_1\left(i+\hat{e}_2\right)\right]. \tag{2.107}$$

In the continuum limit, they become

$$\begin{aligned} \hat{F}_{i\in\Lambda_{even}} &\sim \exp i\left[-\partial_1 A_2 - \partial_2 A_2 - \partial_1 A_1 + \partial_2 A_1\right] \\ &\sim \exp i\sqrt{2}\left[\partial_{l_1} A_2 - \partial_{l_2} A_1\right] \end{aligned} \tag{2.108}$$

and

$$\begin{aligned} F_{i\in\Lambda_{odd}} &\sim \exp i\sqrt{2}\left[-\partial_1 B_1 - \partial_1 B_2 - \partial_2 B_2 + \partial_2 B1\right] \\ &\sim \exp i\sqrt{2}\left[\partial_{l_1} B_2 - \partial_{l_2} B_1\right], \end{aligned} \tag{2.109}$$

where we have defined the new coordinates $\partial_{l_1} \equiv \left(-\partial_1 - \partial_2\right)/\sqrt{2}$ and $\partial_{l_2} \equiv \left(\partial_1 - \partial_2\right)/\sqrt{2}$. The Hamiltonian becomes

$$H \sim -g_1 \int d^2l \cos\left[\sqrt{2}(\partial_{l_1} A_2 - \partial_{l_2} A_1)\right] - g_2 \int d^2l \cos\left[\sqrt{2}(\partial_{l_1} B_2 - \partial_{l_2} B_1)\right]. \tag{2.110}$$

To obtain the low-energy effective action, we can proceed precisely in the same way as we did in the previous section with the Toric code. We construct an action that reproduces the commutation relations (2.105) as well as the ground state constraints,

$$S = \int dt d^2l \frac{N}{2\pi}\left[-B_1\partial_0 A_2 + B_2\partial_0 A_1 - B_0\left(\partial_{l_1} A_2 - \partial_{l_2} A_1\right) - A_0\left(\partial_{l_1} B_2 - \partial_{l_2} B_1\right)\right] \tag{2.111}$$

where A_0 and B_0 are the Lagrange multipliers corresponding to the maximization of the cosines in (2.110) (we have absorbed numerical factors in A_0 and B_0). This action can be compactly written as

$$S = \frac{N}{2\pi}\int d^2l dt\ \epsilon^{\mu\nu\rho} A_\mu \partial_\nu B_\rho, \tag{2.112}$$

where $\partial_1 \equiv \partial_{l_1}$ and $\partial_2 \equiv \partial_{l_2}$, which is nothing else a $\mathbb{Z}_N$ BF topological field theory.

In the continuum limit the Wilson line operators become

$$W(\gamma) \sim \exp\left(-i \oint_{\gamma} A_i dl^i\right), \tag{2.113}$$

and similarly, the 't Hooft lines

$$V(\gamma^*) \sim \exp\left(-i \oint_{\gamma^*} B_i dl^i\right). \tag{2.114}$$

They are exactly the loop operators (1.13) of the BF theory.

Under charge conjugation, $\mathcal{C} : A_i \mapsto -A_1$ and $\mathcal{C} : B_i \mapsto -B_1$. The BF action is invariant under the $\mathcal{C}$ ensured that

$$\mathcal{C} : A_0 \mapsto -A_0 \quad \text{and} \quad \mathcal{C} : B_0 \mapsto -B_0. \tag{2.115}$$

In addition, $\mathcal{T}' : (A_1, A_2, B_1, B_2) \mapsto (A_1, A_2, -B_1, -B_2)$ is a symmetry, ensured that $\mathcal{T}' : (A_0, B_0, t) \mapsto (-A_0, B_0, -t)$, which is precisely the Toric code time-reversal transformation (2.86).

As mentioned previously, the WP model defined on an even $\times$ even lattice is completely equivalent to the Toric Code [32]. As a reflection of this, we have obtained the same low-energy effective theory for both models. The WP model can be mapped into the TC by mapping the clock and shift $\mathbb{Z}_N$ operators into one another, depending whether they belong to even or odd plaquettes. For even plaquettes, we map $X_i \to X_i$ and $Z_i \to X_i$. For odd plaquettes, $Z_i \to Z_i$ and $X \to Z^\dagger$. Then, schematically

$$F_i \text{ with } i \in \Lambda_{even} \leftrightarrow A_s, \quad \text{and} \quad F_i \text{ with } i \in \Lambda_{odd} \leftrightarrow B_p. \tag{2.116}$$

Through this map we see that the WP model is a $\frac{\pi}{4}$-rotated Toric Code, where the sites of the original lattice correspond to the links of the new (Toric code) lattice, as depicted in Figure 13. In this way, the $\mathcal{T}'$ symmetry of the even by even WP model is explicitly mapped into the $\mathcal{T}$ symmetry of the Toric code. The equivalence between both models, however, no longer holds in the case that the WP model is defined on an even $\times$ odd lattice.

2.3.2 Even $\times$ Odd Lattice

The low-energy physical properties of the Wen plaquette model is very sensitive to the microscopic details of the lattice. In fact, as discussed in [33], if it is defined on an even $\times$ odd lattice it exhibits a different spectrum compared to the previous case (even $\times$ even) and the ground state is N-fold degenerate. Due to the periodic boundary conditions, if there is an odd number of sites in the y direction, for example, the parity of the sites is

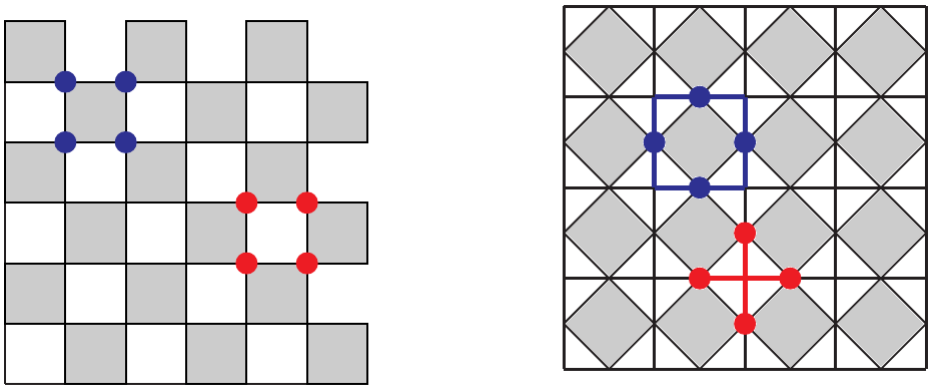

Figura 13 – Map between the operators of Wen Plaquette model and the Toric Code.

not well-defined in such direction. In this case, it is not possible to split the Hamiltonian into two sub-lattices as in (2.99). With no loss of generality, we set $g_i = g$ and write the Hamiltonian (2.96)

$$H = -\frac{g}{2}\sum_i \left(\hat{F}_i + h.c.\right). \tag{2.117}$$

Let N_x and N_y be the number of sites along directions x and y, respectively, with N_x even and N_y odd. As we can no longer distinguish among odd and even plaquettes in the y direction, we cannot distinguish between "electric" and "magnetic" excitations. Therefore, we generically denote them as p-particles. In this case, there are only two independent holonomies which commute with the Hamiltonian

$$W(\gamma_x) = \prod_{\gamma_x} P_i \quad \text{and} \quad W(\gamma_y) = \prod_{\gamma_y} X_i Z_i^\dagger. \tag{2.118}$$

They satisfy

$$W(\gamma_y)W(\gamma_x) = e^{\frac{2\pi i}{N}} W(\gamma_x)W(\gamma_y). \tag{2.119}$$

In the above relations, $W(\gamma_x)$ corresponds to the motion of a p-particle throughout the system around the x direction, whereas $W(\gamma_y)$ represents the motion of a pair of p-particles around the y direction. The Figure 14 shows both non-contractible operators. Since both $W(\gamma_x)$ and $W(\gamma_y)$ commute with the Hamiltonian, the algebra (2.119) implies a N-fold degeneracy of the ground state.

In contrast to the even $\times$ even case, there is no consistent way to introduce two species of fields A and B. Therefore, we are forced to map all the plaquette operators into a single field species A_a:

$$X_i \equiv \exp iA_2(i) \quad \text{and} \quad Z_i \equiv \exp -iA_1(i), \tag{2.120}$$

with the following commutation rule

$$[A_a(\vec{x}), A_b(\vec{y})] = \epsilon_{ab}\frac{2\pi i}{N}\delta_{\vec{x}\vec{y}}. \tag{2.121}$$

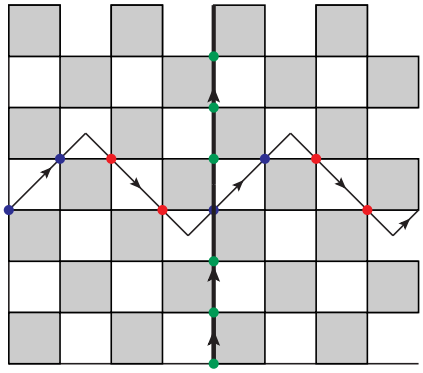

Figura 14 – Line operators around the system. Application of alternating product X (red) and Z (blue) along the x direction and application of $XZ^\dagger$ (green) operators in the vertical direction.

Now we can proceed as in the previous case, i.e., we consider the Hamiltonian in the continuum limit and then construct an action for field configurations that minimize the energy and that reproduces the commutation rule (2.121). This leads to the continuum Chern-Simons EFT

$$S = \frac{N}{4\pi}\int d^2l dt\ \epsilon^{\mu\nu\lambda} A_\mu \partial_{l_\nu} A_\lambda. \tag{2.122}$$

The CS action does capture the low-energy properties of the even $\times$ odd WP model. Through the map (2.120), one can check that the two lattice holonomies, satisfying (2.119), are mapped into the continuum line operators

$$W(\gamma_i) \quad \sim \quad \exp\left\{-i \oint_{\gamma_i} A_i dl^i\right\}. \tag{2.123}$$

Since the sites of the lattice no longer have a well-defined parity in this case, the $\mathcal{T}'$ transformation (2.100) has no a precise meaning. Only the discrete charge conjugation transformation $\mathcal{C}$ remains a symmetry. It can be checked that both the lattice Hamiltonian (2.117) and the continuum action (2.122) are invariant under it. For the case $N = 2$, the Wen Plaquette model is invariant under the discrete transformation (2.63)

$$\mathcal{T} : X \mapsto -X \quad \text{and} \quad \mathcal{T} : Z \mapsto -Z. \tag{2.124}$$

This is nothing else but the usual time-reversal transformations of $\frac{1}{2}$-spin operators, under which the fields transform as

$$\mathcal{T} : A_0 \mapsto -A_0 \quad \text{and} \quad \mathcal{T} : A_a \mapsto A_a - \frac{\pi}{l}. \tag{2.125}$$

Up to total derivative terms, the CS action acquires a global minus signal under $\mathcal{T}$: $S_{CS} \mapsto -S_{CS}$. We note that the EFT is time-reversal symmetric if both levels $N = 2$ and $N = -2$ are identified, i.e., if we consider only the observables that are not sensitive

to the sign of the level. This is also in compliance with the fact that the Pauli algebra $XZ = -ZX$ is reproduced in terms of the fields independent of the sign of the level,

$$[A_1, A_2] = \pm\pi i, \tag{2.126}$$

which naturally leads us to identify the Chern-Simons levels $N = 2$ and $N = -2$.

2.3.3 Odd × Odd Lattice

As a generalization of the even × odd lattice case, we can define the line operator $W_f = \prod_i X_i Z_i^\dagger$ along vertical and horizontal oriented curves γ_1 and γ_2. We can also define line operators W_v along diagonal directions γ_{d_i}, which cross the whole system until they close to itself, without bending, as illustrated in Figure 15. They read [34]

$$W_v = \prod_i P_i, \quad \text{with} \quad P_i = \begin{cases} X_i, \ i \in \gamma_{d1}, \\ Z_i, \ i \in \gamma_{d2}, \end{cases} \tag{2.127}$$

with γ_{d1} and γ_{d2} the principal and secondary diagonal directions, respectively. The Figure 15 represents the principal and secondary diagonals as well as the loops γ_i along the $i = 1$ and 2 directions in a square lattice.

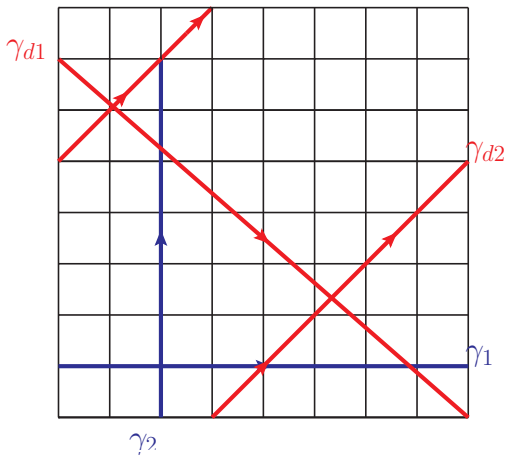

Figura 15 – Line operators on the square lattice. The W_f operators are defined on γ_a (blue) curves while W_v are defined on the γ_{d_b} (red) curves. The curves γ_{d_1} and γ_{d_2} are referred to as the principal and secondary diagonals, respectively.

How many times W_v crosses W_f depends on the lattice size. In fact, for arbitrary odd linear lattice sizes N_1 and N_2, the line operators $W_v(\gamma_{d_b})$ cross $W_f(\gamma_a)$ a number $\rho_a \equiv \text{lcm}(N_1, N_2)/N_a$ of times, with $\text{lcm}(p, q)$ standing for the least common multiple between p and q. In this way, the square lattice with $N_1 = N_2$ shown in Figure 15 is the simplest case in which the line operators cross only once $\rho^a = 1$, for $a = 1, 2$. In contrast, for the case in which N_1 and N_2 share no common factor in their prime decomposition $\text{lcm}(N_1, N_2) = N_1 \times N_2$, we have $\rho_1 = N_2$ and $\rho_2 = N_1$, i.e., they assume their greatest possible values.

The nontrivial algebra between line operators reads

$$W_f(\gamma_a)W_v(\gamma_{d_b}) = e^{\frac{2\pi i\rho_a}{N}}W_v(\gamma_{d_b})W_f(\gamma_a). \tag{2.128}$$

The presence of the factor ρ in the algebra does not change the ground state degeneracy. This quantity represents the topological flux inserted on the non-contractible loops and is defined mod N. In this way, the ground state is N-fold degenerate and ρ is the size of the step in which we go through the $\mathbb{Z}_N$ group. One may be concerned that, if we have, for example, the $\mathbb{Z}_9$ group and we adjust the size of the lattice so that $\rho_1 = 3$ and $\rho_2 = 9$, the sets of ground states $\{0\} = \{|0\rangle, |3\rangle, |6\rangle\}$, $\{1\} = \{|1\rangle, |4\rangle, |7\rangle\}$ and $\{3\} = \{|2\rangle, |5\rangle, |8\rangle\}$ would be inaccessible to each other. In another words, there would be no operators able to take states of $\{0\}$ into states of $\{1\}$, for example. The Figure 16 shows the possible ways to run through the $\mathbb{Z}_9$ group in steps of 3.

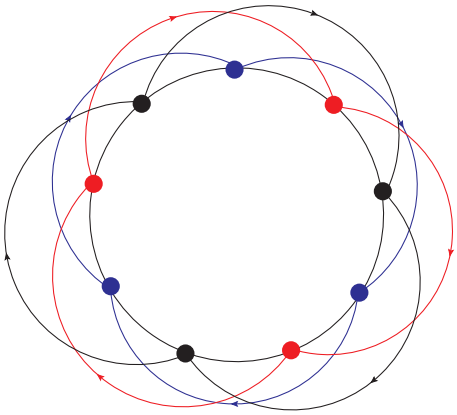

Figura 16 – Going through the $\mathbb{Z}_9$ group in steps of three would make states inaccessible. If you start, for example, in the subset $\{0\}$ (represented in blue) you would be unable to reach states in $\{1\}$ (red) and $\{2\}$ (black).

The fact is that it is always possible to access every elements of $\mathbb{Z}_N$ through applications of $W_v(\gamma_1)$ and $W_v(\gamma_2)$ operators and the example given above can never happen. One can intuitively understand this result by noting that the problematic cases happen when $\rho_1 \neq 1$ and $\rho_2 \neq 1$ are multiple of each other. In these cases, it may happen that one cannot reach all states in the ground state space (as in the previous example). However, from the definition of the ρ factors, ρ_1 and ρ_2 can never be integer multiples of one another. If $\rho_1 = q\rho_2$ for some natural q, then from their definition we would have $N_2 = qN_1$, whose least common multiple is $\text{lcm}(N_1, N_2) = qN_1$. Thus we find that $\rho_1 = q$ and $\rho_2 = 1$, contradicting our hypothesis $\rho_a \neq 1$ for $a = 1, 2$. For the case in at least one of the factors is equal to one, we can go through the group in steps of one and we have no reasons to worry.

As the continuum limit is taken, the microscopic details are forgotten and only the low-energy properties survive. The effective field theory is given by the Chern-Simons-like theory (2.122) and the relevant degrees of freedom are the line operators (2.123).

To summarize, we have obtained EFTs for the Wen Plaquette model in the even $\times$ even, even $\times$ odd, and odd $\times$ odd lattices. The results are in agreement with the proposed EFTs in [35], where the even $\times$ even lattice corresponds to a BF theory and the other two cases correspond to CS theories.

3 Fractonic Exactly Solvable Models

As in the case of the topologically ordered systems discussed previously, fractonic order are usually gapped. In this chapter we study three exactly solvable gapped models: the X-Cube model, the Haah and the Chamon code. We investigate their main properties and see how fractonic signatures, as excitation restricted mobility and UV/IR mixing emerge in such models.

3.1 X-Cube Model

The X-Cube model is a 3-dimensional system defined on a lattice which presents Type I fractons as excitations. Firstly proposed in [11], it is an exactly solvable model and provides a good model to gain some intuition about general properties about fractons. It is a gapped model and presents fractons, lineons and planons as excitations above the ground state.

The X-Cube Hilbert space is defined on a cubic lattice with qubit degrees of freedom living on the links. It is specified by the Hamiltonian

$$H_{XC} = -\sum_{\mathcal{C}} B_{\mathcal{C}} - \sum_{\mu=x,y,z} \sum_{v_\mu} A_v^\mu \tag{3.1}$$

$$= -\sum_{\mathcal{C}} \prod_{l\in\partial\mathcal{C}} X_l - \sum_{\mu=x,y,z} \sum_{v_\mu} \prod_{l\ltimes v_\mu} Z_l. \tag{3.2}$$

The cube terms $B_{\mathcal{C}}$ are products of the twelve X Pauli operators in the cube edges $\partial\mathcal{C}$ and A_v^μ are products of the four Z Pauli operators at the links connected to the vertex v_μ in the plane normal to the μ -direction. The Figure 17 illustrates such operators, where the dots lies on the lattice links.

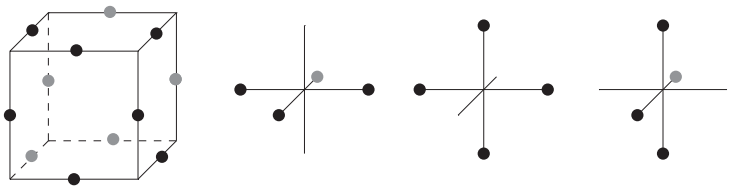

Figura 17 – Cube and star operators.

All the operators mutually commute and their energies can be minimized simultaneously. This is what gives the model its exactly solvable character and its gapped spectrum. Roughly, when the Hamiltonian involves a set of non-compatible operators, the low-energy physics allows gapless fluctuating degrees of freedom in order to minimize the

total energy. This happens, for example, in the $\mathbb{Z}_2$ lattice gauge theory (2.1) in its critical point $g = g_c$, $t = t_c$, where the theory is a CFT.

We must find the ground state $|\psi\rangle$ such that

$$B_{\mathcal{C}}|\psi\rangle = A_v^{\mu}|\psi\rangle = |\psi\rangle, \quad \forall\ \mathcal{C}\ and\ v \in \Lambda. \tag{3.3}$$

Defined on a torus, the ground state is not unique. In fact, if the lattice Λ has $L_x \times L_y \times L_z$ links, the model ground state degeneracy is given by

$$\log_2 \mathrm{GSD}_{\mathrm{XC}} = 2L_x + 2L_y + 2L_z - 3, \tag{3.4}$$

as we shall see soon.

This is a hallmark of fracton systems: the ground state degeneracy depends on the lattice size. Such characteristic brings up some difficulties in finding continuum descriptions of fracton systems, since they usually only takes into account universal properties of physical systems neglecting most of microscopic details. Equation (3.4) signals to UV/IR mixing, as the low-energy physics (IR) is very sensible to UV details.

In order to understand the degeneracy, let us introduce non-contractible loop operators. Let us consider the (μ, n)-plane which is the plane normal to the μ direction lying in the n coordinate in the μ axis. Let $\gamma^{*\nu}_{(\mu,n)}$ be a curve in the dual lattice lying in the (μ, n) plane oriented in the $\nu \neq \mu$ direction, as shown in Figure 18.

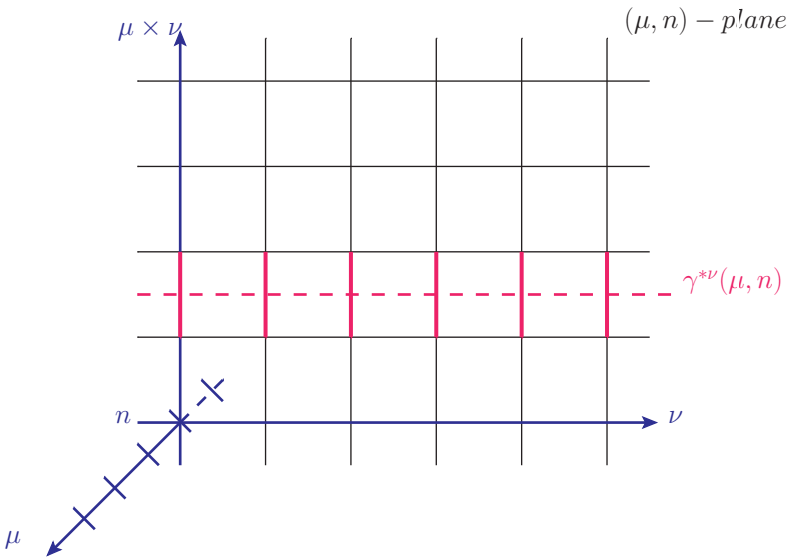

Figura 18 – The curve $\gamma^{*\nu}_{(\mu,n)}$ lying in the dual-lattice of the plane (μ, n) crossing the transverse links (in red).

The set of non-contractible loop operators

$$T\left(\gamma^{*\nu}_{(\mu,n)}\right) = \prod_{\ell \in \gamma^{*\nu}_{(\mu,n)}} Z_\ell \tag{3.5}$$

commutes with the X-Cube Hamiltonian. Thus, if a given state $|0\rangle$ is a ground state of the system with energy E_0, $T\left(\gamma^{*\nu}_{(\mu,n)}\right)|0\rangle$ is also a ground state with the same energy. The

role of the loop operator is to introduce a $\mathbb{Z}_2$ flux in the ν direction of the T^2 torus lying in the (μ, n)-plane. There is two possible $\mathbb{Z}_2$ fluxes ± 1 through the two directions for each of the $L_x \times L_y \times L_z$ planes, telling us that, in principle, we have $2^{2L_x+2L_y+2L_z}$ distinct ground states. However, not all the loop operators are independent. In fact, they must obey the following three constraints:

$$\prod_n T\left(\gamma^{*\nu}_{(\mu,n)}\right) = \prod_n T\left(\gamma^{*\mu}_{(\nu,n)}\right). \tag{3.6}$$

For each pair of distinct directions $x-y$, $y-z$ and $z-x$, we have one of the above constraint. The effect of the constraints is to reduce the "naive" ground state degeneracy $2^{2L_x+2L_y+2L_z}$ by a factor of 2^3, leading us to the final expression in (3.4).

The application of Z operator at a link flips the sign of all the cube operators $B_{\mathcal{C}}$ which has this link in their edges

$$\{Z_{l_1}, B_{\mathcal{C}}\} = 0, \quad l_1 \in \partial\mathcal{C}. \tag{3.7}$$

Since a given link is shared by four cubes, the application of Z creates four cube excitations with eigenvalue -1 of the $B_{\mathcal{C}}$ operator. These four excitations can be separated from each other through the application of Z on the links of a rectangular membrane geometry, as in figure 19.

These "membrane" operators create four excitations in their corners that, individually, are not able to move: the only way to move an individual cube excitation would be applying Z at an edge of the cube. However, this process creates other three excitations, having a large energetic cost. Individual cube excitations have restricted mobility: they are fractons!

In contrast, a pair of adjacent cube excitations in this membrane is allowed to move as a bound state. They can be seen as dipole-like excitations which are two-dimensional particles: planons allowed to move in the normal plane of the dipole axis. The X-Cube model presents Type I fractons. The Figures 19, 20 and 26 were borrowed from Ref. [12].

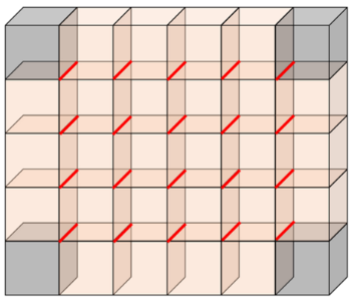

Figura 19 – Four cube excitation spatially spaced by the application of the Z operator on a rectangular membrane.

In addition, the model presents excitations associated with the A^{μ}_{v} terms. The application of the X operator on a string of links anti commutes the vertex terms A^{μ}_{v}.

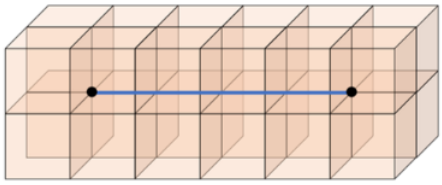

Figura 20 – A pair of lineons, created by a string of X operators on the vacuum state.

These vertex excitations are created in pairs and can move in one dimension through the application of these X string operators. A given vertex excitation is a one-dimensional particle (a lineon) and cannot be moved along other directions since it would create different kind of excitations. A pair of lineons, a dipole-like object, is a dimension-2 particle allowed to move along the normal plane to the dipole axis.

3.2 Chamon Code

Proposed in 2005 by Chamon [9], this exactly solvable model can be thought as the 3D generalization of the 2D Wen's plaquette model 2.96. Firstly investigated due to its quantum glassiness property, it was the first exactly solvable model which presents fracton phenomenology. As we argue in this section, this model is a three-dimensional gapped Type I fractonic system.

The Chamon code is defined on a face-centered cubic lattice with the degrees of freedom living on the faces of the cubes. At each site, both on the cubic vertices and the face centers, we place a spin qubit. More precisely, let us consider the lattice generated by the $\mathbb{R}^3$ canonical basis vectors $\hat{x}_i$, with $\hat{x}_1 \equiv \hat{x}$, $\hat{x}_2 \equiv \hat{y}$ and $\hat{x}_3 \equiv \hat{z}$. We refer to as any site in the lattice through their position vector in relation to some origin $\vec{x} = x_1\hat{x}_1 + x_2\hat{x}_2 + x_3\hat{x}_3$, with $x_i \in \mathbb{Z}$. If a site $\vec{x}$ is such that $\sum_1^3 x_i = odd$, we call $\hat{x}$ an odd site. If, on the other hand, the sum of the $\vec{x}$ site coordinates is even, we call $\hat{x}$ an even site. The set of all even and odd sites constitutes the Λ_{even} and Λ_{odd} sub-lattices, respectively.

The physical system consists of a physical qubit located at every site of Λ_{even}. The sites located in Λ_{odd} play the role of link variables between the qubits. This spin configuration forms a cubic faced-centered qubit structure lattice. The unit cell, in this framework, is not generated by primitive vectors but by the composition of the basis vectors $\hat{x}_i$. For example, the qubits located at the sites associated with the coordinates

$$(0,0,0),\quad (2,0,0),\quad (0,2,0),\quad (0,0,2),\quad (0,2,2)\quad (2,2,0),\quad (2,0,2)$$
$$(2,2,2),\quad (1,1,0),\quad (1,0,1)\quad (0,1,1),\quad (2,1,1),\quad (1,2,1),\quad (1,1,2)$$

form an unit cell in a cubic faced-centered lattice.

Define the "octahedron" operators $S_{\vec{x}}$ in the even sites $\vec{x} \in \Lambda_{odd}$ in terms of the $\mathbb{Z}_2$ Pauli operators P_i acting on the six next-neighbors qubits living at the even sites:

$$S_{\vec{x}} \equiv \prod_{i=1}^{3} P^i_{\vec{x}-\hat{x}_i} P^i_{\vec{x}+\hat{x}_i}. \tag{3.8}$$

The Hamiltonian of this system is defined as the sum of such operators

$$\hat{H} = -h \sum_{\vec{x}\in\Lambda_{odd}} \left(S_{\vec{x}} + S^{\dagger}_{\vec{x}}\right). \tag{3.9}$$

All the $S_{\vec{x}}$ operators commute with each other. If two octahedron operators share just one site, as in Figure 21 a), they apply the same "flavor" of the Pauli operator in the $\vec{x} \in \Lambda_{even}$ site and the commutation follows immediately. If two octahedron operators share two sites $\vec{x} \in \Lambda_{even}$, as in Figure 21 b), the anti commutation relation in both sites cancel each other so that both $S_{\vec{x}}$ operators commute.

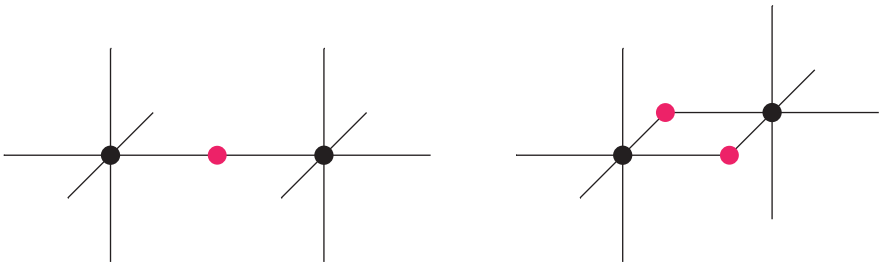

Figura 21 – Possibilities of sharing sites between distinct octahedron operators. The black dot belongs to Λ_{odd} and the red dot belongs to Λ_{even}. In both cases, the operators commute between themselves.

The ground state of the model can be exactly found and simultaneously diagonalizes all octahedron operators. The ground state of the lattice model is such that it corresponds to $S_{\vec{x}} = +1$ for all $\vec{x} \in \Lambda_{odd}$.

Let the lattice Λ be a T^3 torus (periodic boundary conditions in the three directions) with even length dimensions L_x, L_y and L_z. The ground state degeneracy is

$$GSD = 2^{4g}, \quad \text{with} \quad 2g = gcd(L_x, L_y, L_z), \tag{3.10}$$

with $gcd\ (x, y, z)$ the greater common divisor among L_x, L_y and L_z [36]. For the case in which $L_x = L_y = L_z \equiv L$, we have that $2g = L$ and

$$\log_2 (GSD) = 2L. \tag{3.11}$$

Defects in this model correspond to octahedrons with $S_{\vec{x}} = -1$ and they cannot be individually created. If we apply, say, the Z Pauli operator at the site $\vec{u} \in \Lambda_{even}$ above the ground state, the octahedron operators $S_{\vec{x}}$ located at the sites

$$\vec{u} + \hat{x}_1, \quad \vec{u} - \hat{x}_1, \quad \vec{u} + \hat{x}_2 \quad \text{and} \quad \vec{u} - \hat{x}_2 \tag{3.12}$$

will anti commute with it, $\{Z_{\vec{u}}, S_{\vec{x}}\} = 0$, telling us that four excitations are created. This process requires a large energetic cost of $\Delta E \sim 8h \gg 1$ for large coupling h. If we apply the Z operator again, say, at the site $\vec{u} + 2\hat{x}_1$, in an attempting to move an excitation around, we end up with the creation of two other excitations, what it is energetically forbidden. In fact, the excitations, once created cannot be individually moved: they are immobile fractons. As in the X-Cube model, fractons excitations can be separated apart through a membrane operator. As shown in Figure 22, four octahedron excitations are created in the corner of the membrane operator $W(M) = \prod_{\vec{u}\in M} Z_{\vec{u}}$. The Figure 22 were borrowed from Ref. [36].

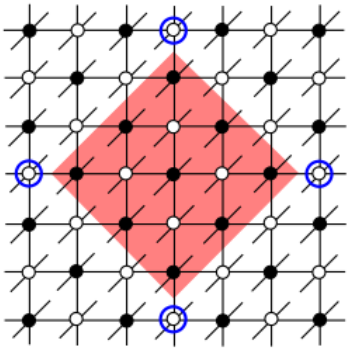

Figura 22 – Membrane operator application above the ground state on a $z = cte$ plane of the lattice. Black dots are even sites, where $Z_{\vec{u}}$ is applied and white dots are odd sites. The four blue circulated white sites are the location of the octahedron excitations.

In every process for excitation creation, both the charge and the dipole momentum are conserved. This is an important feature of this model and will still hold in the effective theory for the low-energy description (see Section 6.3).

There are, however, string operators in this model [36], i.e., there are mobile excitations above the ground state. Consider the four fracton excitations created in the sites (3.12) by the application of $Z_{\vec{u}}$, in the site $\vec{u} \in \Lambda_{even}$ above the ground state. If we apply Z operators along the n-sized string

$$\gamma_n = \{(\vec{u} + 2\hat{x}_1 + 2\hat{x}_2), (\vec{u} + 4\hat{x}_1 + 4\hat{x}_2), \ldots, (\vec{u} + 2n\hat{x}_1 + 2n\hat{x}_2)\} \tag{3.13}$$

we move the two excitations previously in $\vec{u} + \hat{x}_1$ and $\vec{u} + \hat{x}_2$ respectively to the sites $\vec{u} + (2n+1)\hat{x}_1$ and $\vec{u} + (2n+1)\hat{x}_2$. The fractons are able to move along a line as dipole bound states: a dipole of fractons is a lineon. Such lineons are restricted to move only along cube face-diagonal directions. The Chamon code is, indeed, a Type I fracton system, where individual fractons are able to move only as dipole bound states. Further string operators do exist ins this model (as flexible string operators) and are extensively discussed in [36].

The origin of excitations mobility restrictions relies on the octahedron operators structure. Less obviously, another consequence which follows from it is the conser-

vation of the $\mathbb{Z}_2$ charge for any plane $\Sigma_{\vec{t},\alpha}$. The plane $\Sigma_{\vec{t},\alpha}$ is perpendicular to the cube diagonal direction $\vec{t} = (t_x, t_y, t_z)$ and is defined as the set of points $\{(x, y, z) \in \Lambda_{odd} | t_x x + t_y y + t_z z = \alpha\}$. There are, in our system, four cube diagonal directions $\vec{t} = \{(1,1,1), (-1,1,1), (1,-1,1), (1,1,-1)\}$.

Let $s(\vec{x}) = \pm 1$ be the eigenvalue associated to $S_{\vec{x}}$ in the site $\vec{x} \in \Lambda_{odd}$. The $\mathbb{Z}_2$ charges in the planes $\Sigma_{\vec{t},\alpha}$

$$\theta_{\vec{t},\alpha} = \sum_{\vec{x} \in \Sigma_{t,\alpha}} s(\vec{x}), \quad mod\ 2 \tag{3.14}$$

are conserved under the application of any operator and are called topological charges [36]. As mentioned above, the conservation of $\theta_{\vec{t},\alpha}$ in such planes follows from the fact that every process in the theory respects the octahedral symmetry.

3.3 Haah Code

The Haah Code is a three dimensional gapped fractonic model defined on a cubic lattice. In contrast to the X-Cube model and the Chamon code, the Haah code is a type-II fracton model where the fractons are unable to move, neither as bound states. This is a consequence to the fact that there is no string-like operators in this model.

The Haah code was proposed in 2011 by Haah [10] and consists of two qubits per lattice site. The Hamiltonian is written as the sum of two cubic terms

$$H = -\sum_{\mathcal{C}} A_{\mathcal{C}} - \sum_{\mathcal{C}} B_{\mathcal{C}}, \tag{3.15}$$

where $A_{\mathcal{C}}$ and $B_{\mathcal{C}}$ are defined as a product of Pauli operators along the cube edges and are defined in Figure 23. In the operators definition, I refers to the identity operator.

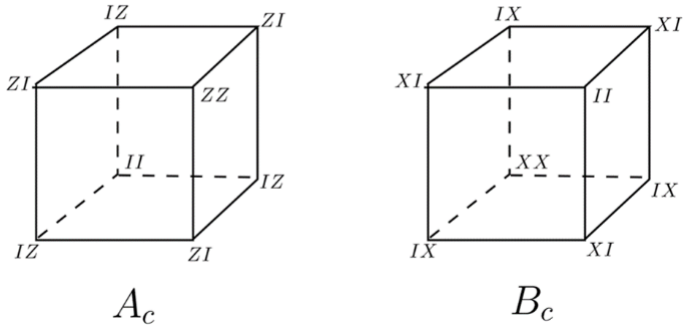

Figura 23 – Cube operators in the Haah code.

As in the X-Cube model, all the operators simultaneously commute

$$[A_{\mathcal{C}}, A_{\mathcal{C}'}] = [B_{\mathcal{C}}, B_{\mathcal{C}'}] = [A_{\mathcal{C}}, B_{\mathcal{C}'}] = 0 \quad \forall \mathcal{C}, \mathcal{C}^{'} \in \Lambda, \tag{3.16}$$

giving the model exactly solvable and gapped properties. The first and second vanishing commutation rules follows trivially. The commutation relations among the $A_{\mathcal{C}}$ and $B_{\mathcal{C}}$ follows trivially when they share no qubits and, otherwise, can be understood in terms of the three cases shown in Figure 24. In all the three cases, one can verify that they

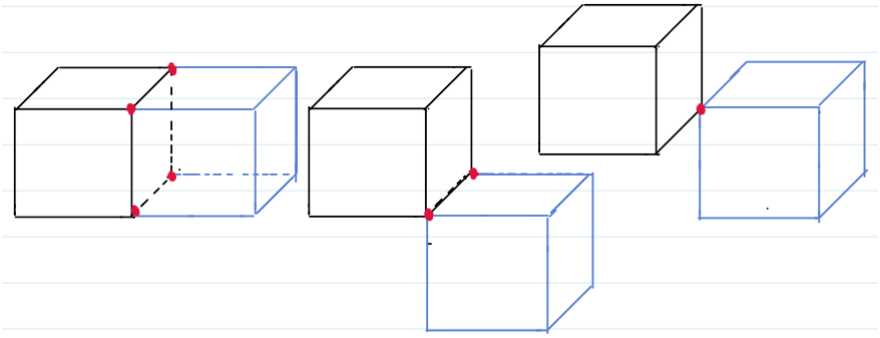

Figura 24 – The cube operators $A_{\mathcal{C}}$ and $B_{\mathcal{C}}$ nontrivial commutators. They can share four, two or one vertices (in red).

always commute. There is always an even number of anti-commutations so that the cube operators always commute.

The ground state of the Haah code is an eigenstate of the cube operators $A_{\mathcal{C}}$ and $B_{\mathcal{C}}$ for every cube $\mathcal{C} \in \Lambda$ with eigenvalue $+1$. For the cases in which Λ is a nontrival topological space, the ground state is degenerate. The counting of the ground state degeneracy, however, is more complicated than in the X-Cube model. In a $L \times L \times L$ torus, GSD is a complicated non-monotonic function of L and is bounded by above by [10]

$$\log_2 GSD < 4L. \tag{3.17}$$

This model possesses a self-duality between the two kinds of operators $A_{\mathcal{C}}$ and $B_{\mathcal{C}}$, such that suffices to study only one excitation flavor. The structure of the Hilbert space and the operators in the Hamiltonian give the excitations a tetrahedron structure. For illustration purposes let us act with, say, the IZ operator on a given vertex of the lattice. Four $\mathcal{B}_{\mathcal{C}}$ cube excitations are created

$$\{\mathcal{B}_{\mathcal{C}}, IZ\} = 0, \tag{3.18}$$

in a tetrahedron structure as shown in Figure 25.

The cube excitations can be separated from one another by applications of IZ operator in other vertices in a tetrahedral structure. Geometrically this is done by inserting tetrahedron structures inside tetrahedron structures as shown in Figure 26. It gives rise to a fractal arrangement and for this reason the application of IZ in such lattice vertices is called tetrahedron fracton operator. The fracton excitations appears always at the corners of the tetrahedron fracton operator.

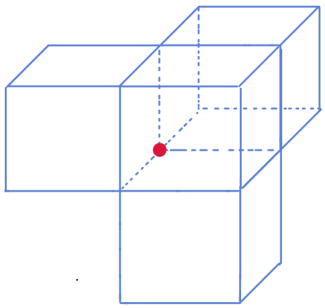

Figura 25 – Application of IZ operator in the indicated (red dot) vertex. It creates four $\mathcal{B}_\mathcal{C}$ excitations in a tetrahedron structure.

Figura 26 – Fracton operator in the Haah code. The individual cube excitations are indicated by the yellow stars.

This can, of course, be done with the application of others operators than IZ, giving rise to different oriented tetrahedron fractal structures. The same is valid for IX and $\mathcal{A}_\mathcal{C}$ operators.

In contrast to the X-Cube model and the Chamon code, dipole bound states of fractons in this model are not mobile. In fact, it can be shown that there are no string operators in the the Haah code [10]. In other words, all possible bound state of fractons are also fractons.

4 Coupled Layers Construction

Topological ordered systems in two dimensions allow us to construct 3d fracton phases. This construction is, in general, non-unique and allow us to build more interesting and richer phases by considering stacks of coupled two-dimensional topological systems. In the infinite coupling limit, stacks of two-dimensional toric code systems result in the three-dimensional X-Cube model. To check this result, we analyze it throughout perturbation theory technology. Up to sixth order in perturbation theory, we recover the X-Cube Hamiltonian while further corrections are suppressed by inverse powers of the infinite coupling constant. The coupling parameter J provides a smooth way to switch between the free toric code layers $J \to 0$ and the X-Cube model $J \to \infty$ through the interpolating Hamiltonian. We are able to understand the X-Cube physics, as the fracton emergence and the ground state degeneracy, in the intermediate coupling limit.

In this chapter we mainly follow [19] and [37].

4.1 X-Cube from Coupled Toric Codes

4.1.1 Strong Coupling

We recover the X-Cube model from two-dimensional layers of toric code models and strongly coupling them. Let us consider a set of toric code planes aligned the xy, yz, and zx planes in a square lattice and let us impose periodic boundary conditions in each one of them. The result is a cubic lattice where each vertex i belongs to three perpendicular planes and each link lies in the intersection of two different orthogonal planes. Let us denote a link which starts in the vertex j aligned with the unit vector $\hat{x}_i$ as $\ell = (j, \hat{x}_i)$. The Hamiltonian of this set of non-interacting toric code models is given by a sum of Hamiltonians (2.31), one for each plane P

$$H_{free} = \sum_{P} \left(- \sum_{i \in P} A_i^{o(P)} - \sum_{p \in P} B_p^{o(P)} \right). \tag{4.1}$$

The upper index $o(P) = \{\hat{x}_1, \hat{x}_2, \hat{x}_3\}$ refers to as the normal direction to the plane P. In the above expression, the $A_i^{o(P)}$ operator is a product of Z Pauli operators on the four links ℓ connected to the vertex i, all lying in the P plane and the $B_p^{o(P)}$ operator is a product of X Pauli operators on the p plaquette boundary, which belongs to the P plane

$$A_i^{o(P)} = \prod_{\ell \perp o(P)} Z_\ell^{o(P)} \quad \text{and} \quad B_p^{o(P)} = \prod_{\ell \in \partial p} X_\ell^{o(P)}. \tag{4.2}$$

The upper index $o(P)$ is necessary on the Pauli operators Z_ℓ and X_ℓ because, from the geometrical arrangement of the toric code planes, there are two qubits lying in every link $\ell = (j, \hat{x}_i)$: one from each of the two planes P which contains ℓ (Figure 27).

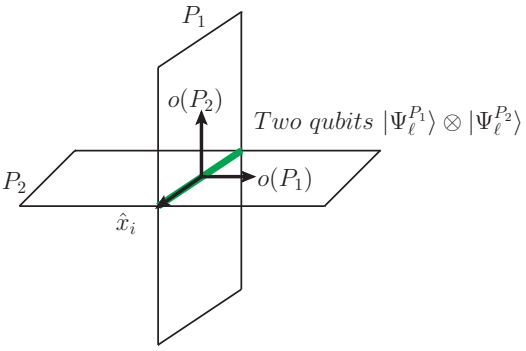

Figura 27 – Two qubits lying in the link ℓ, coming from the planes P_1 and P_2.

The Hamiltonian (4.1) is a free theory in the sense that every plane system is blind to the others. We introduce interactions among them by coupling the two qubits lying in the same geometrical link. The form of the coupling among them will directly affect the resulting theory in the strongly coupling limit. Here we study a ZZ coupling and we are able to recover the X-Cube model in perturbation theory. A different coupling is also possible but gives us a different theory. In fact, a XX coupling in the strongly coupled regime gives us, in perturbation theory, the three dimensional Toric Code system [19].

Let J_z be the coupling constant that measures the strength of the interaction and consider the Hamiltonian

$$H = H_{free} - J_z \sum_\ell Z_\ell^{o(P_1)} Z_\ell^{o(P_2)}, \quad J_z > 0. \tag{4.3}$$

The $o(P_1)$ and $o(P_2)$ upper indices tell us in which planes the qubits relying in the $\ell = (j, \hat{x}_i)$ link belong. Both planes P_1 and P_2 have $o(P_1), o(P_2) \perp \hat{x}_i$ and are perpendicular among themselves $o(P_1) \perp o(P_2)$. In the strong coupling limit $J_z \to \infty$ in order to minimize the energy of the system, the ground state space obeys $Z_\ell^{o(P_1)} = Z_\ell^{o(P_2)}$ for every link ℓ.

Define the operators $\mathcal{Z}_\ell \equiv Z_\ell^{o(P_1)} = Z_\ell^{o(P_2)}$ and the tensorial product $\mathcal{X}_\ell = X_\ell^{o(P_1)} X_\ell^{o(P_2)}$. As we will show in the following, up to sixth order in perturbation theory and discarding constants terms, we recover the X-Cube Hamiltonian

$$H_{XC} = -\sum_i \sum_{\mu=x,y,z} \mathcal{A}_i^\mu - K \sum_{\mathcal{C}} \mathcal{B}_{\mathcal{C}}, \tag{4.4}$$

with the operators

$$A_i^\mu = \prod_{\ell \perp \mu} \mathcal{Z}_\ell, \quad \text{and} \quad \mathcal{B}_{\mathcal{C}} = \prod_{\ell \in \partial \mathcal{C}} \mathcal{X}_\ell \tag{4.5}$$

and the coupling $K \sim J_z^{-5} > 0$.

Let us now formally develop the perturbation theory. Since the ground state of our model is highly degenerated, we make use of degenerate perturbation theory (Brillouin-Wigner Perturbation Theory). The general idea in the following approach is to make use of projectors to separately analyze the perturbation action on the ground state space.

In the strongly coupled regime, we write the complete Hamiltonian (4.3) as $H = H_0 + H_1$, with H_0 the dominant interaction term and treat $H_1 = H_{free}$ perturbatively with perturbation parameter J_z^{-1}. It is convenient to separate the star and plaquette interactions $H_1 = H_{1v} + H_{1p}$ and keep in mind that these two operators commute with each other.

The unperturbed Hamiltonian H_0 forces the two qubits lying in each link to point in the same direction. In the z ket basis, the state in each link ℓ is a (normalized) superposition $|\psi\rangle_\ell = c_{\ell\uparrow} |\uparrow\uparrow\rangle_\ell + c_{\ell\downarrow} |\downarrow\downarrow\rangle_\ell$ so that the system state, lying in the ground state space, is the product state $\prod_\ell \otimes |\psi\rangle_\ell$. The fact of the ground state is product state is a consequence that we have not yet included interactions among qubits lying in different links. The effect of the perturbation H_{1v} and H_{1p} is to favor some spin configurations in star and plaquette clusters and to entangle different links qubits. It is this highly entangled quantum state the responsible for fracton emergence and topological properties.

To have a physical picture in mind, the action of the star perturbation $H_{1v} \sim \sum_P \sum_i \prod_\ell Z_\ell^{o(P)}$ on the ground state will only extract z Pauli operators eigenvalues and will map it into, again, the ground state space (in general, a resulting non-product state). In other words, the H_{1v} operators does not spoil the $Z_\ell^{o(P_1)} = Z_\ell^{o(P_2)}$ constraint. On the other hand, since the $X_\ell^{o(P)}$ Pauli operator flips the P-plane ℓ-qubit and leave the other ℓ links qubits unflipped (spoiling the constraint), the plaquette perturbation $H_{1p} \sim \sum_P \sum_p \prod_{\ell \in \partial p} X_\ell^{o(P)}$ violates the $Z_\ell^{o(P_1)} = Z_\ell^{o(P_2)}$ constraint. That is, when it acts on a ground state, it returns us a state which does not lie in the ground state space. We say that the operator H_{1p} has vanishing projection onto the ground state space.

Let us consider an eigenstate $|\psi\rangle$ of the complete Hamiltonian H with energy E so that it becomes a ground state of H_0 in the absence of the perturbation. Let us decompose it as $|\psi\rangle = |\psi_0\rangle + |\psi_1\rangle$, with $|\psi_0\rangle$ belonging to the ground state space $H_0 |\psi_0\rangle = E_0 |\psi_0\rangle$ and $|\psi_1\rangle$ to the orthogonal complement. Finally, let $\mathcal{P}$ be the projector on the ground state

$$\mathcal{P} = \frac{\prod_\ell \left(1 + Z_\ell^{o(P_1)} Z_\ell^{o(P_2)}\right)}{2} \tag{4.6}$$

and $(1 - \mathcal{P})$ be the projector on the complement space. We write the Schrodinger equation $H |\psi\rangle = E |\psi\rangle$ as

$$(E - H_0) |\psi\rangle = H_1 |\psi\rangle \quad \Rightarrow |\psi\rangle = (E - H_0)^{-1} H_1 |\psi\rangle . \tag{4.7}$$

Applying the $(1-\mathcal{P})$ projector to the left of the previous equation and using that $(1-\mathcal{P})\,|\psi\rangle = |\psi_1\rangle$ and $[P, H_0] = 0$:

$$|\psi_1\rangle = (E - H_0)^{-1}\,(1-\mathcal{P})\,H_1\,|\psi\rangle\,. \tag{4.8}$$

We are able to find a formal expression to the perturbed states replacing (4.8) into $|\psi\rangle = |\psi_0\rangle + |\psi_1\rangle$

$$|\psi\rangle = |\psi_0\rangle + (E - H_0)^{-1}\,(1-\mathcal{P})\,H_1\,|\psi\rangle\,, \tag{4.9}$$

which we can formally solve by recursive iteration

$$\begin{aligned} |\psi\rangle &= \sum_{n=0}^{\infty}\left[\frac{1-\mathcal{P}}{E-H_0}H_1\right]^n|\psi_0\rangle \\ &= \sum_{n=0}^{\infty}(\mathcal{D}H_1)^n\,|\psi_0\rangle\,, \quad \mathcal{D}\equiv\frac{1-\mathcal{P}}{E-H_0}. \end{aligned} \tag{4.10}$$

If we were able to perform the sum in (4.10) we would find the exact lattice ground state of the complete Hamiltonian H. This is, however, a hard task and we ask another question: considering the ground state space (states which obeys the constraint), what is the effect, order by order, of the aplication of the perturbation $\mathcal{D}H_1$ on it? In addition, because $Z_\ell^{o(P_1)} = Z_\ell^{o(P_2)}$ must be strongly implemented, we are interested in the effect of orders of $\mathcal{D}H_1$ on $|\psi_0\rangle$ so that it returns us a state which, again, obeys the constraint. Namely, we are interested in the effect of perturbations on the ground state space. For this purpose, we introduce the notion of the Effective Hamiltonian.

Note that $\mathcal{P}H\,|\psi\rangle = E\mathcal{P}\,|\psi\rangle = E\,|\psi_0\rangle$ and that, applying $\mathcal{P}H$ in the left of the equation (4.10), we get

$$\begin{aligned} E\,|\psi_0\rangle &= \mathcal{P}\,(H_0+H_1)\sum_{n=0}^{\infty}(\mathcal{D}H_1)^n\,|\psi_0\rangle \\ &= E_0\,|\psi_0\rangle + \mathcal{P}H_1\sum_{n=0}^{\infty}(\mathcal{D}H_1)^n\,\mathcal{P}\,|\psi_0\rangle\,. \end{aligned} \tag{4.11}$$

Above, for convenience, we wrote $|\psi_0\rangle = \mathcal{P}\,|\psi_0\rangle$ and used the fact that

$$\begin{aligned} \mathcal{P}H_0\sum_{n=0}^{\infty}(\mathcal{D}H_1)^n\,|\psi_0\rangle &= H_0\mathcal{P}\,|\psi_0\rangle + \underbrace{H_0\mathcal{P}\sum_{n=1}^{\infty}\left[\frac{1-\mathcal{P}}{E-H_0}H_1\right]^n|\psi_0\rangle}_{\text{vanishes, since } \mathcal{P}(1-\mathcal{P})=0} \\ &= E_0\,|\psi_0\rangle\,. \end{aligned} \tag{4.12}$$

From the equations (4.11) and (4.11), we are able to define an effective Hamiltonian which have $|\psi_0\rangle$ as an eigenstate and whose eigenvalue measures the difference between the corrected energy E and the unperturbed energy E_0

$$H_{\text{eff}}\,|\psi_0\rangle = (E - E_0)\,|\psi_0\rangle\,, \tag{4.13}$$

with the definition

$$\begin{aligned} H_{\text{eff}} &\equiv \mathcal{P}H_1 \sum_{n=1}^{\infty} (\mathcal{D}H_1)^{n-1} \mathcal{P} \\ &\equiv \sum_{n=1}^{\infty} \tilde{H}_{\text{eff}}^{(n)} \end{aligned} \tag{4.14}$$

with $\tilde{H}_{\text{eff}}^{(n)}$ being the n-th term in the sum. Albeit each $\tilde{H}_{\text{eff}}^{(n)}$ appears in the n-th term, it is not genuinely of n-th order in the perturbation H_1. This is so because the exact energy E which appears in

$$\tilde{H}_{\text{eff}}^{(n)} = \mathcal{P}H_1 \left(\frac{1-\mathcal{P}}{E - H_0} H_1 \right)^{n-1} \mathcal{P} \tag{4.15}$$

also depends on the perturbative parameter $E = E_0 + \mathcal{O}\left(J_z^{-1}\right)$.

So far, we translated our original problem into finding the effective Hamiltonian perturbation terms in (4.14) such that (4.13) is obeyed. The rightmost and leftmost projectors in the definition of $\tilde{H}_{\text{eff}}^{(n)}$ tells us that $H_1 (\mathcal{D}H_1)^{n-1}$ will always act on the ground state space and return a result that also lies in the ground state space.

The fact is that, analyzing the terms which contribute to the effective Hamiltonian, only the first and the sixth order terms give nontrivial contributions. All other different order operators give us either vanishing or constant contributions, which we conveniently set to zero. In order to not getting lost into too boring calculations, in the following we analyze only these two nontrivial contributions and argue that they really recover the X-Cube Hamiltonian.

The first contribution from the perturbation $H_1 = H_{1v} + H_{1p}$ is

$$\tilde{H}_{\text{eff}}^{(1)} = \mathcal{P}H_{1v}\mathcal{P} + \mathcal{P}H_{1p}\mathcal{P} = \mathcal{P}H_{1v}\mathcal{P}. \tag{4.16}$$

Higher powers of H_{1v} can be simplified using the $Z^2 \sim 1$ property, which gives us constant contributions. Up to fifth order, the action of the H_{1p} operator on the ground state space spoils the constraint $Z_\ell^{o(P_1)} = Z_\ell^{o(P_2)}$ and contributes trivially for the effective Hamiltonian. Extensive analysis can be performed to conclude that, up to fifth order, all other combinations of powers of H_{1v} and H_{1p} either cancels or contributes trivially [19]. Finally, expanding $\tilde{H}_{\text{eff}}^{(n)}$ for $n = 6$ and being careful with the energy expansion $E = E_0 + \mathcal{O}\left(J_z^{-1}\right)$, we have the nontrivial contribution

$$\tilde{H}_{\text{eff}}^{(6)} \supset \mathcal{P} \left(H_{1p}\mathcal{D}_0\right)^5 H_{1p}\mathcal{P}, \quad \mathcal{D}_0 \equiv \frac{1-\mathcal{P}}{E_0 - H_0}. \tag{4.17}$$

Let us analyze the action of this operator, from the right to the left. $H_{1p}\mathcal{P} : |\psi_0\rangle \mapsto |\tilde{\psi}\rangle$ so that $|\tilde{\psi}\rangle$ is a sum of plaquettes in which the constraint is violated; the operator $H_{1p}\mathcal{D}_0$ project $|\tilde{\psi}\rangle$ into the ground space complement, measures its energetic difference in relation to E_0 and apply again the plaquette operator, spoiling the constraint on links

of more plaquettes, resulting in an intermediate state $|\tilde{\psi}_1\rangle$; due to the fifth power of this operator, this process is repeated more four times. Finally the leftmost $\mathcal{P}$ projects the resulting state onto the ground state space.

The physical intuition is that, as each one of the six H_{1p} are applied on the states, more and more plaquettes spoil the constraint $Z_\ell^{o(P_1)} = Z_\ell^{o(P_2)}$ (See Figure 28). However, there is a special combination of spin flipping which survives to the leftmost projector onto the ground space: when the all the links on the plaquettes which constitute a cube are flipped. In this configuration the constraint is again respected and under projection it is able to survive (See Figure 29). The operator (4.17) becomes exactly the X-Cube cubic operator.

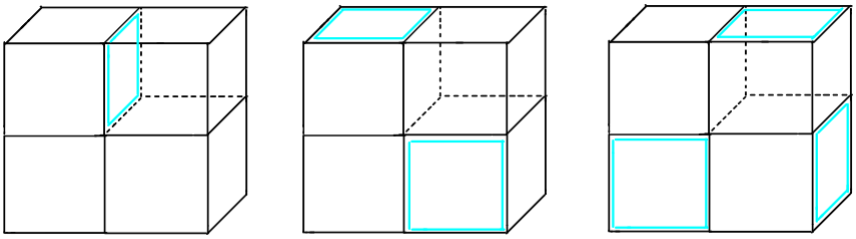

Figura 28 – The blue links represent violated constrains. The figure shows examples of resulting states which violate the constraint when $\sim (H_{1p})^n$ act on $|\psi_0\rangle$ for $n = 1, 2$ and 3 respectively.

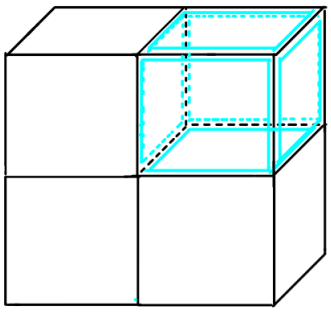

Figura 29 – In sixth order in perturbation theory, there is a special combination of constraint violation that survives to the leftmost projector in (4.17).

The effective Hamiltonian

$$H_{\text{eff}} = \mathcal{P} H_{1v} \mathcal{P} + \mathcal{P} \left(H_{1p} \mathcal{D}_0\right)^5 H_{1p} \mathcal{P} \tag{4.18}$$

is exactly the X-Cube Hamiltonian defined in (4.4). The star operators $\mathcal{A}_i^\mu$ comes from the H_{1v} term and the cubic operators $\mathcal{B}_\mathcal{C}$ from the $\sim (H_{1p})^6$ term. The energy payed for violating the constraint it proportional to J_z, so that, at each energetic measure H_0 in the denominator of $\mathcal{D}_0$, it extracts a J_z factor. The coefficient of the cubic term in (4.4) is proportional to J_z^{-5}.

4.1.2 Mapping Between the Degrees of Freedom

The Hamiltonian (4.3) for a generic J_z value interpolates between the free toric code models ($J_z = 0$) and the X-Cube system ($J_z \to \infty$). It suggests a smooth connection between the fractonic and toric code topological orders. Let us consider the effect of the interaction term in the weak and intermediate coupling regime. This regime allows us to map the properties of the X-Cube model to the toric code degrees of freedom. For this purpose it is useful to introduce the concept of $p-$*strings*.

Let us consider the coupling term $Z_\ell^{o(P_1)} Z_\ell^{o(P_2)}$ in the interpolating Hamiltonian. It anti-commutes with the four plaquettes operators $B_p^{o(P)}$ so that $\ell \in \partial p$ in both planes P that contain the link ℓ

$$\{Z_\ell^{o(P_1)} Z_\ell^{o(P_2)}, B_p^{o(P)}\} = 0. \tag{4.19}$$

The action of the coupling operator $Z_\ell^{o(P_1)} Z_\ell^{o(P_2)}$ on the link $\ell = (j, \hat{x}_i)$ creates four plaquette defects $B_p = -1$, as indicated by the black crosses in the Figure 30 (a). This is a collection of m-excitations of the toric code, two in each plane P such that $o(P) \perp \hat{x}_i$. To further analyze, it is useful to represent such a collection of magnetic excitations in a string picture. Let us draw a perpendicular crossing line through each plaquette where m particles lie and let us join line segments entering into the same cube. In this picture, the action of the coupling operator creates a closed string - a closed $p-$string, as indicated in blue in the Figure 30 (a). Larger closed $p-$strings can be created through the action of the coupling operator at links lying in a membrane operator (Figure 30 (b)). The letter p, from $p-$strings, refers to "particles". The Figures 30, 31 and 32 were borrowed from Ref. [37].

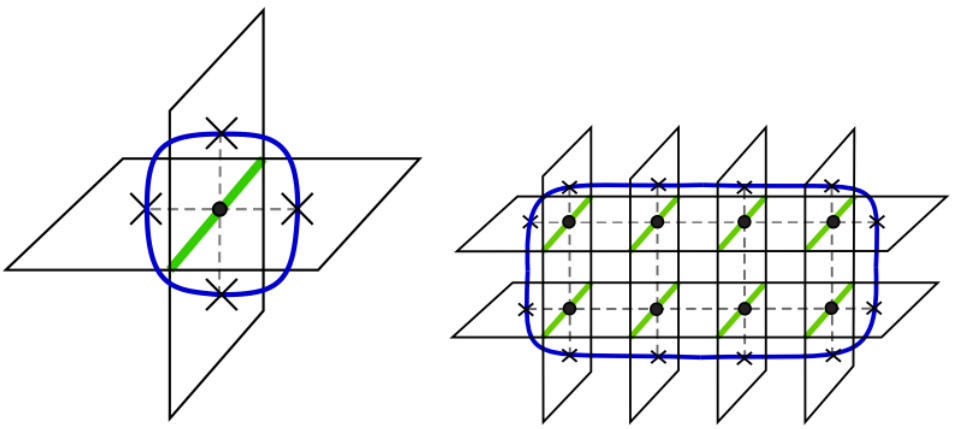

Figura 30 – (a) Closed $p-$string formed by the four m excitations in the two toric code planes. (b) Larger closed $p-$strings can be achieved through the application of the coupling operator on transversal links on a rectangular membrane.

In the decoupled phase ($J_z = 0$), the ground state is an eigenstate of the Hamiltonian H_{free} such that $B_p = A_i^{o(P)} = 1$ every where. As $J_z > 0$ is increased, the ground

state of H contains more and more closed $p-$strings, until certain limit where the coupling operator induces a string condensate ground state. In the limit $J_z \to \infty$, where we recover the X-cube model, the ground state contains strings of all sizes which are free to propagate throughout the system.

We can now ask how the X-cube physics emerge in $J_z \to \infty$ limit in terms of the toric code planes degrees of freedoms. Let us consider electrical excitations (e particles) on toric code planes. As we will argument, in the condensed phase individual e excitations are confined. To see this, let us calculate the mutual statistics between e particles and $p-$strings.

Let $e_{P_0^\mu}$ refers to as an electric particle belonging to the toric code in the plane P_0^μ such that $o(P_0^\mu) = \hat{\mu}$. The process we investigate is the braiding of a $p-$string at a fixed $e_{P_0^\mu}$ particle located at the origin of our coordinate system so that $o(P_0^\mu)$ can be $\hat{x}_1, \hat{x}_2$ or $\hat{x}_3$ corresponding, receptively, to the planes yz, zx and xy indicated in the Figure 31.

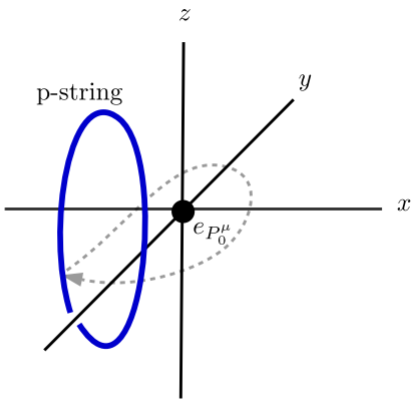

Figura 31 – Braiding of a $p-$string around an e excitation located in the P_0^μ plane. The process is performed so that the right side ($x > 0$) of the string is kept immobile and the left side is continuously deformed along the gray dashed path.

In the magnetic particle picture, for each plane P^ν that the $p-$string intersects there is a magnetic m_{P^ν} particle lying in that plane. As we braid a magnetic particle around an electric particle, both lying in the same plane, the quantum state gets a π phase (See 2.2 section). This result, which follows from the toric code model, holds individually for each plane in the coupled layers system. From the Figure 31 the $m_{P_0^z}$ particles associated to the $p-$string in the plane $z = 0$ braids around the $e_{P_0^\mu}$ particle during the process and get a π phase only if $\hat{\mu} = \hat{z}$. If $\hat{\mu} \neq \hat{z}$, the $e_{P_0^\mu}$ mutual statistics with the $m_{P_0^z}$ particles is trivial

$$\theta_{e_{P_0^\mu}, m_{P_0^z}} = \pi \delta_{\mu,z}. \tag{4.20}$$

The very same arguments apply to the yz and the zx planes. Along the braiding process

present in the Figure 31, the quantum state gets a nontrivial phase

$$\theta_{e_P\mu,\ p-\text{string}} = \sum_{\nu=x,y,z} \theta_{e_{P_0^\mu}, m_{P_0^\nu}} = \pi. \tag{4.21}$$

Because this braiding phase is nontrivial, all individual e_P particles become confined in the $p-$string condensate phase. The Figure 33 schematically shows the two phases of the model (4.3).

There are, however, allowed excitations in this phase. Let us consider two electric excitations e_{P_i} and e_{Q_i} lying in the vertex i of two distinct planes P and Q so that $o(P) \neq o(Q)$. The bound state of such particles

$$\mathfrak{e}^i_\mu = e_{P_i^\nu} \times e_{P_i^\lambda}, \tag{4.22}$$

with $\hat{\mu} = o(\hat{\nu}, \hat{\lambda})$ the orthogonal direction to both $\hat{\nu}$ and $\hat{\lambda}$, is an allowed excitation in the p-string condensate. The $\mathfrak{e}$ excitations have trivial mutual statistics with the $p-$strings and are deconfined in the $J_z \to \infty$ phase. This follows from the fact that the mutual phase (4.21) receives the contribution of π from two distinct planes and sums to zero modulo 2π.

The fusion rules for two $\mathfrak{e}$ particles lying in the same lattice vertex i can be derived from the toric code fusion rules (2.52)

$$\mathfrak{e}^i_\mu \times \mathfrak{e}^i_\nu = \left\{ \begin{array}{ll} \mathfrak{e}^i_{o(\mu,\nu)}, & \hat{\mu} \neq \hat{\nu} \\ 1, & \hat{\mu} = \hat{\nu} \end{array} \right\}. \tag{4.23}$$

We can understand the above result in terms of the toric code electric excitations. For $\hat{\mu} \neq \hat{\nu}$

$$\mathfrak{e}^i_\mu \times \mathfrak{e}^i_\nu = (e_{P_i^\lambda} \times e_{P_i^\alpha}) \times (e_{P_i^\lambda} \times e_{P_i^\beta}) = e_{P_i^\alpha} \times e_{P_i^\beta} = \mathfrak{e}^i_{o(\mu,\nu)}, \tag{4.24}$$

with $\hat{\mu} = o(\lambda, \alpha)$, $\hat{\nu} = o(\beta, \lambda)$ and naturally $o(\alpha, \beta) = o(\mu, \nu)$. For $\hat{\mu} = \hat{\nu}$ the four e_P particles pairwise annihilate each other and results in 1.

For the following result, it is important to stress that given an electric excitation e_P at a plane P, there is no way to move this excitation in the $o(P)$ direction. Then, if we try to move $\mathfrak{e}_\mu$ particles in any direction perpendicular to the $\hat{\mu}$ direction, the bound state $e_{P^\nu} \times e_{P^\lambda}$ is broken. In fact, to preserve the bound state, we can only move it the $\hat{\mu}$ direction, i.e., along the intersection line of the planes P^ν and P^λ. These one-dimensional particles are exactly the lineons found in the X-Cube model (3.1) associated to the A^μ_ν operators.

We can also understand the fractons associated to the cube operator $B_\mathcal{C}$ excitations in terms of the 2d toric code excitations. In the coupled layers model, they correspond to the endpoints of open $p-$strings. To see it, let us first analyze the decoupled limit $J_z = 0$. A stack of m particles in the xy planes (Figure 32 (a)) forms a finite open $p-$string in the z-direction. Deformations of the string-bulk can be performed by applying the coupling

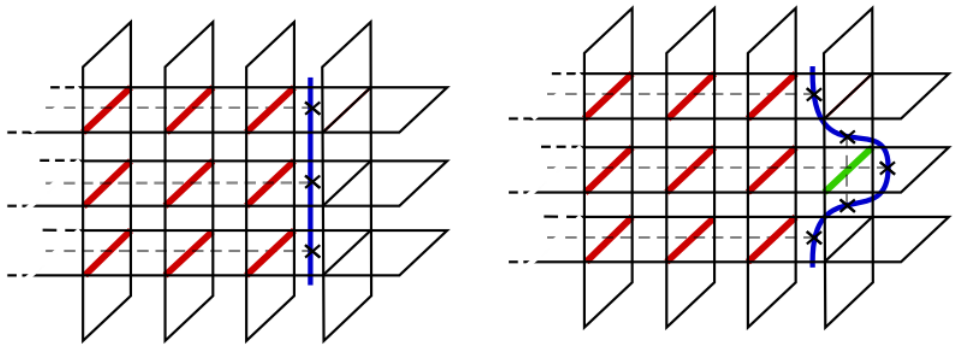

Figura 32 – (a) Open $p-$string formed by a stack of m excitations in the 2d toric code systems. (b) Deformation of the open string throughout the application of the $Z^x_\ell Z^z_\ell$ operator.

$Z^x_\ell Z^z_\ell$ operator. Albeit the bulk of the string can be freely deformed, the application of the coupling operator fails to move the string endpoints around. It follows from the the fact that the coupling operator preserves the $\mathbb{Z}_2$ flux through the cubes. In the condensate phase $J_z \to \infty$, infinite open-string bulk fluctuations size are allowed at zero energetic cost, indicating us they no longer carry physical meaning but only their endpoints.

The $\mathbb{Z}_2$ cube flux conservation under $Z^{\mu_1}_\ell Z^{\mu_2}_\ell$ tell us that there is no local operator able to change such flux. As a consequence, open-string endpoints excitations are not allowed to move. They correspond to the cube fracton excitations $B_\mathcal{C}$ in the X-Cube model (3.1) and we denote them by $\mathfrak{m}_\mathcal{C}$. In terms of the toric code variables, the fusion rules for such particles are $\mathfrak{m}_\mathcal{C} \times \mathfrak{m}_\mathcal{C} = 1$. Let σ be a rectangular membrane in the lattice. Then the following operator creates four $\mathfrak{m}_\mathcal{C}$ excitations, one in each of its corners

$$M_\sigma = \prod_{\ell | \ell \cap \sigma \neq 0} Z^z_\ell, \tag{4.25}$$

which in the $J_z \to \infty$ limit becomes

$$\mathcal{M}_\sigma = \prod_{\ell | \ell \cap \sigma \neq 0} \mathcal{Z}_\ell. \tag{4.26}$$

It is exactly the membrane operator in the X-Cube model (19). For the case in which the membrane operator acts only along a line, it creates one $\mathfrak{m}_\mathcal{C}$ excitation in each of its two endpoints. That is how the toric code m excitations survive to the strong coupling $J_z \to \infty$ limit in the X-Cube picture.

To summarize, we have seen how the X-Cube fracton excitations can be directly mapped into the 2d toric code m and e particles: the e particles survive as bound states of two-dimensional particles (each e_P particle can move along its belonging plane) and result into a one-dimensional particle (X-Cube lineons). The m particles survive by breaking them into pairs of immobile particles (X-Cube fractons).

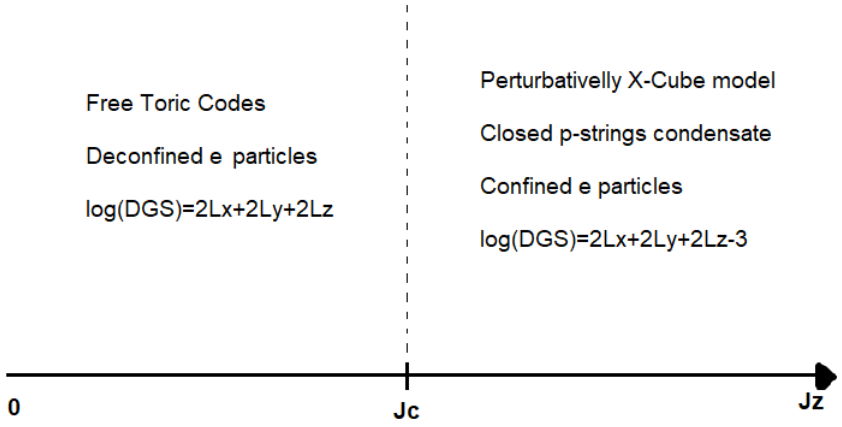

Figura 33 – Two phases of the interpolating Hamiltonian. For small J_z we have a system of free toric codes and for $J_z \gg 1$ we perturbatively recover the X-Cube Hamiltonian.

4.1.3 Ground State Degeneracy

The layer construction approach allows us not only to understand the excitations nature, but also to understand the ground state degeneracy from the toric code degrees of freedom. Let our system be defined on a T^3 torus with dimensions $L \times L \times L$. As we explicitly saw in the Section 2.31, the ground state degeneracy for the 2d toric code system defined on a T^2 torus is $2^2 = 4$.

To do it, let us count how many independent logical operators there are in the system. With periodic boundary conditions, each one of the $3L$ planes constitutes a T^2 torus. Let (μ, n) be the plane orthogonal to the μ direction with μ coordinate n. Let also $\gamma^{*\nu}_{(\mu,n)}$ be the closed loop oriented in the ν direction and which belongs to the dual lattice of the $(\mu, n)-$plane. The 't Hooft loop operators

$$\mathcal{T}_m(\gamma^{*\nu}_{(\mu,n)}) = \prod_{\ell \in \gamma^{*\nu}_{(\mu,n)}} Z^{\mu}_{\ell} \tag{4.27}$$

commute with the Hamiltonian (4.3) and their role is to introduce $\mathbb{Z}_2$ flux throughout the $(\mu, n)-$plane along the ν direction. In the system there are $3L$ planes, resulting in $6L$ logical operators - 2 logical operators for each plane, as in the toric code.

The $6L$ operators, however, are not all independent. Indeed, one can see that for any two distinct directions μ and ν, the logical operators obey

$$\prod_{0 \leq n < L} \mathcal{T}_m\left(\gamma^{*\nu}_{(\mu,n)}\right) = \prod_{0 \leq n < L} \mathcal{T}_m\left(\gamma^{*\mu}_{(\nu,n)}\right) \equiv \mathcal{M}_{\mu\nu}, \tag{4.28}$$

In the strongly coupled limit, the $M_{\mu\nu}$ quantity is the membrane operator on the entire plane orthogonal to $o(\mu, \nu)$. There are three pairs of distinct planes, namely xy, yz and zx and, consequently, three constraints $M_{\mu\nu} = M_{\nu\mu}$. Thus, there are in the total $6L - 3$ independent logical operators in the system, each one contributing with a factor of 2 to

the ground state degeneracy. Thus

$$\log_2(GSD_{XC}) = 6L - 3, \tag{4.29}$$

which agrees with our previous result (3.4) for the case in which $L_x = L_y = L_z \equiv L$.

The coupled layer construction philosophy is very similar to quantum wires approach in the sense we understand complicated systems in terms of simpler "building blocks". Coupling many layers of two-dimensional toric codes we were able to recover, in degenerate perturbation theory, the X-Cube Hamiltonian, to understand the fracton degrees of freedom in terms of the electric and magnetic toric code excitations and to successfully count the ground state degeneracy.

5 Fracton Effective Theories: Bottom-Up Approach

So far, we are familiarized with two mechanisms to study fractonic phases: their emergence in exactly solvable models and their appearance in coupled layer construction. In this chapter we study Abelian low-energy effective field theories where fractons may appear, making use of general arguments of effective field theories. The algorithm is to add all the operators which are compatible with the symmetries of the system in the Lagrangian and then analyze their relevance in low-energy physics.

5.1 Gapless Tensor Gauge Theory

Tensor gauge field theories can be thought as the tensor generalization of vector field theories and are expressed in terms of higher-rank gauge tensor fields $A_{ij}(\vec{x},t)$. In an attempt to generalize Maxwell theory, we can build both scalar charge gauge and vector charge gauge theories. As we will argue, both of them are able to describe fractonic phenomena. In general, scalar charge gauge theory means that, as in usual Maxwell theory, our charge density is described by a scalar quantity. In the other hand, in a vector tensor gauge theory the charges are described by a vector.

Let us first consider a 3D symmetric scalar charge tensor gauge theory $A_{ij} = A_{ji}$ with the symmetric tensor gauge transformation $A_{ij} \to A_{ij} + \partial_i\partial_j\alpha$. Higher-rank gauge tensor theories naturally leads to higher momentum conservation laws. To see it, we follow [12] and consider the Gauss law in the charged sector. Let $E_{ij} = E_{ji}$ be the conjugate electric fields and its Gauss law in the presence of charged matter

$$\partial_i\partial_j E^{ij} = \rho. \tag{5.1}$$

The above equation reproduces the main characteristic of fracton systems: it restricts particles mobility. Note that the charge, in a region Γ

$$Q = \int_\Gamma d^3x\rho = \int_\Gamma d^3x\partial_i\partial_j E^{ij} = \oint_{\partial\Gamma} dn_j\partial_i E^{ij}, \tag{5.2}$$

can only change through the charge flux through the boundary, that is, it is a locally conserved quantity. Just as in the usual Maxwell vector gauge theory, the Gauss law forbids the creation, say, of single particles in a region of space. In addition, the dipole moment

$$P_i = \int_\Gamma d^3x\rho x^i = \int_\Gamma d^3\left(\partial_k\partial_j E^{kj}\right)x^i = \oint_{\partial\Gamma} dn_k\left(x^i\partial_j E^{jk} - E^{ik}\right), \tag{5.3}$$

which is expressed as a integral on the boundary of the Γ region is also locally conserved. The conservation law (5.3) accounts for the fractons phenomenology. One charge, alone, is unable to move, since it would violate local dipole momentum conservation. Charges are allowed to move only as dipole bound states as long as they preserve the modulo and direction of the dipole momentum. The charged particles of this model are prototypes for describing fractons. The key fact responsible for the particle mobility restriction is the second derivative structure of the Gauss law, so that we are able to integrate by parts the above relations.

As mentioned, we can also define a symmetric vector charge tensor gauge theory, that is, a theory in which we promote our charge density to a rank 1 vector. In such theory we are able to construct a theory whose Gauss law reads

$$\partial_i E^{ij} = \rho^j. \tag{5.4}$$

This set of equations, in contrast to the previous one, leads to the conservation of both charge

$$\vec{Q} = \int_\Gamma d^3x \vec{\rho} = \int_\Gamma d^3x \partial_i \vec{E}^i = \oint_{\partial\Gamma} dn_j \vec{E}^j \tag{5.5}$$

and angular charge moment

$$\vec{M} = \int_\Gamma d^3x \left(\vec{\rho} \times \vec{x}\right) = \int_\Gamma d^3x \left(\partial_i \vec{E}^i \times \vec{x}\right) = \oint_{\partial\Gamma} dn_i \left(\vec{E}^i \times \vec{x}\right), \tag{5.6}$$

where we have made use of the electric field tensor symmetry $E^{ij} = E^{ji}$ and defined $\vec{E}^i \equiv \left(E^{i1}, E^{i2}, E^{i3}\right)$. The above conservation relation tell us that in every local process that occurs inside Γ, $\vec{M}$ must be conserved. So, not all particles are allowed to move in any direction. Instead, a particle charged with ρ^i is allowed to only move along the i direction. This phenomenology accounts for the one dimensional *lineons* particles.

So far we have described how restricted mobility can be naturally embedded in terms of a symmetric tensor gauge field. In the following, we construct an effective field theory that describes fractonic matter and see how gauge tensor fields arise naturally.

5.1.1 Gauge Principle

In the previous section, we explored mobility restriction properties of charged matter due to the Gauss law in the corresponding symmetric gauge tensor theory. In this section develop, from an EFT viewpoint, a tensor gauge theory for both scalar and vector symmetric tensor gauge theories [15]. The tensor gauge fields emerges from the gauge principle, which consists of "gauging" a global symmetry, i.e., we make a global symmetry also valid locally.

Symmetries and conservation laws requirements will be our leading guide to construct such EFT. Let Φ represent the fractonic matter field. We require the theory to be

invariant under the transformations

$$\Phi \to e^{i\alpha}\Phi \quad \text{and} \quad \Phi \to e^{i\vec{\lambda}\cdot\vec{x}}\Phi \tag{5.7}$$

with α and λ^i real constants. These symmetry transformations are associated, respectively, to charge and dipole conservation. The imposition of the second transformation to be a symmetry restricts the allowed derivative structure in the theory. The usual spatial derivatives are not allowed to be in the Lagrangian since they do not transform in a covariant way:

$$\begin{aligned}
\partial_i\Phi^*\partial^i\Phi &\to \partial_i\left(e^{-i\vec{\lambda}\cdot\vec{x}}\Phi^*\right)\partial^i\left(e^{i\vec{\lambda}\cdot\vec{x}}\Phi\right) \\
&\to e^{-i\vec{\lambda}\cdot\vec{x}}\left(-i\lambda_i\Phi^* + \partial_i\Phi^*\right)e^{i\vec{\lambda}\cdot\vec{x}}\left(i\lambda^i\Phi + \partial^i\Phi\right) \\
&\to \partial_i\Phi^*\partial^i\Phi + \left(\lambda_i^2\left|\Phi\right|^2 + i\lambda^i\Phi\partial_i\Phi^* - i\lambda^i\Phi^*\partial_i\Phi\right) \neq \partial_i\Phi^*\partial^i\Phi.
\end{aligned} \tag{5.8}$$

Instead, note that:

$$\begin{aligned}
\partial_i\Phi\partial_j\Phi - \Phi\partial_i\partial_j\Phi &\to e^{2i\vec{\lambda}\cdot\vec{x}}\Big(\Phi\partial_i\partial_j\Phi - \partial_i\Phi\partial_j\Phi + i\lambda_i\Phi\partial_j\Phi + i\lambda_j\Phi\partial_i\Phi - \lambda_i\lambda_j\Phi^2 \\
&+ \lambda_i\lambda_j\Phi^2 - i\lambda_i\Phi\partial_j\Phi - i\lambda_j\Phi\partial_i\Phi\Big) \\
&\to e^{2i\vec{\lambda}\cdot\vec{x}}\left(\partial_i\Phi\partial_j\Phi - \Phi\partial_i\partial_j\right).
\end{aligned} \tag{5.9}$$

Following the philosophy of EFT, we write all symmetry compatible operators in the action

$$\begin{aligned}
S[\Phi,\Phi^*] &= \int d^3xdt\left|\partial_t\Phi\right|^2 - m^2|\Phi|^2 - g\left|\Phi\partial_i\partial_j\Phi - \partial_i\Phi\partial_j\Phi\right|^2 \\
&- h\ \Phi^{*2}\left(\Phi\partial^2\Phi - \partial_i\Phi\partial^i\Phi\right) + \cdots .
\end{aligned} \tag{5.10}$$

where $\cdots$ contains an infinity quantity of operator terms.

In natural units and mass dimension, fixing $[x^i] = [t] = -1$,

$$[\Phi] = 1, \quad [m^2] = 2, \quad [g] = -4 \quad \text{and} \quad [h] = -2, \tag{5.11}$$

which follows from the requirement of the action to be dimensionless. Introducing large mass scale parameter Λ, we define dimensionless parameters

$$g \equiv \frac{\tilde{g}}{\Lambda^4} \quad \text{and} \quad h \equiv \frac{\tilde{h}}{\Lambda^2}. \tag{5.12}$$

They are useful to note that, in a physical process in energy scale $E \ll \Lambda$,

$$\begin{aligned}
\int d^3xdth\ \Phi^{*2}\left(\Phi\partial^2\Phi - \partial_i\Phi\partial^i\Phi\right) &\sim \tilde{h}\left(\frac{E}{\Lambda}\right)^2 \\
\int d^3xdtg\left|\Phi\partial_i\partial_j\Phi - \partial_i\Phi\partial_j\Phi\right|^2 &\sim \tilde{g}\left(\frac{E}{\Lambda}\right)^4,
\end{aligned} \tag{5.13}$$

which tell us that, the the non-Gaussian term h has a major contribution to the low energy physics than the Gaussian one g.

The infinite terms inside ... in (5.10) will have coupling constants with more and more negative as their operator dimensions get higher and higher. As irrelevant terms, they contribute less and less for in the infrared regime of the theory such that, in practice, we can neglect them.

Interactions with other fields can be introduced by "gauging" the global symmetries (5.7). We gauge the continuous symmetry so that it becomes invariant under transformations with local parameters $\alpha(x)$ and $\lambda^i(x)$. As in usual vector gauge theories, the price we must pay to ensure gauge invariance is the introduction of gauge fields. Under local phase transformations $e^{i\alpha(x)}$

$$\begin{aligned}\partial_i\Phi\partial_j\Phi - \Phi\partial_i\partial_j\Phi &\rightarrow e^{i2\alpha}\left(\Phi\partial_i\partial_j\Phi - \partial_i\Phi\partial_j\Phi\right.\\ &+ i\partial_i\alpha\Phi\partial_j\Phi + i\partial_j\alpha\Phi\partial_i\Phi - \left(\partial_i\alpha\partial_j\alpha - i\partial_i\partial_j\alpha\right)\Phi^2\\ &+ \left.\partial_i\alpha\partial_j\alpha\Phi^2 - i\partial_i\alpha\Phi\partial_j\Phi - i\partial_j\alpha\Phi\partial_i\Phi\right)\\ &\rightarrow e^{i2\alpha}\left(\Phi\partial_i\partial_j\Phi - \partial_i\Phi\partial_j\Phi + \left(i\partial_i\partial_j\alpha\right)\Phi^2\right), \end{aligned} \tag{5.14}$$

showing that an extra term $\left(i\partial_i\partial_j\alpha\right)\Phi^2$ emerges. To get rid of it we introduce a symmetric tensor field $A_{ij} = A_{ji}$ that also transforms under local phase change and cancels the additional term. Under gauge transformation

$$\Phi \rightarrow e^{i\alpha}\Phi, \quad A_{ij} \rightarrow A_{ij} + \partial_i\partial_j\alpha, \tag{5.15}$$

the derivative operator defined by

$$D_{ij}\Phi^2 = \partial_i\Phi\partial_j\Phi - \Phi\partial_i\partial_j\Phi - iA_{ij}\Phi^2, \tag{5.16}$$

transforms in a covariant way, namely,

$$D_{ij}\Phi^2 \rightarrow e^{2i\alpha}D_{ij}\Phi^2. \tag{5.17}$$

A gauge invariant theory is then reached by the replacement of the usual derivative operators by covariant derivatives ones D_{ij}. They provide the coupling between the fractonic field Φ and the U(1) tensor gauge field A_{ij}. At leading order,

$$S = \int d^3xdt\left|D_t\Phi\right|^2 - m^2|\Phi|^2 - g\left|D_{ij}\Phi^2\right|^2 - h\left(\Phi^{*2}D_i^i\Phi^2 + \text{ c.c. }\right) \tag{5.18}$$

$$+ E^{ij}E_{ij} - B^{ij}B_{ij}, \tag{5.19}$$

where we have introduced the covariant time derivative $D_t\Phi \equiv \left(\partial_t - iA_0\right)\Phi$ so that, under a time depend gauge transformation

$$A_0 \rightarrow A_0 + \partial_t\alpha \tag{5.20}$$

and we introduced the gauge invariant electric and magnetic fields

$$E_{ij} = \partial_tA_{ij} - \partial_i\partial_jA_0, \quad \text{and} \quad B_{ij} = \epsilon_{ikl}\partial^kA_j^l. \tag{5.21}$$

The theory in (5.18) is a scalar symmetric gauge tensor field theory and has the phenomenology discussed in the previous section with charge density $\rho \sim (\Phi \partial_t \Phi^* - \Phi^* \partial_t \Phi)$.

The field theory constructed above is a scalar charge tensor gauge theory. We can also obtain a vector charge tensor gauge theory introducing many "flavors" of matter fields Φ_a and gauge transformations $e^{i\alpha_a(x)}$ in a similar way.

The terms $\sim E^2 - B^2$ in the action, in analogy with usual Maxwell theory, leads to gapless theories for both scalar and vector charge tensor gauge theories. The massless excitations are analogous to the photons in vector gauge theories, but with more degrees of freedom. As they are associated with a symmetric rank 2 tensor, they are very close cousins to gravitons. The gravitational aspect of fractons is exploited in [15].

It is interesting to look for gapped fractonic theories, since the exactly solvable lattice models in Section 3 are all gapped. The fractonic theory (5.18) can be turned gapped through the Higgs mechanism, generating mass to the gapless excitations. Pursuing a gapped theory, in the next section we investigate Chern-Simons-like theories in 3+1 dimensions. This type of continuum field theory succeeds to provide low-energy descriptions to the lattice models previously seen .

5.2 Chern-Simons and BF-like Theories

BF-theories can be thought as generalizations of Chern-Simons theories for other dimensions. In general, BF theories involve topological interaction terms $A \wedge \mathrm{d}B$, with A a one-form and B a $(D-2)-$form fields in a D dimensional spacetime. For the case in $2+1$ dimensions, dB is the topological conserved current, and the BF term is the current coupling with a vector field A. In this section, however, we study generalizations of this type theory, where we may have the A field as a tensor field. Here we mainly follow [17].

Due to the Levi-Civita symbol structure with only three indices, topological terms between two gauge fields $\epsilon^{\mu\nu\rho} A_\mu \partial_\nu B_\rho$ are defined in $2+1$ dimensions. The generalization to $3+1$ dimensions we look for keeps this structure intact. As its cousins in $2+1$, our theory will have only two spatial components A_1 and A_2. The price to be paid is the rotational symmetry. The system, instead, remains invariant only under discrete rotations now. Actually, the fracton excitations structure itself, as lineons and planons, doesn't obey rotational symmetry.

Consider two component field A_1 and A_2 so that under an U(1) gauge transformation, they transform as

$$A_1 \to A_1 + D_1 \alpha, \quad A_2 \to A_2 + D_2 \alpha \tag{5.22}$$

with D_i a derivative operator. The operators D_i are generalization of the usual ∂_i operators: They may contain more derivatives $\partial_i \partial_j \ldots$. Let the time component of this theory A_0

transform as $A_0 \to A_0 + \partial_t \alpha$. Then, the Chern-Simons Lagrangian is

$$\mathcal{L}_{CS} = \frac{s}{4\pi} \left(A_1 E_2 - A_2 E_1 - (-1)^\eta A_0 B \right), \tag{5.23}$$

where

$$E_i \equiv \partial_t A_i - D_i A_0, \quad \text{and} \quad B \equiv D_1 A_2 - D_2 A_1 \tag{5.24}$$

are the gauge invariant electric and magnetic fields. In the above, $\eta = 1$ if there are even derivatives and $\eta = 2$ if there are an odd number of derivatives in D_i. This takes into account how many integration by parts must be taken so that this theory is gauge invariant. This theory contains gapped degrees of freedom in the bulk with an energy gap $\Delta E \sim s$.

The $\mathcal{L}_{CS}$ Lagrangian is gauge invariant, up to a boundary term

$$\begin{aligned} \delta\mathcal{L}_{CS} &= \frac{s}{4\pi} \left(D_1\alpha E_2 - D_2\alpha E_1 - (-1)^\eta \partial_t \alpha B \right) \\ &= \frac{s}{4\pi} \left(D_1\alpha \partial_t A_2 + (-1)^\eta \partial_t\alpha D_1 A_2 \right. \\ &- \left(D_2\alpha \partial_t A_1 + (-1)^\eta \partial_t \alpha D_2 A_1 \right) \\ &+ \left. D_2\alpha D_1 A_0 - D_1\alpha D_2 A_0 \right), \end{aligned} \tag{5.25}$$

so that, for closed or infinite manifolds, the theory is gauge invariant. If the underlying spacetime manifold contains boundaries, in order to ensure gauge invariance, additional edge degrees of freedom are needed. In this way, as in the case of usual CS theory, higher-rank Chern-Simons-like theory may be very useful in describing fractonic systems with gapless edge excitations. This is the core idea behind bulk-edge correspondence, where the physics in the bulk and the boundary of the system are intrinsically related.

In the absence of matter, the Chern-Simons constraint enforces $B = 0$. The physical observables of this gapped theory are determined by the gauge invariant holonomies $e^{i \int A_i}$. Irrespective the choice of the D_i operators, A_1 and A_2 are conjugated to each other. For A_i compact, we have discrete and compact Wilson operators. In closed manifolds, this a provides large ground state degeneracy. As we will see in the next chapter, this class of theory is able to provide an EFT for the Chamon Code.

Matter is added to the CS Lagrangian by the coupling $\mathcal{L} = \mathcal{L}_{CS} + A_0 \rho - A_i J^i$, provided that the current satisfies

$$\partial_t \rho - D_i J^i = 0. \tag{5.26}$$

BF-like theories constructions can be realized in a similar way. With the appropriate derivative operators D_i such theories are able to describe Type II fractonic order [38]. We consider two gauge fields (A_0, A_1, A_2) and (B_0, B_1, B_2) with the following gauge transformations

$$\begin{aligned} &A_0 \to A_0 + \partial_t \alpha, \quad B_0 \to B_0 - \partial_t \alpha \\ &A_1 \to A_1 + D_1 \alpha, \quad B_1 \to B_1 + \tilde{D}_1 \alpha \\ &A_2 \to A_2 + D_2 \alpha, \quad B_2 \to B_2 + \tilde{D}_2 \alpha \end{aligned} \tag{5.27}$$

where $D_i \equiv D_i^{(e)} + D_i^{(o)}$, $\tilde{D}_i \equiv D_i^{(e)} - D_i^{(o)}$. $D_i^{(e)}$ is a differential operator containing an even number of derivatives whereas $D_i^{(o)}$ an odd number. The BF-like Lagrangian is

$$\mathcal{L}_{BF} = A_0 \left(\tilde{D}_1 B_2 - \tilde{D}_2 B_1\right) + B_0 \left(D_1 A_2 - D_2 A_1\right) + A_1 \partial_t B_2 - A_2 \partial_t B_1. \tag{5.28}$$

Analogously to the Lagrangian (5.23), $\mathcal{L}_{BF}$ is gauge invariant up to boundary terms. In the presence of sources

$$\begin{aligned} \left(\tilde{D}_1 B_2 - \tilde{D}_2 B_1\right) &= \rho_A \\ \left(D_1 A_2 - D_2 A_1\right) &= \rho_B, \end{aligned} \tag{5.29}$$

with ρ_A and ρ_B charges coupled to A and B fields. If D_1 and D_2 do not share any common factor, the constraint suffices to kill any propagating degree of freedom in low-energy physics, leading to a completely gapped theory. The A_1 field is canonically conjugated to B_2 and the same is valid for A_2 and B_1. It may induce nontrivial mutual statistic between ρ_A and ρ_B particles.

In both the Chern-Simons-like and BF-like theories, the form of the derivative operator is the input of the theory and will determine the physics of the excitations. The gauge structure may allow (or not) gapless boundary modes in the theory and the conservation law, on its turn, may restrict (or not) excitation mobility throughout higher multipole momentum conservation.

6 Fracton Effective Theories: Top-Down Approach

In the previous chapter we constructed effective field theories for fracton systems based on symmetries, conservation laws and operator relevance. In this chapter, on the other hand, we shall discuss a top-down approach, i.e., starting from the microscopic theory, we shall derive their corresponding field theory descriptions. The precise map between the lattice and continuum degrees of freedom is able to provide insights not only about fracton physics but in general properties of topological ordered systems.

6.1 Two-dimensional Type-I Fracton System

In this section we will consider gapped fractonic systems in two spatial dimensions. First we propose an exactly solvable lattice model, adapted from the $\mathbb{Z}_N$ Wen plaquette model, which presents fracton phenomenology. Following the approach in Chapter 2, we use the map present in Ref [18] and find a gapped EFT for it. In addition, we generalize such EFT by allowing the existence of higher order derivative operators and study the consequences on the excitations mobility.

Lattice Model

Let us consider a two-dimensional microscopic model defined on a periodic square lattice which presents Type-I fracton phenomenology. In the following, there are $\mathbb{Z}_N$ qubits lying on the sites of both the original and the dual lattices, as shown in Figure 34.

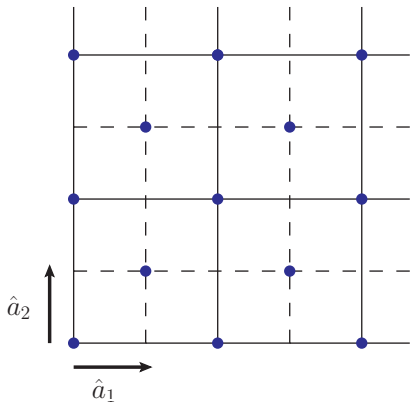

Figura 34 – $\mathbb{Z}_N$ qubits (blue dots) on the sites of the lattice (full lines) and the dual lattice (dashed lines).

The interacting Hamiltonian is given by a sum of plaquette operators

$$H_{frac} = -\frac{h}{2}\sum_{p}\left(\hat{B}_p + \hat{B}_p^{\dagger}\right), \tag{6.1}$$

with

$$\hat{B}_p \equiv X_{p-\hat{a}_1-\hat{a}_2} Z_{p+\hat{a}_1-\hat{a}_2} \mathcal{O}_p X_{p+\hat{a}_1+\hat{a}_2} Z_{p-\hat{a}_1+\hat{a}_2} \quad \text{and} \quad \mathcal{O}_p \equiv \left(X_p^{\dagger}\right)^2 \left(Z_p^{\dagger}\right)^2. \tag{6.2}$$

In the above, p denotes the center of the plaquette and can be located either on the original lattice or on the dual one. The $\mathcal{O}_p$ term is introduced to keep the B_p plaquette operators neutral under the $\mathbb{Z}_N$ group. For the $N = 2$ case, the model results in two copies of the $\mathbb{Z}_2$ Wen Plaquette model. In such case, the system does not exhibit fracton phenomenology. The price for the emergence of fractonic properties is the presence of interactions among multiple $\mathbb{Z}_N$ degrees of freedom in the B_p operators. In the present case, the B_p plaquette operators provide the interaction among five neighboring $\mathbb{Z}_N$ qubits. In this section, we are mainly interested in the $N \neq 2$ case.

This model is exactly solvable, which follows from the fact that all the plaquette operators in the Hamiltonian are compatible. All the possibilities in that two distinct plaquette operators share common sites is depicted in Figure 35. From this, we can immediately check that all the plaquette operators commute.

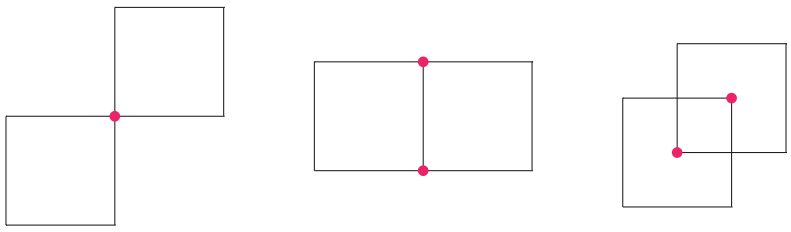

Figura 35 – Basic possibilities for two plaquette operators to share common sites (in red).

The plaquette operators obey $B_p^N = 1$ telling us this is a $\mathbb{Z}_N$ lattice theory. The ground state is such that $B_p |0\rangle = |0\rangle$ for all plaquettes p of the lattice, which is, however, non-unique. In the $N_x \times N_y$ lattice, the dimension of the Hilbert space is $N^{N_x N_y}$. Due to the constraint $\prod_p B_p = e^{i\delta}$, there are $N^{N_x N_y}/N$ independent labels B_p. It indicates us that all the states, including the ground state, are N-fold degenerate.

Excitations above the ground state are well localized in space and correspond to $B_p |\psi\rangle = e^{\frac{2\pi i}{N}} |\psi\rangle$. It is not possible to create isolated excitations through the application of local operators. In addition, isolated particles are completely immobile: they are fractons. There are, as shall see, string operators which are able to move bound states of fractons along straight lines. Therefore, this model corresponds to a Type-I fracton system.

There are two kinds of line operators, characterizing the mobility of two types of lineons. Let γ be a straight line oriented in either vertical or horizontal directions and γ_d

be a rigid line which can cross the plaquettes either in the principal (p.d.) or secondary diagonal (s.d) directions. We define

$$W(\gamma) \equiv \prod_{\gamma} X_i Z_i \quad \text{and} \quad V(\gamma_d) \equiv \begin{cases} \prod_{\gamma_d} X_i, \gamma_d \text{ is oriend with p.d.,} \\ \prod_{\gamma_d} Z_i^\dagger, \gamma_d \text{ is oriend with s.d..} \end{cases} \tag{6.3}$$

The excitations above the ground state created by $W(\gamma)$ and $V(\gamma_d)$ are shown in Figure 36 and Figure 37, respectively. The operator $W(\gamma)$ creates two dipoles, one at each endpoint of the line, which are able to move along the perpendicular direction of the dipole orientation. In contrast, the $V(\gamma_d)$ operator creates two dipoles which are, alone, able to move along the dipole axis.

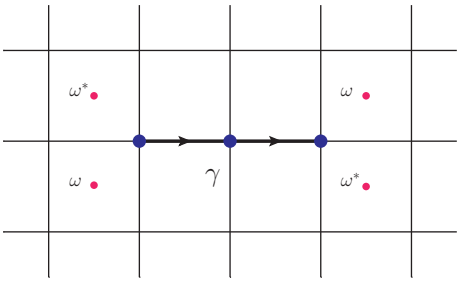

Figura 36 – String operator $W(\gamma)$ (in blue) creating four excitations at its endpoints (in red). Although here γ is oriented with the horizontal direction, a vertical aligned operator is similarly possible.

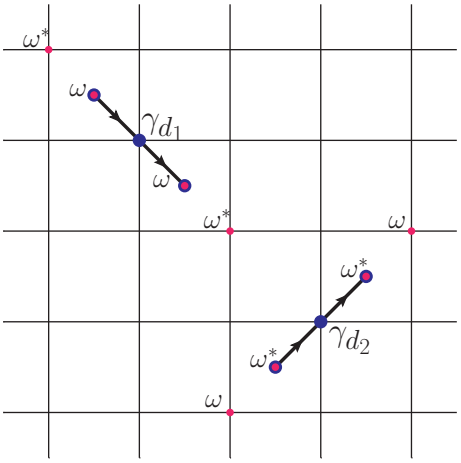

Figura 37 – String operator $V(\gamma_d)$ (in blue) creating four excitations at its endpoints (in red). Above, γ_d is oriented with p.d. and bellow it is parallel to s.d. direction.

The two line operators (6.3), defined on non-contractible loops γ and γ_d obey the algebra

$$V(\gamma_d)W(\gamma) = e^{\frac{2\pi i \rho_a}{N}} W(\gamma)V(\gamma_d), \tag{6.4}$$

where $\rho_a = \text{lcm}(N_x, N_y)/N_a$ for $a = x, y$ depending whether γ is x or y oriented. Since both operators commute with the Hamiltonian, such algebra is responsible for the N-fold degeneracy of the ground state.

The only way to separate fractons apart is through the application of a membrane operator

$$M(\sigma) = \prod_{\tilde{\sigma}} X_i Z_i, \tag{6.5}$$

where $\tilde{\sigma}$ means that we apply $X_i Z_i$ on sites of the lattice and not on the ones of the dual lattice. The membrane creates four fractons, one at each corner of it, as show in Figure 38.

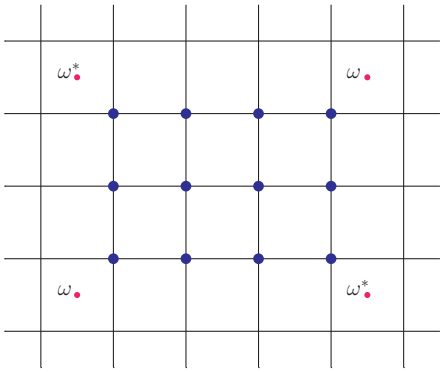

Figura 38 – Creation of four fractons through the application of the membrane operator.

Effective Field Theory

We may find the corresponding EFT for such fractonic model by applying the maps (2.65) and (2.66) with the rescaled field $A \to NA$

$$X_i = \exp iA_2 \quad \text{and} \quad Z_i = \exp -iA_1. \tag{6.6}$$

We get the continuum B operators

$$\hat{B} = \exp ia^2 \left(\partial_{l_2}^2 A_1 - \partial_{l_2}^2 A_2 + \mathcal{O}(a^2)\right) \tag{6.7}$$

and the continuum Hamiltonian

$$H \sim -h \int d^2 l \cos a^2 \left(\partial_{l_2}^2 A_1 - \partial_{l_2}^2 A_2 + ...\right). \tag{6.8}$$

The derivative are defined as $\partial_{l_1} \equiv -\partial_1 - \partial_2$ and $\partial_{l_2} \equiv \partial_1 - \partial_2$. It leads to the Chern-Simons-like effective action

$$S_{CS} = -\frac{N}{2\pi} \int_{T^2 \times \mathbb{R}} d^2 l dt \left[A_1 D_0 A_2 + A_0 \left(D_1 A_2 - D_2 A_1\right)\right], \tag{6.9}$$

with $D_0 \equiv \partial_t$, $D_1 \equiv \partial_{l_1}^2$ and $D_2 \equiv \partial_{l_2}^2$. It is useful to write the above action in a more symmetric way, which resembles the original Chern-Simons theory, namely

$$S_{CS} = -\frac{N}{4\pi} \int_{T^2 \times \mathbb{R}} d^2 l dt \left[A_1 \left(D_0 A_2 - D_2 A_0\right) + A_2 \left(D_1 A_0 - D_0 A_1\right) + A_0 \left(D_1 A_2 - D_2 A_1\right)\right]. \tag{6.10}$$

The non-relativistic character of the above theory leads us to an anisotropic dimensional analysis. Let us set $[l] = -1$ and $[t] = -2$, then

$$[D_0] = [D_i] = 2 \quad \text{and} \quad [A_0] = [A_i] = 1. \tag{6.11}$$

The action (6.10) is invariant under gauge transformations

$$A_0 \to A_0 + D_0\Lambda, \quad A_1 \to A_1 + D_1\Lambda \quad \text{and} \quad A_2 \to A_2 + D_2\Lambda, \tag{6.12}$$

up to boundary terms. A gauge-invariant coupling to external currents is of the form

$$S_{int} = \int dt d^2l \left[A_0 J_0 - A_1 J_1 - A_2 J_2\right], \tag{6.13}$$

provided that they obey the continuity equation

$$\partial_t J_0 = D_1 J_1 + D_2 J_2, \tag{6.14}$$

which leads to the conservation of the global charge $Q = \int d^2l J_0$. In addition, given the form of the derivative operators D_1 and D_2, the generalized charges

$$Q_f \equiv \int d^2l J_0 f(l_1, l_2), \quad \text{with} \quad f(l_1, l_2) = a l_1 l_2 + b l_1 + c l_2, \tag{6.15}$$

are also conserved for arbitrary $a, b, c \in \mathbb{R}$. The existence of such generalized charges gives rise to higher multipole moments conservation and can account for the fracton restricted mobility. The form of $f(l_1, l_2)$ follows from the requirement $\partial_t f = D_1 f = D_2 f = 0$.

To investigate the mobility properties of excitations, let us first consider a single charge localized at $(l_1(t), l_2(t))$:

$$J_0(l_1, l_2, t) = \delta(l_1 - l_1^0(t))\delta(l_2 - l_2^0(t)). \tag{6.16}$$

From previous arguments, the generalized charges (6.15)

$$Q_f = a l_1^0(t) l_2^0(t) + b l_1^0(t) + c l_2^0(t) = cte \tag{6.17}$$

are conserved for all values of the parameters a, b, c. At first sight, it seems that we could find a solution of (6.17) allowing certain mobility for the charges compatible with

$$l_2^0 = \frac{\text{constant} - b l_1^0}{a l_1^0 + c}. \tag{6.18}$$

This solution, however, is not valid for all values of the parameters. Indeed, the case $a = c = 0$ implies

$$l_1^0(t) = \text{constant} \quad \text{and} \quad l_2^0(t) = \text{constant}, \tag{6.19}$$

showing there is no mobility of single charges. Nonetheless, dipole-like objects are able to move. Suppose two opposite charged particles, located at $(l_1^a(t), l_2^a(t))$ in the instant of time t with $a = 1, 2$,

$$J_0 = \delta(l_1 - l_1^1(t))\delta(l_2 - l_2^1(t)) - \delta(l_1 - l_1^2(t))\delta(l_2 - l_2^2(t)). \tag{6.20}$$

The conservation of charges in (6.15) yields to

$$a(l_1^1 l_2^1 - l_1^2 l_2^2) + b(l_1^1 - l_1^2) + c(l_2^1 - l_2^2) = cte, \tag{6.21}$$

where time dependence is implicit. In contrast to the previous case, there are non-constant solutions for arbitrary a, b and c, e.g.,

$$l_2^1(t) = l_2^2(t) = cte \quad \text{and} \quad l_1^1(t) = \frac{cte}{b} + l_1^2(t), \tag{6.22}$$

showing that dipole bound states may be mobile through the system. This mobility is represented by the Wilson lines (6.3)

$$W(\gamma) = e^{-i\int_\gamma A_1 dl^i}. \tag{6.23}$$

Bulk-Edge Correspondence

So far, we have studied the system defined on a closed manifold (torus), i.e., in a manifold without boundaries. The fact that the effective action (6.10) is invariant under gauge invariant up to total derivatives implies that in a manifold with a boundary, there may be gapless degrees of freedom living at the edges. The peculiar form of the derivative operators in (6.10) naturally rises the question about the properties of the edge states.

Let us consider the system defined on the manifold $\Omega \times \mathbb{R}$, with $\Omega = \{(l_1, l_2) | \, l_1 \in \mathbb{R}, l_2 \leq 0\}$. In the presence of boundaries, the theory (6.10) is no longer invariant under (6.12), instead it changes by

$$\begin{aligned} \delta S_{CS} &= -\frac{N}{4\pi}\int dt d^2 l \partial_{l_2} \left[(\partial_{l_2}\Lambda)(D_1 A_0 - D_0 A_1) - \Lambda \partial_{l_2}(D_1 A_0 - D_0 A_1) \right] \\ &= -\frac{N}{4\pi}\int dt dl_1 \left[(\partial_{l_2}\Lambda)(D_1 A_0 - D_0 A_1)\Big|_{l_2=0} - \Lambda \partial_{l_2}(D_1 A_0 - D_0 A_1)\Big|_{l_2=0} \right] \end{aligned} \tag{6.24}$$

We see that $\delta S = 0$ only for restricted gauge transformations with

$$\Lambda\Big|_{l_2=0} = 0 \quad \text{and} \quad \partial_{l_2}\Lambda\Big|_{l_2=0} = 0. \tag{6.25}$$

Alternatively, we can restore gauge invariance by introducing an edge action S_{edge} and demanding that the whole system $S_{CS} + S_{edge}$ is gauge invariant, that is, $\delta S_{CS} = -\delta S_{edge}$ (see, for example [39]). We consider an edge action involving two scalar fields ϕ and $\tilde{\phi}$:

$$S_{edge} = \frac{N}{4\pi}\int dt dl_1 \left[\tilde{\phi}(D_1 A_0 - D_0 A_1)\Big|_{l_2=0} - \phi\left(D_1 \tilde{A}_0 - D_0 \tilde{A}_1\right)\Big|_{l_2=0} \right], \tag{6.26}$$

where we have defined $\tilde{A}_\mu\Big|_{l_2=0} \equiv \partial_{l_2} A_\mu\Big|_{l_2=0}$. Under a gauge transformation, the variation this action cancels precisely δS_{CS} in (6.24) provided that the scalar fields transforms as

$$\phi \to \phi + \Lambda \quad \text{and} \quad \tilde{\phi} \to \tilde{\phi} + \partial_{l_2}\Lambda. \tag{6.27}$$

In this way, the whole action $S_{CS} + S_{edge}$ is gauge invariant.

We wish to extract the physical content of the edge action (6.26). With this purpose, we shall examine eventual gauge invariance exclusive of the edge action (without involving the bulk action). If this is the case, it can be used to get rid of gauge degrees of freedom at the edge. The action (6.26) is invariant under the gauge transformations

$$A_\mu \to A_\mu + D_\mu \alpha \quad \text{and} \quad \tilde{A}_\mu \to \tilde{A}_\mu + D_\mu \tilde{\alpha}, \quad \text{for } \mu = 0, 1. \tag{6.28}$$

This allows us to fix the gauge as

$$A_0\Big|_{l_2=0} = vA_1\Big|_{l_2=0} \quad \text{and} \quad \tilde{A}_0\Big|_{l_2=0} = \tilde{v}\tilde{A}_1\Big|_{l_2=0}. \tag{6.29}$$

In this way, the edge action becomes

$$S_{edge} = \frac{N}{4\pi}\int dt dl_1 \left[\tilde{\phi}\left(vD_1 - D_0\right)A_1 - \phi\left(\tilde{v}D_1 - D_0\right)\tilde{A}_1\right]. \tag{6.30}$$

There is still a residual gauge invariance that preserves the gauge choice (6.29), namely, transformations of the form (6.28) but now with the gauge functions satisfying $\left(D_0 - vD_1\right)\alpha = 0$ and $\left(D_0 - \tilde{v}D_1\right)\tilde{\alpha} = 0$. These residual transformations imply that not all the fields in the above action are physical. In fact, let us consider the equations of motion for $\phi, \tilde{\phi}, A_1$ and $\tilde{A}_1$,

$$\begin{aligned}
\phi:\ &\left(\tilde{v}D_1 - D_0\right)\tilde{A}_1 = 0 \quad &\Rightarrow \quad &\tilde{A}_1\left(\frac{l_1^2}{2} + \tilde{v}t\right),\\
\tilde{\phi}:\ &\left(vD_1 - D_0\right)A_1 = 0 \quad &\Rightarrow \quad &A_1\left(\frac{l_1^2}{2} + vt\right),\\
A_1:\ &\left(vD_1 + D_0\right)\tilde{\phi} = 0 \quad &\Rightarrow \quad &\tilde{\phi}\left(\frac{l_1^2}{2} - vt\right),\\
\tilde{A}_1:\ &\left(\tilde{v}D_1 + D_0\right)\phi = 0 \quad &\Rightarrow \quad &\phi\left(\frac{l_1^2}{2} - \tilde{v}t\right).
\end{aligned} \tag{6.31}$$

As A_1 and $\tilde{A}_1$ have the same dependence on coordinates as the functions α and $\tilde{\alpha}$, respectively, the residual gauge invariance can be used to eliminate both A_1 and $\tilde{A}_1$. Therefore, the boundary action contains two physical propagating degrees of freedom ϕ and $\tilde{\phi}$ with "velocities"v and $\tilde{v}$, respectively. There are two special cases that are interesting:

- For $\tilde{v} = v$, we can use the residual gauge invariance to fix $A_1 = \tilde{A}_1$ so that

$$\begin{aligned}
S_{edge} &= \frac{N}{4\pi}\int dt dl_1 \left(\tilde{\phi} - \phi\right)\left(vD_1 - D_0\right)A_1\\
&= \frac{N}{4\pi}\int dt dl_1 \varphi\left(vD_1 - D_0\right)A_1.
\end{aligned} \tag{6.32}$$

  In this case, the two scalar fields combine into a single field $\varphi \equiv \tilde{\phi} - \phi = \varphi\left(l_1^2/2 - vt\right)$ that propagates along the edge.

- For $\tilde{v} = -v$, we are able to fix $A_1 = \phi$ and $\tilde{A}_1 = \tilde{\phi}$, so that the resulting theory is

$$\begin{aligned} S_{edge} &= \frac{N}{4\pi}\int dtdl_1 \left[\tilde{\phi}\left(vD_1 - D_0\right)\phi - \phi\left(-vD_1 - D_0\right)\tilde{\phi}\right] \\ &= \frac{N}{2\pi}\int dtdl_1 \tilde{\phi}\left(vD_1 - D_0\right)\phi. \end{aligned} \tag{6.33}$$

We see that the bulk-edge correspondence leads to unusual propagating degrees of freedom in the edge of the system. In fact, the equation of motion for such fields is the heat dispersion equation in one spatial dimension. Further investigation of the meaning and implications of this fact are currently under investigation.

Generalized derivative operators EFTs

Modifications in the structure of the derivative operator which appears in the CS or BF theories may give rise to restricted mobility, and consequently, fracton phenomenology. This were the case of the $2D$ Type-I model (6.10) previously studied, where we considered second order derivative operators. In this section we generalize such model and consider

$$D_1 \equiv \partial_1^n, \quad D_2 \equiv \partial_2^n \quad \text{for } n \in \mathbb{N} \quad \text{and} \quad D_0 \equiv \partial_t. \tag{6.34}$$

In this fashion, the action defined on compact manifolds

$$\begin{aligned} S = -\frac{N}{4\pi}\int d^2xdt \left[(-1)^n A_1\left(D_0A_2 - D_2A_0\right) + (-1)^n A_2\left(D_1A_0 - D_0A_1\right)\right. \\ \left. + A_0\left(D_1A_2 - D_2A_1\right)\right], \end{aligned} \tag{6.35}$$

describes a gapped system and remains invariant under gauge transformations

$$\begin{aligned} A_i &\to A_i + D_i\lambda \\ \text{and} \quad A_0 &\to A_0 + D_0\lambda. \end{aligned} \tag{6.36}$$

Excitations can be introduced through the coupling to external currents $\int d^3x[A_0J_0 + A_1J_1 + A_2J_2]$, which is gauge invariant provided that the continuity equation is satisfied

$$\partial_t J_0 = (-1)^n D_1J_1 + (-1)^n D_2J_2. \tag{6.37}$$

This leads to the conservation of the global charge, $\int d^2x J_0$. In addition, the form of the derivative operators in this equation implies that there is also a generalized conserved charge

$$Q_P = \int d^2x J_0(x,t)P(x), \tag{6.38}$$

where $P(x)$ is an arbitrary polynomial of degree $n-1$ in spatial coordinates, i.e, it satisfies $\partial_t P = D_1P = D_2P = 0$. This extra conserved charge associated with the polynomial P is closely related to the conservation of multipole moments [15]. Indeed, consider a

theory with charged matter described in terms of a complex scalar field $\Phi = \rho e^{i\phi}$. Next we consider a shift transformation of the form

$$\delta\phi = \sum_{I,a} \lambda_a^I P^{I,a}(x), \tag{6.39}$$

where $P^{I,a}(x)$ is a polynomial, with the index I corresponding to its order and the index a labeling distinct polynomials of the same order I. If this transformation corresponds to a symmetry of the theory, then the quantity (6.38) is the associated Noether charge [38]. For the case in which the polynomials are homogeneous, namely,

$$P^{I,a}(x_1, x_2) = \sum_{\substack{q_1,q_2 \\ q_1+q_2=I}} \mu^{I,a}_{q_1,q_2} \left(x_1\right)^{q_1} \left(x_2\right)^{q_2}, \tag{6.40}$$

the conserved charges $Q^{I,a}$ are the components of multipole moments

$$\int d^2x \underbrace{\frac{\partial \mathcal{L}_{matter}}{\partial\left(\partial_0\phi\right)}}_{\rho(x)} \delta\phi \quad \Rightarrow \quad Q^{I,a} \equiv \sum_{q_1,q_2} \int d^2x \mu^{I,a}_{q_1,q_2}(x_1)^{q_1}(x_2)^{q_2}\rho(x). \tag{6.41}$$

Effective field theories with the derivative operators (6.34) conserve all the 2^I-pole moments, for $I \leq n-1$. They describe Type-I fracton systems with the line operators

$$W \sim e^{i\int A_i dx^i}, \tag{6.42}$$

which correspond to the motion of the 2^{n-1}-pole bound states.

We can further generalize the fractonic effective field theories by considering derivative operators that mix the spatial derivatives, for example,

$$D_1 = \partial_1^2 + \partial_2^2 \quad \text{and} \quad D_2 = \partial_1\partial_2, \tag{6.43}$$

which are able to annihilate the polynomial

$$f(x,y) = a\left(x_1^2 - x_2^2\right) + bx_1 + cx_2 + d. \tag{6.44}$$

The additional structure $x^2 - y^2$ of the above expression compared to the previous case with $n = 2$ (see (6.15)) yields to the conservation not only of the dipole moment, but also the diagonal elements of the quadrupole moment

$$Q_{ij} = \int d^2x \left(2x_ix_j - \vec{x}\cdot\vec{x}\delta_{ij}\right)\rho(x). \tag{6.45}$$

Such extra conservation law restricts, still more, the mobility of the dipole bound states. As we shall discuss below, dipoles can only move along horizontally or vertically oriented directions.

The gauge invariant line operators $e^{i\int dx_1 A_2}$ and $e^{i\int dx_2 A_2}$ create dipole bound states which are able to move in the horizontal and vertical directions, while $e^{i\int dl_1(A_1-2A_2)}$

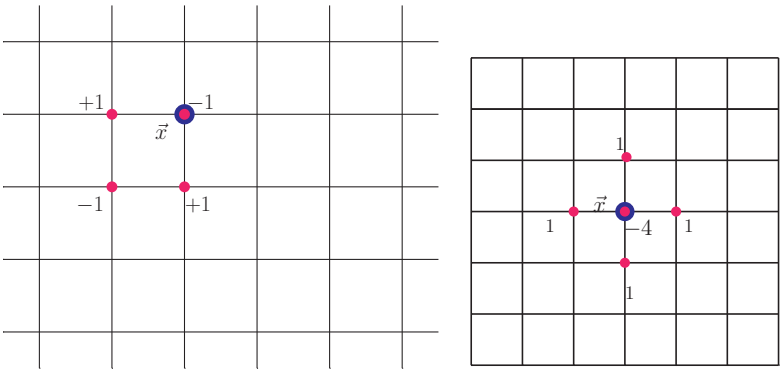

Figura 39 – The application of the $e^{iA_2(x)}$ and $e^{iA_1(x)}$ operators above the ground state.

and $e^{i\int dl_2(A_1+2A_2)}$ create quadrupole bound states which are able to move along diagonal directions. To see it, we investigate the excitations above the ground state created by the operators e^{iA_1} and e^{iA_2}. It is useful to note that there are no excitations at the vacuum $J_0\left|0\right\rangle = 0$ and that

$$\begin{aligned}\left[e^{iA_2(\vec{x})}, J_0\left(\vec{x}'\right)\right] &= \frac{N}{2\pi}\left[e^{iA_2(\vec{x})}, D_1A_2 - D_2A_1\left(\vec{x}'\right)\right] \\ &= -\frac{N}{2\pi}D_2'\left[e^{iA_2(\vec{x})}, A_1\left(\vec{x}'\right)\right] \\ &= -iD_2'\frac{\delta}{\delta A_2\left(\vec{x}'\right)}e^{iA_2(\vec{x})} \\ &= \left(\partial_{1'}\partial_{2'}\right)\delta\left(\vec{x}-\vec{x}'\right)e^{iA_2(\vec{x})}.\end{aligned} \tag{6.46}$$

In this fashion, by discretizing the two-dimensional space into a square lattice with a "lattice spacing"a, we see that the e^{iA_2} operator creates four excitations above the vacuum

$$\begin{aligned}J_0\left(\vec{x}'\right)e^{iA_2(\vec{x})}|0\rangle = -\frac{1}{a^2}\Big(\delta(x_1-x_1'-a)-\delta(x_1-x_1')\Big)\times \\ \Big(\delta(x_2-x_2'-a)-\delta(x_2-x_2')\Big)e^{iA_2(\vec{x})}|0\rangle.\end{aligned} \tag{6.47}$$

A similar analysis shows us that the operator e^{iA_1} creates the following charge pattern

$$\begin{aligned}J_0\left(\vec{x}'\right)e^{iA_1(\vec{x})}|0\rangle = \frac{1}{a^2}\Big[\Big(\delta(x_1-x_1'-a)-2\delta(x_1-x_1')+\delta(x_1-x_1'+a)\Big)\delta(x_2-x_2') \\ +\Big(\delta(x_2-x_2'-a)-2\delta(x_2-x_2')+\delta(x_2-x_2'+a)\Big)\delta(x_1-x_1')\Big]e^{iA_1(\vec{x})}|0\rangle\end{aligned} \tag{6.48}$$

The Figure 39 (a) and (b) show, in units of $1/a^2$, the charge distribution created by $e^{iA_2(\vec{x})}$ and $e^{iA_1(\vec{x})}$, respectively. In addition, in the Figures 40 (a) and (b) we illustrate how the application of the operators e^{iA_2} and $e^{A_1-2A_2}$ in consecutive sites are able to move particle bound states around. In the figures, the blue dots represent the sites $\vec{x}$ where the operators are applied and the red dots indicate excitations.

Such charge configurations and mobility are in complete in agreement with the conservation laws. For a two particle configuration

$$J_0 = q\delta(x_1-x_1^1(t))\delta(x_2-x_2^1(t)) - q\delta(x_1-x_1^2(t))\delta(x_2-x_2^2(t)), \tag{6.49}$$

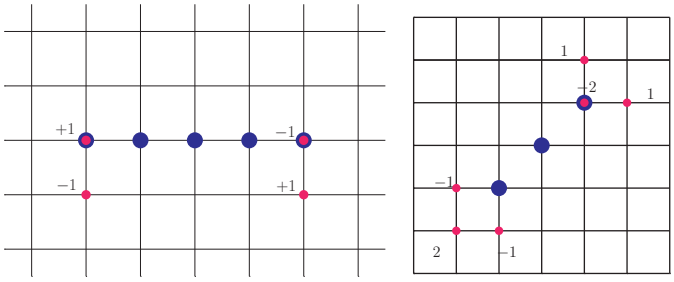

Figura 40 – (a) A string of the operator e^{iA_2} is able to move the dipole bound states along a line while (b) a string of $e^{A_1-2A_2}$ is able to move quadrupole bound states along the diagonal direction.

the Noether conserved charges following from the shift symmetry under (6.44) impose that

$$cte = qa((x_1^1)^2 - (x_1^2)^2 - (x_2^1)^2 + (x_2^2)^2) + b(x_1^1 - x_1^2) + c(x_2^1 - x_2^2). \tag{6.50}$$

The non-trivial solutions of such equation, for all a, b and c in $\mathbb{R}$ is

$$x_2^{(1)}(t) = cte, \quad x_2^{(2)}(t) = cte \quad \text{and} \quad x_1^{(1)}(t) = x_1^{(2)}(t), \tag{6.51}$$

which is precisely the movement described by the line operator $e^{i\int dx_1 A_2(x)}$ in Figure 40 (a).

6.2 X-Cube Model

In Section 3, we have studied the lattice description of the X-Cube model. A natural question that arises is: are we able to write down a continuum field theory that captures the phenomenology of such model? In this section we will see that it is possible to find such EFT, which resembles a CS topological field theory. In this discussion, we mainly follow Ref [16].

Let us consider the $\mathbb{Z}_N$ generalization of the X-Cube model (See Appendix A for a review of $\mathbb{Z}_N$ Pauli operators). The Hamiltonian is given by

$$\hat{H}_{\text{X-cube}} = -\sum_{\ell}\left(\hat{\mathcal{B}}_\ell + \hat{\mathcal{B}}_\ell^\dagger\right) - \sum_{\ell,a}\left(\hat{\mathcal{A}}_\ell^{(a)} + \hat{\mathcal{A}}_\ell^{(a)\dagger}\right), \tag{6.52}$$

where $\ell = (\mathbf{x}, a)$ denotes a link in the $3D$ lattice in terms of the site $\mathbf{x}$ and the direction $a = 1, 2, 3$. The operators $\hat{\mathcal{B}}_\ell$ and $\hat{\mathcal{A}}_\ell$ are the $\mathbb{Z}_N$ cube and star analogous of (17) and are defined according to Figure 41. The Figure 41 were adapted from Ref. [16].

The process of finding the X-Cube model EFT is very similar to the process we developed in Chapter 2 for the Toric Code and Wen Plaquette model. The lattice degrees

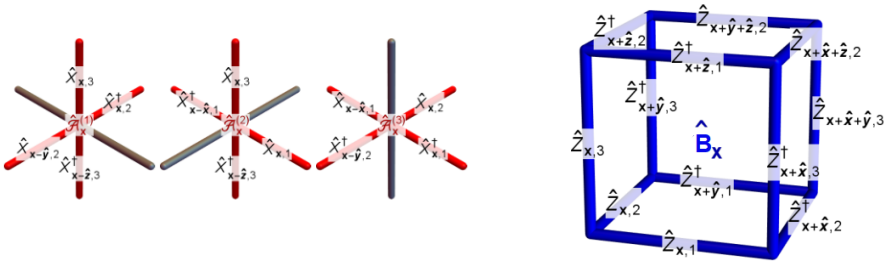

Figura 41 – $\mathbb{Z}_N$ cube and star operators of the X-Cube model.

of freedom are roughly given in terms of real-valued $U(1)$ continuum variables

$$\begin{aligned}
\hat{Z}_{\mathbf{x},a}(t) &\sim \exp\left(\mathrm{i}\int_a^{\prime} Z_a(t,\mathbf{x})\right),\\
\hat{X}_{\mathbf{x},a}(t) &\sim \exp\left(\mathrm{i}\int_{\perp a}^{\prime\prime} X^a(t,\mathbf{x})\right),\\
\hat{\mathcal{B}}_{\mathbf{x}}(t) &\sim \exp\left(\frac{2\pi\mathrm{i}}{N}\int^{\prime} i^0(t,\mathbf{x})\right),\\
\hat{\mathcal{A}}^{(a)}_{\mathbf{x}}(t) &\sim \exp\left(\frac{2\pi\mathrm{i}}{N}\int^{\prime\prime} j^{0;a}(t,\mathbf{x})\right).
\end{aligned} \tag{6.53}$$

In the above relations, we introduced continuum sources i^0 and $j^{0,a}$ for cube and star excitations. Roughly, the integral $\int_a^{\prime}$ is performed over the link $\ell = (\mathbf{x}, a)$, and $\int_{\perp a}^{\prime\prime}$ is performed on the dual plaquette, orthogonal to $\ell = (\mathbf{x}, a)$. Finally, $\int^{\prime}$ integrates over the cube centered at $\mathbf{x}$ and $\int^{\prime\prime}$ integrates over the plaquette centered at $\mathbf{x}$ and orthogonal to a. In $j^{0;a}$, the semicolon is used to indicate that the a index does not transform under spacetime transformations.

The $\mathbb{Z}_N$ Pauli algebra implies nontrivial equal-time commutation relations between Z and X fields

$$\left[Z_a(t,\mathbf{x}), X^b\left(t,\mathbf{x}'\right)\right] = \frac{2\pi\mathrm{i}}{N}\delta_a^b\delta^3\left(\mathbf{x}-\mathbf{x}'\right). \tag{6.54}$$

From the operators $\hat{\mathcal{A}}_{\mathbf{x}}$ and $\hat{\mathcal{B}}_{\mathbf{x}}$ operators and the definitions in (6.53), we see that

$$i^0 = \frac{N}{2\pi}\left|\epsilon^{0abc}\right|\frac{1}{2}\partial_a\partial_b Z_c \quad \text{and} \quad j^{0;a} = \frac{N}{2\pi}\sum_{b,c}\epsilon^{0abc}\partial_c X^c. \tag{6.55}$$

We can immediately construct a theory which is able to give the above relations (6.54) and (6.55) as

$$\begin{aligned}
\tilde{L}_{\text{X-cube}} = &\frac{N}{2\pi}X^a\partial_0 Z_a + X_0\frac{N}{2\pi}\left|\epsilon^{0abc}\right|\frac{1}{2}\partial_a\partial_b Z_c + Z_{0;a}\frac{N}{2\pi}\epsilon^{0abc}\partial_c X^c\\
&- Z_{0;a}j^{0;a} - Z_a j^a - X_0 i^0 - X^a i_a.
\end{aligned} \tag{6.56}$$

The first term is responsible to lead to (6.54) under quantization, while the X_0 and $Z_{0;a}$ terms are responsible to ensure (6.55) through Lagrange multipliers. The other two terms $Z_a j^a$ and $X^a i_a$ are generic coupling of the Z and X fields. The lattice constraint

$\prod_a \hat{\mathcal{A}}^{(a)} = 1$ implies $\sum_a j^{0;a} = 0$, which follows directly from the definition (6.55). It also implies that the multipliers obey $\sum_a Z_{0;a} = 0$.

In order to write (6.56) in a more familiar way, let us redefine the fields as

$$\begin{aligned} A_{0;a} &\equiv Z_{0;a}, & J^{0;a} &\equiv j^{0;a}, \\ A_a &\equiv Z_a, & J^a &\equiv j^a, \\ B_0 &\equiv X_0, & I^0 &\equiv i^0, \\ B_{ab} &\equiv |\epsilon_{0abc}|\, X^c, & I^{ab} &\equiv \left|\epsilon^{0abc}\right| i_c, \\ X^a &\equiv \left|\epsilon^{0abc}\right| \tfrac{1}{2} B_{bc}, & i_a &\equiv |\epsilon_{0abc}|\, \tfrac{1}{2} I^{bc}. \end{aligned} \tag{6.57}$$

In terms of such variables, the EFT for the X-cube model is given by

$$\begin{aligned} S_{\text{X-Cube}} = \frac{N}{2\pi} \int d^4x \left(\left|\epsilon^{0abc}\right| \frac{1}{2} B_{ab} \partial_0 A_c + B_0 \left|\epsilon^{0abc}\right| \frac{1}{2} \partial_a \partial_b A_c + A_{0;a} \epsilon^{0abc} \partial_c B_{ab} \right) \\ - \int d^4x \left(A_{0;a} J^{0;a} + A_a J^a + B_0 I^0 + B_{ab} \frac{1}{2} I^{ab} \right), \end{aligned} \tag{6.58}$$

with the constraint $\sum_a A_{0;a} = 0$.

The conserved charges $\int_{\mathbf{x}'} I^0(t, \mathbf{x}')$ and $\int_{\mathbf{x}'} J^{0;b}(t, \mathbf{x}')$ induce a local transformation on the fields

$$\begin{aligned} B_{ab}(t, \mathbf{x}) &\to B_{ab}(t, \mathbf{x}) + \mathrm{i} \int_{\mathbf{x}'} [B_{ab}(t, \mathbf{x}), \underbrace{\frac{N}{2\pi} \left|\epsilon^{0cde}\right| \frac{1}{2} \partial'_c \partial'_d A_e \left(t, \mathbf{x}'\right)}_{I^0(t, \mathbf{x}')}] \chi\left(t, \mathbf{x}'\right) \\ &= B_{ab} + \partial_a \partial_b \chi \end{aligned} \tag{6.59}$$

$$\begin{aligned} A_a(t, \mathbf{x}) &\to A_a(t, \mathbf{x}) + \mathrm{i} \int_{\mathbf{x}'} [A_a(t, \mathbf{x}), \underbrace{\frac{N}{2\pi} \epsilon^{0bcd} \partial'_d B_{bc} \left(t, \mathbf{x}'\right)}_{J^{0;b}(t, \mathbf{x}')}] \zeta_b\left(t, \mathbf{x}'\right) \\ &= A_a - \epsilon^{0abc} \partial_a \zeta_c. \end{aligned} \tag{6.60}$$

Provided that the Lagrange multipliers transform as $A_{0;a} \to A_{0;a} + \partial_0 \zeta_a$, $B_0 \to B_0 + \partial_0 \chi$ and the currents satisfy appropriate conservation laws (see below), the theory (6.58) is gauge invariant. In order to the constraint on $A_{0;a}$ be consistent, we must have $\sum_a \zeta_a = 0$.

We see that the EFT for the X-Cube model resembles a topological BF theory, but with slight differences. This is appropriate since, the topological robustness of fracton phases require a topological description but its UV sensitivity forbids the EFT to be an absolute TQFT.

Conservation Laws

Let us investigate how the conservation laws impose restrictions on the excitations mobility. The conservation laws for the currents I and J are

$$\partial_0 I^0 - \frac{1}{2} \partial_a \partial_b I^{ab} = 0 \tag{6.61}$$

$$\partial_0 J^{0;a} + \epsilon^{0abc} \partial_c J^c = 0. \tag{6.62}$$

The EFT does capture the lattice fracton creation phenomenology. Indeed, the current

$$\begin{aligned} I^0 &= \sum_{\mu,\nu=\pm 1} \mu\nu\theta(t)\delta(x-\mu a)\delta(y-\nu a)\delta(z), \\ I^{12} &= \delta(t)\theta(a+x)\theta(a-x)\theta(a+y)\theta(a-y)\delta(z), \\ I^{23} &= I^{13} = 0 \end{aligned} \tag{6.63}$$

describes the creation process of four fracton excitations at $t = 0$ at the positions $\mathbf{x} = (\pm a, \pm a, 0)$. Note that I_{12} is non-zero only for $t = 0$, which is when the process takes place. Analogously, the current which describes a z-lineon moving along the z-axis is given by

$$\begin{aligned} J^{0;1} &= -J^{0;2} = J^3/v = \delta(x)\delta(y)\delta(z-vt), \\ J^{0;3} &= J^1 = J^2 = 0. \end{aligned} \tag{6.64}$$

The fusion rules between star excitations (4.23) is also recovered by the EFT. Let us consider both an x- and an y-lineon at the origin

$$J^{0;b} = \sum_{a=1,2} \sum_{c=1,2,3} \epsilon^{0abc}\delta(x)\delta(y)\delta(z) \quad \text{and} \quad J^b = 0. \tag{6.65}$$

We see that, performing the sum, it is equivalent to a $z-$lineon

$$J^{0;b} = -\sum_{c} \epsilon^{03bc}\delta(x)\delta(y)\delta(z). \tag{6.66}$$

It is possible to show that the ground state degeneracy can be recovered by the EFT and is a generalization of (3.4) to the $\mathbb{Z}_N$ case. Since the continuum field theory (6.58) has an infinite ground state degeneracy, we regularize it by introducing a short-distance cutoff a. The topological operators with nontrivial commutation relations on a $L_1 \times L_2 \times L_3$ 3-torus allow us to count the ground state space dimension

$$\log_N DGS = 2L_1/a + 2L_2/a + 2L_3/a - 3. \tag{6.67}$$

The -3 factor comes from a redundancy between the topological operators, analogously to (3.6). Further details of the calculations can be found in [16].

6.3 Chamon Code

In Section 5.2 we discussed an effective field theory with the potential to describe the low-energy physics of the Chamon code. The EFT was proposed based in general arguments of operators relevance, symmetries and conservation laws. In the work presented in [18], a generalization for odd dimensions of the Chamon code is presented, as well as a precise way to find the continuous descriptions of the lattice models. In this section

we review their construction and use an explicit map between the lattice and continuum degrees of freedom in order to find a EFT for Chamon code in 3 dimensions.

We map the Pauli operators $P^i_{\vec{x}}$ defined in the microscopic model to continuous fields $A_a(\vec{x})$ as

$$P^i_{\vec{x}} = \exp\Big(it^i_a K_{ab} A_b(\vec{x})\Big), \tag{6.68}$$

with $K = (K_{ab})$ a 2×2 invertible matrix to be determined and $t^i = (t^i_a) = (t^i_1, t^i_2)$ three two-component vectors for $i = 1, 2, 3$. Because Pauli operators 'redundancies' $X_{\vec{x}} Y_{\vec{x}} \sim Z_{\vec{x}}$, the t vectors must satisfy $\sum_{j=1}^{3} t^j_a = 0$. We choose

$$t^i_a = \delta^i_a, \text{ for } i, a = 1, 2 \quad \text{and} \quad t^3_a = -1 \quad \text{for } a = 1, 2. \tag{6.69}$$

In order to this map hold, the $A_i(\vec{x})$ fields must replicate the Pauli matrices algebra. Let $x, y \in \Lambda_{even}$

$$P^i_{\vec{x}} P^j_{\vec{y}} = \exp\Big(it^i_a K_{ab} A_b(\vec{x})\Big) \exp\Big(it^j_c K_{cd} A_d(\vec{y})\Big). \tag{6.70}$$

Using the BCH theorem and imposing that the resulting commutator is a c-number $e^A e^B = e^{[A,B]} e^B e^A$ we have

$$P^i_{\vec{x}} P^j_{\vec{y}} = \exp\Big(-[t^i_a K_{ab} A_b(\vec{x}), t^j_c K_{cd} A_d(\vec{y})]\Big) P^j_{\vec{y}} P^i_{\vec{x}}. \tag{6.71}$$

The different Pauli operators must commute for different sites $\vec{x}$ and $\vec{y}$, but anti commute for $\vec{x} = \vec{y}$. In order this to be true in the $A_i(\vec{x})$ picture, we demand that

$$[t^i_a K_{ab} A_b(\vec{x}), t^j_c K_{cd} A_d(\vec{y})] = i\pi \delta_{\vec{x}\vec{y}} \quad \Rightarrow \quad [A_b(\vec{x}), A_d(\vec{y})] \equiv \pi i \left(K^{-1}\right)_{bd} \delta_{\vec{x}\vec{y}}, \tag{6.72}$$

together with the condition that

$$t^i_a \left(K^T\right)_{ab} t^j_b = \begin{cases} 1 \mod 2, & i \neq j \\ 0 \mod 2, & i = j. \end{cases} \tag{6.73}$$

The commutation relation between the A_1 and A_2 fields can be thought as the canonical commutation relation at equal times, ensuring that the momentum conjugated to the $A_a(\vec{x})$ field is

$$\Pi_a(\vec{x}) = \frac{1}{\pi} (K^T)_{ab} A_b. \tag{6.74}$$

The general idea is to replace the Pauli operators in the microscopic model (3.9) for two independent fields $A_1(\vec{x})$ and $A_2(\vec{x})$. The octahedron operators (3.8) at the site $\vec{x}$ are translated in the field theory counterpart as

$$S_{\vec{x}} = \exp i \left(\sum_{j=1}^{3} t^j_a K_{ab} A_b\left(\vec{x} + \hat{x}_j\right) + t^j_a K_{ab} A_b\left(\vec{x} - \hat{x}_j\right) \right). \tag{6.75}$$

Since this operator involves the product of the Pauli operators in different sites, which trivially commute with each other, the BCH formula is not needed in order to arrange all the A fields in the same exponential argument.

The exactly solvable character of the microscopic model is one of the key aspects of the theory, which follows the trivial commutation among all octahedron operators. In the EFT, this impose restrictions on the matrix K.

Let us consider two sites $\vec{x}$ and $\vec{x}+\hat{x}_i+\hat{x}_j$, with $i \neq j$ belonging to Λ_{odd}. In this case, the octahedron operators $S_{\vec{x}}$ and $S_{\vec{x}+\hat{x}_i+\hat{x}_j}$ share two sites: the site at $\vec{x}+\hat{x}_i$ and the one at $\vec{x}+\hat{x}_j$. Imposing that $[S_{\vec{x}}, S_{\vec{x}+\hat{x}_i+\hat{x}_j}] = 0$, follows from (6.75)

$$C_{ij} = t_a^i K_{ab} t_b^j + t_a^j K_{ab} t_b^i \equiv 0 \tag{6.76}$$

For the case in witch $i = j$, it is zero automatically from (6.73) and tell us that $K_{11} = K_{22} = 0$. For the case in which $i \neq j$ it gives us information about the off-diagonal elements. For $i = 1$ and $j = 2$ we see that $K_{12} = -K_{21}$. Thus, the K matrix is an anti symmetric 2×2 matrix, which we write as

$$K = \begin{pmatrix} 0 & k \\ -k & 0 \end{pmatrix} \quad \text{and} \quad K^{-1} = \begin{pmatrix} 0 & -\frac{1}{k} \\ \frac{1}{k} & 0 \end{pmatrix}. \tag{6.77}$$

We now take the continuum limit of the model. Let a be the lattice spacing length and let us replace the unitary vectors $\hat{x}_i$ that measures the distances between sites by $\vec{a}_i = (a_i^1, a_i^2, a_i^3) \equiv a\hat{x}_i$. In the continuum limit $a \to 0$ we Taylor expand the A_b fields in the $\vec{x} \pm \vec{a}_j$ sites:

$$A_b\left(\vec{x} \pm \vec{a}_j\right) = A_b(\vec{x}) \pm \sum_i a_j^i \partial_i A_b + \frac{1}{2} \sum_{i,k} a_j^i a_j^k \partial_i \partial_K A_b + \cdots . \tag{6.78}$$

Higher orders of derivatives are suppressed by higher powers of a. Let us replace the field expansion and the components for the $\vec{a}_i$ vectors $a_i^j = a\delta_i^j$ in (6.75)

$$S_{\vec{x}} = \exp i \left(\sum_{j=1}^{3} t_a^j K_{ab} \partial_j^2 A_b + \cdots \right). \tag{6.79}$$

All the terms with odd order in derivatives cancel due to the contributions of $A_b(\vec{x}+\vec{a}_j)$ and $A_b(\vec{x}-\vec{a}_j)$ in (6.75). The zero-th order term is canceled due to the condition that $\sum_j t_a^j = 0$:

$$2 \sum_{j=1}^{3} t_a^j K_{ab} A_b\left(\vec{x}\right) = 2 K_{ab} A_b(\vec{x}) \sum_{j=1}^{3} t_a^i = 0. \tag{6.80}$$

Thus, in the continuum limit, the Hamiltonian (3.9) becomes

$$\hat{H} = -h \sum_{\vec{x} \in \Gamma_{odd}} \left(S_{\vec{x}} + S_{\vec{x}}^{\dagger} \right) \quad \Rightarrow \quad H \sim -2h \int d^3x \cos M(\vec{x}), \tag{6.81}$$

with the operator $M(\vec{x})$, in dominant order, defined as

$$M(\vec{x}) \equiv \sum_{j=1}^{3} t_a^j K_{ab} \partial_j^2 A_b(\vec{x}). \tag{6.82}$$

To explicitly show the gauge invariance this model possesses, it is useful to write the $M(\vec{x})$ operator as

$$\begin{aligned} M(\vec{x}) &= \sum_{j=1}^{2} t_a^j K_{ab} \partial_j^2 A_b(\vec{x}) - K_{ab} \partial_3^2 A_b(\vec{x}) \\ &= K_{ab} \sum_{j=1}^{2} t_a^j \left(\partial_j^2 - \partial_3^2\right) A_b(\vec{x}) \\ &= K_{ab} \mathcal{D}_a A_b(\vec{x}), \end{aligned} \tag{6.83}$$

where we used $t_a^3 = -1$ from the first to the second line and defined the differential operator $\mathcal{D}_a \equiv \sum_{j=1}^{2} t_a^j \left(\partial_j^2 - \partial_3^2\right)$.

The continuous model, defined in (6.81) depends only on the $M(\vec{x})$ operator, which depends on the A_b fields only through the relation (6.83). Due to the anti-symmetry of the K matrix, this theory is invariant under the gauge transformation

$$\begin{aligned} A_a &\rightarrow A_a + \mathcal{D}_a \lambda, \\ \Rightarrow M &\rightarrow K_{ab} \mathcal{D}_a A_b + K_{ab} \mathcal{D}_a D_b \lambda \\ &\rightarrow K_{ab} \mathcal{D}_a A_b(\vec{x}) = M. \end{aligned} \tag{6.84}$$

We consider only the dominant terms in the $A_b(\vec{x})$ field expansion (6.78) since we are interested only in the low-energy physics of the theory. By the same reason, we consider only the field configurations that maximize the cosine function, i.e., minimize the Hamiltonian energy function. These field configurations obey

$$M(\vec{x}) = 2\pi m, \quad m \in \mathbb{Z}. \tag{6.85}$$

We are ensure our EFT describes the low-energy physics of the Chamon code enforcing the previous relation through a Lagrange multiplier A_0. The Lagrangian can be found by Legendre transforming the Hamiltonian

$$\mathcal{L} = \Pi_a \partial_0 A_a - \mathcal{H}. \tag{6.86}$$

The Hamiltonian density is given in the integral argument of (6.81) and the conjugated momentum is given in (6.74). Thus

$$\mathcal{L} = \frac{1}{\pi} (K)_{ab} A_a \partial_0 A_b + 2A_0 \left(K_{ab} \mathcal{D}_a A_b - 2\pi m\right) \tag{6.87}$$

The low-energy effective theory is then

$$S = \int d^3x dt \frac{1}{2\pi} \left[K_{ab} A_a \partial_0 A_b + 2A_0 \left(K_{ab} \mathcal{D}_a A_b - 2\pi m\right)\right]. \tag{6.88}$$

The requirement that the theory is gauge invariant, up to boundary terms, of the theory is that the Lagrange multiplier transforms as

$$A_0 \to A_0 + \partial_0 \lambda. \tag{6.89}$$

The charged sector of this theory is associated to the coupling $A_0 m$, with $m = 0$ being the zero charge sector. The theory we obtained is a Chern-Simons like action, defined in three spatial dimensions. In terms of the gauge-invariant electric and magnetic fields $E_a = \partial_0 A_a - \mathcal{D}_a A_0$ and $B = \mathcal{D}_1 A_2 - \mathcal{D}_2 A_1$, the action becomes

$$S = \int d^3x dt \frac{k}{2\pi} \left[A_1 E_2 - A_2 E_1 + A_0 B \right], \quad \left[A_1(\vec{x}), A_2\left(\vec{x}'\right) \right] = -\frac{\pi i}{k} \delta_{\vec{x},\vec{x}'}. \tag{6.90}$$

This is exactly the EFT for the Chamon code presented at the work [17] which we discussed in section 2.112. To completely compare both theories, we redefine $A_1 \to -A_2, A_2 \to A_1, \mathcal{D}_1 \to -\mathcal{D}_2$, and $\mathcal{D}_2 \to \mathcal{D}_1$ and identify $k = s/2$.

Conservation Laws

As mentioned previously, the conserved quantities in the effective field theory are the charges in certain planes. With our modified derivative operator, in order to keep the theory gauge invariant, the current must obey

$$\partial_0 J_0 - \mathcal{D}_a J_a = 0. \tag{6.91}$$

It gives us a conserved charge not only in the whole system

$$\frac{dQ}{dt} = \frac{d}{dt} \int d^3x J_0 = \int d^3x \mathcal{D}_a J_a = 0, \tag{6.92}$$

but also in some specific planes. Let $\sigma_i = \pm 1$ and $\vec{u}_1^{\sigma_1} = \hat{x}_1 + \sigma_1 \hat{x}_3$ and $\vec{u}_2^{\sigma_2} = \hat{x}_2 + \sigma_2 \hat{x}_3$ face-diagonals coordinates. Integrating on any of the four plans

$$\begin{aligned} \frac{d}{dt} \int du_1^{\sigma_1} du_2^{\sigma_2} J_0 &= \int du_1^{\sigma_1} du_2^{\sigma_2} \mathcal{D}_a J_a \\ &= \int du_1^{\sigma_1} du_2^{\sigma_2} \left(\partial_1^2 - \partial_3^2 \right) J_1 + \left(\partial_2^2 - \partial_3^2 \right) J_2 \\ &= \int du_1^{\sigma_1} du_2^{\sigma_2} \left(\partial_{u_{1_+}} \partial_{u_{1_-}} \right) J_1 + \left(\partial_{u_{2_+}} \partial_{u_{2_-}} \right) J_2 = 0, \end{aligned} \tag{6.93}$$

where we have used the explicit definition of $\mathcal{D}_a$ operators and written $\partial_{u_{i_\pm}} = \partial_i^2 \pm \partial_3^2$. The perpendicular directions of such planes

$$\vec{u}_1^{\sigma_1} \times \vec{u}_2^{\sigma_2} = -\sigma_1 \hat{x}_1 - \sigma_2 \hat{x}_2 + \hat{x}_3 \tag{6.94}$$

are the cube-diagonal vectors $\vec{t} = \{[111], [\bar{1}11], [1\bar{1}1], [\bar{1}\bar{1}1]\}$. The conserved charges along the perpendicular planes $\Sigma_{\vec{t}} = \{-\sigma_1 x_1 - \sigma_2 x_2 + x_3 = cte\}$ in this continuous field description are exactly the topological charges (3.14) in the lattice model.

Note that the dipole momentum $\vec{P} = \int_{\Sigma_{\vec{t}}} J_0 \vec{t}$ in any $\vec{t}$ cube-diagonal direction is conserved along the planes $\Sigma_{\vec{t}}$,

$$\partial_0 \vec{P} = \int_{\Sigma_{\vec{t}}} \partial_0 J_0 \vec{t} = \int_{\Sigma_{\vec{t}}} (\mathcal{D}_a J_a)\vec{t} \tag{6.95}$$

$$= \int du_1^{\sigma_1} du_2^{\sigma_2} \mathcal{D}_a (J_a \vec{t}) = 0, \tag{6.96}$$

where we used that the $\mathcal{D}_a$ derivatives act on the orthogonal planes to $\vec{t}$ and $\mathcal{D}_a \vec{t} = 0$ for $a = 1, 2$.

Ground State Degeneracy

As a check consistency of our description, we recover the ground state degeneracy (3.10) in the effective low-energy description. In the continuum limit $L \to \infty$, the ground state is infinitely degenerate. We regularize this divergence by reintroducing the lattice spacing length a in a convenient way. We take advantage of the conservation laws in the $\Sigma_{\vec{t}}$ sub manifolds and discretize our model as stacks of such cube-diagonal perpendicular planes. Basically, we think of it as a collection of four 2d planar systems stacked along a cubic diagonal line. In the action (6.88), we discretize the transverse direction. For this, we perform the variables change

$$(x_1, x_2, x_3) \to (u_1^{\sigma}, u_2^{\sigma}, x_{\perp}), \tag{6.97}$$

with $x_{\perp}$ being the cube-diagonal variable, normal to the planes $u_1^{\sigma_1} u_2^{\sigma_2}$. In order to discretize this direction, we introduce the lattice distance a, where the distance between two planes in the stack is $2a$

$$\int dx_{\perp} \to \sum_{i=1}^{N} 2a. \tag{6.98}$$

In this way, the action (6.88) becomes a sum in N A_a fields, corresponding to their respective layer. That is, we have a bunch of $2+1$ dimensional theories

$$S = \sum_{i=1}^{N} \int dt dx_{13}^{\sigma_1} dx_{23}^{\sigma_2} \frac{k}{\pi} A_1^i \partial_0 A_2^i + \cdots . \tag{6.99}$$

In order to get rid of the $2a$ factor, we have properly scaled the gauge fields $A_a\left(t, u_a^{\sigma_a}, x_{\perp}\right) \to \frac{1}{\sqrt{2a}} A_a^i\left(t, u_a^{\sigma_a}\right)$, so that now $[A_a^i] = 1$. In this parametrization, $L = 2a \times N$. In the following, to be compatible with our previous discussion in section 3.2 we set $a = 1$.

Note that, for each one of the N two-dimensional systems, due to the periodic boundaries conditions, we have a T^2 torus. The nontrivial topology of the lattice allows large gauge transformations. Namely, the gauge transformation implemented by

$$\zeta^i = \frac{2\pi n_1^i}{l_i} u_1^+ u_1^- + \frac{2\pi n_2^i}{l_i} u_2^+ u_2^-, \quad n_1^i, n_2^i \in \mathbb{Z}, \tag{6.100}$$

give us the transformation for the A_a^i fields as

$$A_1^i \cong A_1^i + \frac{2\pi}{l_i} m_1^i \quad \text{and} \quad A_2^i \cong A_2^i + \frac{2\pi}{l_i} m_2^i, \quad m_1^i, m_2^i \in \mathbb{Z}. \tag{6.101}$$

The holonomy operators

$$\exp\left(i \oint_0^{l_i} du_1^{\sigma_1} A_1^i\right) \quad \text{and} \quad \exp\left(i \oint_0^{l_i} du_2^{\sigma_2} A_2^i\right) \tag{6.102}$$

where l_i the linear dimension of the $i-$th torus, are gauge invariant even under large transformations. The holonomies are the relevant degrees of freedom in low-energy physics and provide us a way to count the ground state degeneracy.

The CS-like theory (6.99) for each plane is completely gapped. There is no propagating degrees of freedom in the spectrum and he physics of the model relies on global aspects. That is why we are interested in the "global" holonomies degrees of freedom. By the same reason, we are interested in the zero modes solutions

$$A_a^i\left(t, u_1^+, u_2^-\right) = \frac{1}{l_i} \bar{A}_a^i(t), \tag{6.103}$$

which reflects the topological aspects of the theory. In terms of these solutions, the action becomes

$$S = \sum_{i=1}^{N} \int dt \frac{k}{\pi} \bar{A}_1^i \partial_0 \bar{A}_2^i. \tag{6.104}$$

The commutation rule for each plane variable is

$$\left[\bar{A}_1^i, \bar{A}_2^j\right] = -\frac{i\pi}{k} \delta^{ij}. \tag{6.105}$$

The associated holonomies in the i-th plane $e^{i\bar{A}_1^i}$ and $e^{i\bar{A}_2^i}$ obey

$$e^{i\bar{A}_1^i} e^{i\bar{A}_2^i} = e^{i\bar{A}_2^i} e^{i\bar{A}_1^i} e^{\frac{i\pi}{k}}, \tag{6.106}$$

which implies a 2k-fold degeneracy for each plane i.

In our regularization, there are $4N$ independent $\Sigma_{\vec{t}}$ planes (N for each one of the four cube-diagonals), so that the total system ground state degeneracy is

$$\text{GSD} = (2k)^{4N} = 2^{2L}. \tag{6.107}$$

We set $k = 1$ and replaced $N = L/2$. This successfully recover the result in (3.11).

Final Remarks and Perspectives

In this work we have studied and developed several methods that are quite useful to investigate certain topologically ordered systems, as QSL and fracton models. To briefly summarize the main points of the work, within the context of QSL, we studied two exactly solvable lattice models, the Toric Code and the Wen Plaquette model. We were able to find the corresponding effective descriptions that properly capture the low-energy properties. Moreover, we studied in some details the three-dimensional lattice models X-Cube and Chamon codes, as well as their EFTs, and also discussed general aspects of fractonic field theories. In addition, we proposed and explored an exactly solvable $2D$ Type-I fracton model both in the lattice as in the continuum.

Most of the studies carried in this thesis dealt with Type-I fracton models, which are more abundant in examples than the Type-II ones. Nevertheless, Type-II fracton systems are the subject of great interest, not only due their potential technological applications, but also because of their even more intriguing physical properties. In particular, the study of Type-II fractonic field theories is in its initial stage and in developing process. We do expect that the methods discussed here can be directly applied to the study of Type-II fracton lattice models that are given in terms of commuting projectors, as in the case of the Haah code and the model discussed in Ref. [40]. Although the latter model is not strictly a Type-II fracton, since it contains lineons along one direction, it presents Type-II phenomenology in a submanifold and still is written in terms of commuting projectors. These investigations are currently in progress.

To conclude, it is worth to stress that the methods developed along this work pave the way for the investigation of several open questions. Among them, we would like to highlight the following: i) the study of layer construction from the perspective of continuum descriptions along the lines of Ref. [41]; ii) investigation of the duality relations between the BF-like theories and Higgsed higher-rank gauge theories; iii) full classification of the $2+1$ dimensional fracton systems; iv) construction of non-Abelian fractonic phases; v) extension of the commuting projectors formalism for the case of non-exactly solvable models.

Referências

[1] GROSS, D. et al. Quantum fields and strings. a course for mathematicians. In: . [S.l.: s.n.], 1999.

[2] ANDERSON, P. W. More is different. *Science*, American Association for the Advancement of Science, v. 177, n. 4047, p. 393–396, 1972. ISSN 0036-8075.

[3] ZENG, B. *Quantum information meets quantum matter: from quantum entanglement to topological phases of many-body systems*. [S.l.]: Springer, 2019.

[4] WEN, X. G. *Quantum Field Theory of Many-Body Systems: From the Origin of Sound to an Origin of Light and Electrons*. [S.l.: s.n.], 2004. v. 9780199227. 1–520 p. ISBN 9780191713019.

[5] WITTEN, E. Three lectures on topological phases of matter. *Rivista del Nuovo Cimento*, v. 39, n. 7, p. 313–370, 2016. ISSN 0393697X.

[6] TONG, D. Lectures on the Quantum Hall Effect. n. January, 2016.

[7] LERDA, A. *Anyons quantum mechanics of particles with fractional statistics*. [S.l.]: Springer, 1992.

[8] SAVARY, L.; BALENTS, L. Quantum spin liquids. *Reports on Progress in Physics*, v. 80, 2016. ISSN 01430807.

[9] CHAMON, C. Quantum Glassiness in Strongly Correlated Clean Systems: An Example of Topological Overprotection. *Physical Review Letters*, v. 94, n. 4, 2005.

[10] HAAH, J. Local stabilizer codes in three dimensions without string logical operators. *Physical Review A - Atomic, Molecular, and Optical Physics*, v. 83, n. 4, p. 1–16, 2011. ISSN 10502947.

[11] VIJAY, S.; HAAH, J.; FU, L. A new kind of topological quantum order: A dimensional hierarchy of quasiparticles built from stationary excitations. *Physical Review B - Condensed Matter and Materials Physics*, v. 92, n. 23, 2015. ISSN 1550235X.

[12] PRETKO, M.; CHEN, X.; YOU, Y. Fracton phases of matter. *International Journal of Modern Physics A*, v. 35, n. 6, p. 1–71, 2020.

[13] NANDKISHORE, R. M.; HERMELE, M. Fractons. *Annual Review of Condensed Matter Physics*, v. 10, n. 1, p. 295–313, 2019.

[14] SEIBERG, N.; SHAO, S.-H. Exotic Symmetries, Duality, and Fractons in 2+1-Dimensional Quantum Field Theory. 3 2020.

[15] PRETKO, M. Emergent gravity of fractons: Mach's principle revisited. *Physical Review D*, v. 96, n. 2, p. 1–16, 2017. ISSN 24700029.

[16] SLAGLE, K.; KIM, Y. B. Quantum field theory of X-cube fracton topological order and robust degeneracy from geometry. *Physical Review B*, v. 96, n. 19, p. 1–20, 2017. ISSN 24699969.

[17] YOU, Y. et al. Fractonic Chern-Simons and BF theories. *Physical Review Research*, v. 2, n. 2, 2020.

[18] FONTANA, W. B.; GOMES, P. R. S.; CHAMON, C. Lattice Clifford fractons and their Chern-Simons-like theory. 2020. Disponível em: <http://arxiv.org/abs/2006.10071>.

[19] MA, H. et al. Fracton topological order via coupled layers. *Physical Review B*, v. 95, n. 24, p. 1–20, 2017. ISSN 24699969.

[20] HSIEH, T. H.; HALÁSZ, G. B. Fractons from partons. *Physical Review B*, v. 96, n. 16, p. 1–6, 2017. ISSN 24699969.

[21] DUNNE, G. V. Aspects Of Chern-Simons Theory. In: *Aspects topologiques de la physique en basse dimension. Topological aspects of low dimensional systems*. [S.l.: s.n.], 2007. p. 177–263.

[22] BALENTS, L. Spin liquids in frustrated magnets. *Nature*, v. 464, n. 7286, p. 199–208, 2010. ISSN 00280836.

[23] SACHDEV, S. Topological order, emergent gauge fields, and Fermi surface reconstruction. *Reports on Progress in Physics*, v. 82, n. 1, 2019. ISSN 00344885.

[24] POLYAKOV, A. Quark confinement and topology of gauge theories. *Nuclear Physics B*, v. 120, n. 3, p. 429 – 458, 1977. ISSN 0550-3213.

[25] RYDER, L. H. *Quantum field theory*. [S.l.]: Cambridge university press, 1996.

[26] KITAEV, A. Y. Fault-tolerant quantum computation by anyons. *Annals of Physics*, v. 303, n. 1, p. 2–30, 2003. ISSN 00034916.

[27] LEVIN, M. A.; WEN, X. G. String-net condensation: A physical mechanism for topological phases. *Physical Review B - Condensed Matter and Materials Physics*, v. 71, n. 4, p. 1–21, 2005. ISSN 10980121.

[28] KITAEV, A.; LAUMANN, C. Topological phases and quantum computation. 2009. Disponível em: <http://arxiv.org/abs/0904.2771>.

[29] ARAKAWA, G.; ICHINOSE, I. Zn gauge theories on a lattice and quantum memory. *Annals of Physics*, v. 311, n. 1, p. 152 – 169, 2004. ISSN 0003-4916.

[30] HANSSON, T.; OGANESYAN, V.; SONDHI, S. Superconductors are topologically ordered. *Annals of Physics*, v. 313, n. 2, p. 497 – 538, 2004. ISSN 0003-4916.

[31] WEN, X. G. Quantum Orders in an Exact Soluble Model. *Physical Review Letters*, v. 90, n. 1, p. 4, 2003. ISSN 10797114.

[32] SCHULZ, M. D. et al. Breakdown of a perturbed $\mathbb{Z}_n$ topological phase. *New Journal of Physics*, IOP Publishing, v. 14, n. 2, p. 025005, feb 2012.

[33] GUO, C.-X. et al. Non-hermitian dynamic strings and anomalous topological degeneracy on a non-hermitian toric-code model with parity-time symmetry. *Phys. Rev. B*, American Physical Society, v. 101, p. 144439, Apr 2020.

[34] YU, J.; KOU, S.-P. Macroscopic quantum tunneling effect of Z_2 topological order. *Phys. Rev. B*, American Physical Society, v. 80, p. 075107, Aug 2009.

[35] KOU, S.-P.; LEVIN, M.; WEN, X.-G. Mutual chern-simons theory for Z_2 topological order. *Phys. Rev. B*, American Physical Society, v. 78, p. 155134, Oct 2008.

[36] BRAVYI, S.; LEEMHUIS, B.; TERHAL, B. M. Topological order in an exactly solvable 3D spin model. *Annals of Physics*, v. 326, n. 4, p. 839–866, 2011. ISSN 00034916.

[37] MA, H. *Mechanisms for Fracton Phases*. Tese (Doutorado) — University of Colorado, 2019.

[38] GROMOV, A. Towards Classification of Fracton Phases: The Multipole Algebra. *Physical Review X*, v. 9, n. 3, p. 1–17, 2019. ISSN 21603308.

[39] GOMES, P. R. S. et al. Effective field theory for the bulk-edge correspondence in a two-dimensional $_2$ topological insulator with rashba interactions. *Phys. Rev. B*, American Physical Society, v. 90, p. 115144, Sep 2014.

[40] CASTELNOVO, C.; CHAMON, C. Topological quantum glassiness. *Philosophical Magazine*, Taylor & Francis, v. 92, n. 1-3, p. 304–323, 2012.

[41] SHIRLEY, W.; SLAGLE, K.; CHEN, X. Twisted foliated fracton phases. *Phys. Rev. B*, American Physical Society, v. 102, p. 115103, Sep 2020.

Apêndices

APÊNDICE A – $\mathbb{Z}_N$ Pauli Operators

In this work we make use of the generalized $\mathbb{Z}_N$ "clock" Z and "shift" X Pauli operators. They satisfy

$$XZ = \omega ZX \quad \text{with} \quad \omega = e^{\frac{2\pi i}{N}} \tag{A.1}$$

and $Z^N = X^N = I$. In opposition to the $N = 2$ case, where we have the usual Pauli matrices σ^z and σ^x algebra, such operators are not Hermitian and have eigenvalues $1, \omega, \cdots, \omega^{N-1}$. They can be represented as $N \times N$ unitary matrices

$$Z_{xi} = \begin{pmatrix} 1 & 0 & . & . & 0 \\ 0 & \mathrm{e}^{\frac{2\pi i}{N}} & 0 & . & 0 \\ . & . & . & . & . \\ . & . & . & . & 0 \\ 0 & . & . & . & \mathrm{e}^{\frac{2\pi(N-1)i}{N}} \end{pmatrix} \quad \text{and} \quad X = \begin{pmatrix} 0 & 1 & 0 & . & 0 \\ 0 & 0 & 1 & 0 & 0 \\ . & . & . & . & . \\ 0 & 0 & . & 0 & 1 \\ 1 & 0 & . & . & 0 \end{pmatrix}. \tag{A.2}$$

For future purposes, it is useful to investigate how time-reversal transforms the $\mathbb{Z}_N$ operators. It is implemented by an anti-unitary transformation $\mathcal{T} = U\hat{K}$ and $\mathcal{T}^{-1} = \hat{K}U^\dagger$ with U unitary and $\hat{K}$ the complex conjugation operator. It transforms (A.1) as

$$\begin{aligned} \mathcal{T}XZ\mathcal{T}^{-1} = \mathcal{T}\omega ZX\mathcal{T}^{-1} \quad \Rightarrow \quad \underbrace{\mathcal{T}X\mathcal{T}^{-1}}_{X'}\underbrace{\mathcal{T}Z\mathcal{T}^{-1}}_{Z'} &= \omega^*\mathcal{T}Z\mathcal{T}^{-1}\mathcal{T}X\mathcal{T}^{-1} \\ \Rightarrow \quad X'Z' &= \omega^* Z'X', \end{aligned} \tag{A.3}$$

where we have used that $\mathcal{T}\omega = \omega^*\mathcal{T}$. We can explicit find the $\mathbb{Z}_N$ operators transformations generalizing the $\mathbb{Z}_2$ case $qU = e^{i\delta}\sigma^y$ where a physical spin $1/2$ transforms $\mathcal{T} : \hat{S}^i = \sigma^i/2 \mapsto -\hat{S}^i$. Define $Y = iXZ$, then under time reversal $\mathcal{T} = e^{i\alpha}XZ\hat{K}$

$$X \to X' = \mathcal{T}X\mathcal{T}^{-1} = \omega^* X \quad \text{and} \quad Z \to Z' = \mathcal{T}Z\mathcal{T}^{-1} = \omega^* Z^\dagger, \tag{A.4}$$

where we have used the algebra $XZ^\dagger = \omega^* Z^\dagger X$, that $\hat{K}X\hat{K} = X$ and $\hat{K}Z\hat{K} = Z^\dagger$. This representation for $\mathcal{T}$ transformation successfully reproduces (A.3).